

A N N U A L R E P O R T 1964
of the
Institut für Plasmaphysik GmbH
Munich - Garching
and of the
Experimental Department (Plasma Physics)
of the Max-Planck-Institut für Physik
and Astrophysik, Munich

I N S T I T U T F Ü R P L A S M A P H Y S I K
G A R C H I N G B E I M Ü N C H E N

P R E F A C E

The purpose of the Institut für Plasmaphysik, as laid down by its constitution, is to conduct research in plasma physics and allied fields and also to develop the methods and equipment required for such research.

At present the Institute comprises three Experimental Departments, a Theory Department, an Engineering Department, Central Workshop, Administration and General Services. The "Scientific Supervisory Board" consisted in the period covered by the present report of the five departmental heads and the two directors of the Max-Planck-Institut für Physik und Astrophysik who held office when the Institute was founded. One of the duties of this board is to decide on the type of research and how it is to be conducted, close contact being maintained at all times with the business management. Organization and administration are based on the successful principles adopted by the Max-Planck-Gesellschaft and geared to the special requirements of the work being done at the Institute.

The collaboration with EURATOM dating back to 1961 under the terms of an agreement to conduct a joint research programme was continued.

In the report year the main object of the scientific work undertaken was again to investigate the possibility of producing hot plasmas and maintaining them over such long periods and at such high temperatures that a substantial quantity of plasma (if it consists of suitable hydrogen isotopes) is converted by energy-yielding thermonuclear reactions. So far this objective has not been achieved anywhere in the world, not even with a modest degree of success. Nor were any of the experiments conducted, started or planned in the Institute intended to bring about these conditions directly. Even the relatively large experiments constitute only preliminary stages for clarifying in three ways the conditions essential for realizing the state sought.

The first approach consists in producing by rapid magnetic compression (theta pinch) a plasma of as high temperature as possible and of not too low density. This way comes nearest to achieving the state sought but in its analysis certain difficulties arise, firstly because of the complications involved here in all measurements of physical quantities and secondly because of the essentially dynamic behaviour of the plasma, which has to be clarified by elaborate numerical calculations. In order to achieve any worthwhile progress by this method the confinement times have to be extended considerably. Special attention is therefore devoted to the phenomena at the ends of elongated devices and to the possibilities of devices closed upon themselves ("M+S").

The second approach consists in producing an almost fully ionized plasma in almost stationary thermal equilibrium. Such a plasma therefore has properties that are largely understood. By methods which can be regarded as relatively conventional temperatures of 10^5 degrees (C) and a little over have been reached (Experimental Plasma Physics 3, "Hour-glass") so as to produce a plasma particularly suitable for experiments that point the way ahead.

The third approach consists in investigating model plasmas, there being no intention of seeking an approximation to the state variables of a fusion plasma. This way does allow, however, a detailed analysis of the behaviour of the charged particles confined by a magnetic field. For this purpose alkali plasmas in various geometric configurations are used.

All these experiments and also a large number of others which are concerned with subordinate problems in physics, or clarify technical difficulties, or devise new measuring methods are being conducted more and more in collaboration with theorists. The report therefore describes a fairly large amount of theoretical work connected with the relevant experiments.

Both the investigations at the Institute and the knowledge gained from the remarkably close cooperation with a large number of other laboratories, mostly abroad, indicate that the desired extension of the confinement time, in particular, is possible with magnetic fields which are stable against so-called "exchange". Appropriate experiments with plasmas produced in various ways are being prepared.

Work in the field of magnetohydrodynamic generators was continued in the report year. This involved, in particular, investigating the possibility of maintaining the electrons at a higher temperature than the rest of the gas. Shock tubes are used for supplementary measurements.

The sections of the report relating to the various groups of the Engineering Department describe the extensive work being done in the field of technical developments, such as were necessary, for instance, for constructing the 1.5/2.6-MJ capacitor bank, and in special fields of physics, such as ultra-high-vacuum physics.

The Institute arranged two international conferences: "International Symposium on Diffusion Across a Magnetic Field" from 29th June till 3rd July 1964 in Feldafing and "Third Symposium on Engineering Problems in Thermonuclear Research" in Munich. An account of the proceedings was published by the Institute.

C O N T E N T S

Page

EXPERIMENTAL PLASMA PHYSICS I (PROF. DR. FÜNFER)

1. <u>Summary</u>	1
2. <u>Theta-Pinch</u>	4
2.1 Theta Pinch I (H. Herold, G. Decker, M. Kornherr, F.L. Ribe, H. Röhr)	4
2.2 Theta Pinch II (A. Eberhagen, M. Bernstein, H. Glaser, H. Griem)	8
2.3 Theta Pinch 1.5/2.6 MJ (C. Andelfinger, A. Eberhagen, M. Ulrich, R. Wunderlich)	11
2.4 Pinch Dynamics (D. Düchs)	12
2.5 Theoretical Studies of the Behaviour of a Theta Pinch at Extremely Low Plasma Density (R. Chodura)	12
2.6 Experimental Investigations of the Collisionless Compression of a Low-Density Theta Pinch Plasma (P. Igenbergs)	14
2.7 Vacuum Magnetic Field in Theta Pinch Coils and Cusped Geometries (F. Pohl)	14
2.8 Brightness Distribution along the Axis of a Theta Pinch with Unperturbed Coil Geometry (E. Glock, K. Hübner)	15
2.9 Preionization in the Theta Pinch	15
2.9.1 z-Pinch Preionization (R. Wunderlich)	15
2.9.2 Conical z-Pinch as Preionization Method (C. Andelfinger, E. Glock, R. Wunderlich)	15
2.9.3 Preionization by UV Radiation (G. Hofmann)	16
3. <u>Antipinch</u> (W. Engelhardt, W. Köppendörfer, P. Merkel)	17
4. <u>z-Pinch</u>	17
4.1 X-Radiation in the Linear z-Pinch (J. Sommer)	17
4.2 Electron Density Measurements with Microwaves (H. Hermansdorfer)	17
5. <u>Fieldless Plasma Configurations in Equilibrium with Plane Magnetic Fields</u> (P. Merkel)	18
6. <u>Measuring Methods</u>	18
6.1 Use of the Laser in Plasma Diagnostics (B. Kronast, H.-J. Kunze, H. Röhr, G. Weiser, H. Zietemann)	18
6.2 Frequency Shifting of Laser Radiation by the Doppler Effect (F.P. Küpper)	20
6.3 Laser Light Source for the Interferometer (R. Beck)	20
6.4 Differential Interferometer (A. Heiss)	20
6.5 Testing Electric Double Probes in Hot Plasmas (D. Combecker)	21
6.6 Development of Piezoelectric Probes for Pressure Measurement in Very Fast Discharges (W. Katsaros)	23
6.7 Infra-red Radiation of Plasma (D. Gross)	23
6.8 Infra-red Radiation in an Inhomogeneous Cylindrical Plasma Column in an Axial Magnetic Field (H. Gratzl)	23
6.9 Recording of Rapidly Varying Optical Line Profiles with Image Converter and Multiplier (W. Nässl)	24
6.10 Spectroscopic Measuring Devices (E. Glock)	24
6.11 Further Development of a Neutron Source (H.-J. Schneider-Muntau)	24
6.12 Electronic Systems (F. Lindenberger, M. Ulrich)	25

	Page
<u>EXPERIMENTAL PLASMA PHYSICS 2 (DR. G. VON GIERKE)</u>	
1. <u>Summary</u>	26
2. <u>High-Temperature Plasmas (F. Boeschoten)</u>	27
2.1 Proposed Method for Producing High-Temperature Plasmas (HELIOS and HELIOSIS) (F. Boeschoten, A. Borer, G. Cattanei, H. Grawe, W. Herrmann, G. Lisitano, G. Siller, K.H. Wöhler)	27
2.2 WW I (W. Herrmann)	28
2.3 Ion Beam Interaction (JO-JO) (A. Borer)	28
2.4 CABINET I (F. Boeschoten, K. Geissler, G. Siller)	28
2.5 CABINET III (K. Geissler)	28
2.6 Microwaves (G. Lisitano)	29
2.7 Hoke (K. Weinhardt)	29
3. <u>Thermal Plasmas and Probe Diagnostics (G. Müller)</u>	30
3.1 Particle Losses of a Cs Plasma Column in Straight and Curved Magnetic Fields (E. Guilino, in collaboration with the "Wendelstein" Group, MPI)	30
3.2 Excitation and Propagation of Plasma Oscillations	30
3.2.1 Bernstein Waves and Self-Excitation of Plasma Oscillations in the Vicinity of the Electron Cyclotron Harmonics (R.S. Harp, G. Müller)	30
3.2.2 Low-Frequency Electrostatic Ion Oscillations ($k//B$) (E. Guilino)	30
3.3 Probe Diagnostics	31
3.3.1 Investigation of the Velocity Distribution of the Electrons in a Hg Low-Pressure Discharge (W. Troppmann)	31
3.3.2 Investigations of Ion Current with a Grid Probe (V. Joshi)	31
3.3.3 RF Plasma Resonance Probe (G. Müller, W. Ott, G. Peter)	32
3.3.4 Plasma Boundary Sheaths (Electron Beam Probe) (W. Ott)	33
3.3.5 Comparative Density and Temperature Measurements with Probes and Spectroscopic Methods (A. van Oordt)	33
4. <u>Ultra-high Vacuum (E.W. Blauth)</u>	34
4.1 Surfaces	34
4.1.1 Sputtering of Solid Material (R. Behrisch)	34
4.1.2 Investigations of Field Emission (H. Vernickel)	34
4.2 Mass Spectrometers (E.W. Blauth, H. Hötzel, E.H. Meyer)	35
4.3 UHV Measurements	35
4.3.1 Oil Flow in the UHV (H.E. Schulze)	35
4.3.2 Initial Flow (B.M.U. Scherzer)	35
4.3.3 Base Pressures of Hg Diffusion Pumps (B.M.U. Scherzer)	35
4.3.4 Ion-Electron Converter (B.M.U. Scherzer)	35
4.3.5 Two-Chamber Ionization Gauge (G. Venus)	36

EXPERIMENTAL DEPARTMENT (PLASMA PHYSICS) OF THE MAX-PLANCK-INSTITUT
FÜR PHYSIK UND ASTROPHYSIK, MUNICH (DR. G. VON GIERKE)

1. <u>Summary</u>	37
2. <u>Hourglass (P. Grassmann, O. Klüber, H. Wulff)</u>	37

	Page
3. <u>Wendelstein</u> (D. Eckhartt, G. Grieger, M. Hashmi, H.P. Zehrfeld) (Engineers: C. Freudenberger, J. Kolos, M. Zippe)	38
3.1 Particle Losses of a Cs Plasma in a Stellarator	38
3.2 Particle Losses of a Cs Plasma in a Magnetic Field with Variable Curvature (experiments on ALMA II in collaboration with E. Guilino, IPP)	39
3.3 Particle Losses of a Cs Plasma in a Homogeneous Magnetic Field	39
3.4 Equilibrium in Toroidally Closed Configurations	40
3.5 Ba Plasma (in collaboration with F.W. Hofmann, Princeton, and A. van Oordt, IPP)	40
3.6 "Ambipol" (F. Karger)	40
4. <u>Theta Pinch in Toroidal Magnetic-Field Configurations (M+S)</u> (H. Bialas, J. Junker, W. Lotz, F. Rau, E. Remy, K.I. Uo, H. Wobig, G.H. Wolf) (Engineers: H. Finkelmeyer, F. Hartz, H. Schuhbäck, D. Seewald)	41
4.1 Theory	41
4.1.1 Numerical Calculations of the Magnetic Field in the Space Outside a M+S Plasma	41
4.1.2 New M+S Surfaces	41
4.2 Experiments	41
4.2.1 "Drehfeld" Measuring Station - up to 16 kJ	41
4.2.2 "Zwilling" Measuring Station	43
4.2.3 "Quickly" Measuring Station - 4 kJ	43
4.2.4 Measuring Station T-2 - 4 to 16 kJ	43
4.2.5 "Limpus" - 380 kJ (planned)	44
4.2.6 "Copper Plasma"	44
4.3 Technical Aspects	44
4.3.1 "Capacitor Unit with Ignitrons" Fatigue Test	44
4.3.2 "Spark Gaps" Fatigue Test	44
4.3.3 Short-circuiting Device	44
4.4 Data Processing	45
4.4.1 Preliminary Programme	45
4.4.2 Probe Measurements	45
4.4.3 Spectroscopy	45
5. <u>Spectroscopy</u> (K. Bergstedt, C.-R. Vidal)	45
6. <u>RF Plasma Interaction</u> (H.M. Mayer)	46
7. <u>Vacuum Spectroscopy</u> (G. Boldt)	46
7.1 Si I, II Oscillator Strengths in the Region of $1000 < \lambda < 1800 \text{ \AA}$ (F. Labuhn)	46
7.2 Si I, II Oscillator Strengths in the Region of $1100 < \lambda < 2000 \text{ \AA}$ (W. Hofmann)	46
7.3 Line Wing Profile of the Hydrogen Line α (G. Boldt, W.S. Cooper)	47
7.4 H ₂ Oscillator Strengths in the Region of $900 < \lambda < 1100 \text{ \AA}$ (G. Boldt, E.H. Pinnington)	47
7.5 Comparison of Various Intensity Normals in the Vacuum UV Spectral Range (G. Boldt, F.W. Hofmann)	47
7.6 Intermittence Effect on Various Photographic Emulsions (K.H. Stephan)	47
8. <u>Microwaves</u> (U. Hopf, F. Klan, G. Landauer, B. O'Brien, M. Tutter)	48
8.1 Longitudinal Waves (M. Tutter)	48
8.2 Resonance Experiment on a Low-Pressure Discharge (B. O'Brien)	48

	Page
8.3 PIG I (G. Landauer)	48
8.4 PIG III (F. Klan)	49
8.5 Miscellaneous (U. Hopf)	50
8.6 Use of Microwave Technique on Physico-chemical and Biochemical Problems (N. Kaiser as guest)	50
9. <u>Electronic Workshop</u> (K. Moustafa, J. Machate, H. Utzat)	51

EXPERIMENTAL PLASMA PHYSICS 3 (PROF. DR. R. WIENECKE)

1. <u>Summary</u>	53
2. <u>Stationary Heating of High-Density Plasmas</u> (S. Witkowski)	54
2.1 Helium Arc in a Magnetic Field (C. Mahn, S. Witkowski)	54
2.2 Hydrogen Arc in a Magnetic Field (C. Mahn, H. Ringler, G. Zankl)	54
2.3 Calculation of the Characteristic of a Hydrogen Arc in a Magnetic Field with Due Allowance for the Radiation (U. Heidrich)	55
2.4 Doppler Temperature Measurement (K. Büchl)	56
2.5 Experimental Investigations of the Pressure Profile in a Hydrogen Arc with Superimposed Magnetic Field (H.F. Döbele, S. Witkowski)	56
2.6 Consideration of the Pressure Increase in an Arc Column with Superimposed Axial Magnetic Field (S. Witkowski)	57
2.7 Velocity Measurement by "Colouring" a Plasma Beam (H.Salzmann, G.Zankl)	58
2.8 Population of Energy Levels with Due Allowance for the Radiation Field (S. Ramer)	58
3. <u>Magnetoplasmdynamics</u> (M. Salvat)	59
3.1 Theoretical Studies on Raising the Electron Temperature in a Rare-Gas Alkali Generator (M. Salvat, G. Brederlow, W. Ohlendorf)	59
3.2 Measurements of Electron Temperature and Conductivity in the Argon-Potassium Plasma of a MHD Generator (G. Brederlow)	60
3.2.1 Measurements of the Electron Temperature Field without Magnetic Field (G. Brederlow, W. Riedmüller)	60
3.2.2 Measurements of the Electron Temperature and Electric Conductivity in a MHD Generator and with Applied Crossed Electric and Magnetic Fields (G. Brederlow, R. Hodgson)	60
3.2.3 Electron Temperature Distribution in a Segmented Argon-Potassium MHD Generator (F. Fischer)	60
3.3 Measurements of the Temperature and Velocity Profiles in a MHD Generator (Z. Celinski)	61
3.4 Vector Representation and Analysis of the Principle of Various MHD Generator Types (Z. Celinski)	61
3.5 Two-Dimensional Analysis of the MHD Generator with Segmented Electrodes (Z. Celinski, M. Fischer)	62
3.6 Calculation of the Transport Properties of Weakly Ionized Rare-Gas Alkali Plasmas (R.T. Hodgson)	63
3.7 MHD Generator with Non-thermal Radio-Frequency Ionization (W. Ohlendorf)	63
3.8 Plasma Acceleration (G. Hahn, M. Salvat)	63
4. <u>Shock Wave Experiments and Problems of Non-stationary MHD Conversion</u>	
(H. Muntenbruch)	64
4.1 Investigations of a Rail Spark Gap (L. Liebing)	64
4.2 Investigations of T Tubes	64
4.2.1 Interferometric Measurements (H. Brinkschulte)	64

	Page
4.2.2 Microwave Investigations (W. Makios)	65
4.2.3 Measurement of Currents and Magnetic Fields (H. Kolig)	65
4.3 Diaphragm Tube Device for Investigating the Interaction between Shock Wave and Magnetic Field	65
4.3.1 Theoretical Consideration of the "Reflection" of Shock Waves in Magnetic Fields (E. Rebhan)	67
4.3.2 Preliminary Experimental Investigations (H. Brinkschulte)	68
4.3.3 Calculation of the Optimum Dimensions for the Device (P. Javel, H. Nett)	68
4.3.4 Technical Problems of the Diaphragm Tube (P. Javel, H. Nett)	68
4.3.5 Initial Experiments (H. Nett)	68
5. <u>Construction of Laboratory Block L 5 and Rectifier Centre L 5 E</u>	
(H. Dickopp, H. Muntenbruch, R. Wienecke, S. Witkowski)	69

THEORY (PROF. DR. SCHLÜTER)

1. <u>Summary</u>	70
2. <u>Macroscopic Theory</u>	70
2.1 Two-Dimensional Theta Pinch Calculations (F. Hertweck)	70
2.2 One-Dimensional Pinch Calculations (H. Fisser)	73
2.3 Transport Coefficients (W. Feneberg, H. Fisser)	73
2.4 Equilibrium with Plane Magnetic Fields (R. Gorenflo, P. Merkel)	73
2.5 Stability of M+S Surfaces (D. Pfirsch, H. Wobig, MPI)	73
2.6 Diffusion of a Plasma in a Magnetic Field (G. Knorr, D. Pfirsch)	74
2.7 Equilibrium between Surface Currents (Magnetic Laval Valve) (W. Lünow)	74
3. <u>Microscopic Theory</u>	74
3.1 Microinstabilities in Homogeneous Plasmas (D. Pfirsch, MPI)	74
3.2 Kinetic Equations	74
3.2.1 Derivation of Kinetic Equations by Time Scale Formalism (S. Priess)	74
3.2.2 Kinetic Equations and Correlations (P.P.J.M. Schram)	75
3.3 Spatial Correlations (M. Feix, K. von Hagenow, W. Kegel, P.P.J.M. Schram)	75
3.3.1 Classical Treatment of the Spatial Correlation Function of a Single-Component Plasma (K. von Hagenow)	75
3.3.2 Quantum Theoretical Treatment of Thermal Equilibrium (K. von Hagenow)	75
3.3.3 Correlation in Non-equilibrium (M. Feix, K. von Hagenow)	76
3.3.4 Correlations and Scattering Cross Section (W.H. Kegel, P.P.J.M. Schram)	76
3.4 Electrostatic Instability (H. Völk)	76
3.5 Thermalization by Coulomb Collisions (B. Lamborn)	76
3.6 Theory of the Resonance Probe (H.K. Wimmel)	77
3.7 The Adiabatic Approximation to the Motion of a Charged Particle	77
3.7.1 Motion in a Time-Constant Inhomogeneous Magnetic Field (P.P.J.M. Schram, H. Völk)	77
3.7.2 The Adiabatic Invariant for the Time-Dependent Harmonic Oscillator (G. Knorr, D. Pfirsch)	77
3.8 Thermal Deviations from the Holtmark Line Profile (H.K. Wimmel)	77

	Page
4. <u>Radiation and Waves</u>	77
4.1 Non-linear Plasma Optics	77
4.1.1 Coherent Scattered Light (W.H. Kegel)	77
4.1.2 Incoherent Scattered Light (A. Salat)	78
4.1.3 Light Mixing in Finite Plasma Volumes (A. Salat)	78
4.1.4 Emission of the Second Harmonic (A. Salat, A. Schlüter)	78
4.1.5 Direct Numerical Treatment (W. Lünow, A. Schlüter)	78
4.2 Interaction with Laser Radiation	78
4.2.1 Heating Plasmas with Laser Radiation (H. Hora)	78
4.2.2 Ionization of Gases by Laser Radiation (H. Hora, D. Pfirsch MPI)	78
4.2.3 Absorption Constants of Dense Plasmas (H. Hora)	79
4.3 The Harmonics of the Electron Cyclotron Frequency in Plasmas (E. Canobbio, R. Croci)	79
4.4 Dispersion at the Harmonics of the Cyclotron Frequency (B. Lamborn)	79
4.5 Electron Cyclotron Resonance Heating in a Plasma (H.K. Wimmel, K.H. Wöhler)	79
5. <u>Other Theoretical Work</u>	81
5.1 Gas Discharge Diode with Laser Anode (H. Hora)	81
5.2 Light Distribution in a Ruby Laser (H. Hora, B. Kronast, H.J. Kunze)	81
5.3 Scattering Coefficient in Stars (W.H. Kegel)	81
5.4 Knudsen Flow (R. Gorenflo, M. Pacco)	81
6. <u>Numerical Mathematics and Data Processing</u>	82
6.1 Evaluation of Spectroscopic Measurements (R. Gorenflo, H. Hora, Y. Kovetz, W. Lünow)	83
6.2 Investigations on Numerical Stability (O. Eder)	82
6.3 Interpolation (O. Eder)	83
6.4 Calculation of Plasma Density Profiles (O. Eder)	83
6.5 Numerical Solution of Differential Equations (O. Eder)	83
6.6 Training of Programmers (O. Eder)	83
6.7 Formulation of a Script (O. Eder)	83
6.8 Computer IBM 7090	84
6.9 Increasing the Input/Output Capacity	84
7. <u>Scientific Documentation of Plasma Physics (D. Hilsenbeck)</u>	85

ENGINEERING DEPARTMENT (DIPL.-ING. K.H. SCHMITTER)

1. <u>Summary</u>	86
2. <u>Planning Group (A. Knobloch)</u>	87
2.1 Project Supervision and Technical Clarification for the 1.5 (2.6)-MJ Capacitor Bank (A. Knobloch, H. Schlageter, in collaboration with Dept. 1)	87
2.2 Planning (A. Knobloch)	89
2.3 Elaboration of the Analogue Method ((J. Deleplanque), G. Herppich, A. Knobloch, H. Schlageter, F. Werner)	89
2.4 Plans, Design Principles and Mathematical Data for Dimensioning Discharge Devices (K.H. Fertl, A. Knobloch, H. Schlageter)	90
2.5 Experimental Bank (F. Werner)	92

	Page
2.6 Special Assignments ((J. Deleplanque), J. Mantel)	92
2.7 General Assignments in the Engineering Department (J. Mantel, H. Schlageter)	92
3. <u>Design Group</u> (G. Wulff)	92
4. <u>High-Voltage Group</u> (R.-C. Kunze)	95
4.1 Work relating to the 2.6-MJ Bank (J. Bäumlner, J. Gruber, R.-C. Kunze, G. Klement)	95
4.2 Magnetic-Field Bank for Dept. 1 (G. Klement, R.-C. Kunze)	97
4.3 Crowbar Bank for Dept. 3 (J. Gruber, G. Klement)	97
4.4 Crowbar Bank for Dept. 4 (R.-C. Kunze, E. von Mark)	98
4.5 Chargers for Capacitor Banks (J. Bäumlner)	98
4.6 Crowbar Spark Gap (R.-C. Kunze, E. von Mark)	98
4.7 Investigations of Pulse Ignitrons (J. Gruber)	99
4.8 Miscellaneous Work	101
5. <u>Electronics Group</u> (A. Steinhausen)	101
5.1 Power Sources	101
5.2 Measuring Amplifiers	103
5.3 Fast Control System (F. Skerjanc)	103
5.4 Slow Control System (W. Melkus)	103
5.5 Image Converters	104
5.6 Ruby Lasers	104
5.7 Other Diagnostic Tools	105
5.8 Transmitters	105
5.9 Maintenance (B. Heine)	106
6. <u>Magnetic-Field Group</u> (B. Oswald)	106
6.1 Intense Stationary Magnetic Fields (B. Oswald)	106
6.2 Water-Cooled Coils (H. Lohnert)	106
6.3 Coils for Hourglass Magnetic Fields (A. Kellerbauer, P. Krüger, B. Oswald)	106
6.4 Magnetic Field for Shock Tube (A. Kellerbauer, P. Krüger)	107
6.5 B-min Field (P. Krüger, B. Oswald, R. Pöhlchen)	107
6.6 Superconducting Coils (H. Lohnert, P. Krüger, B. Oswald)	107
6.7 Magnetic Energy Storage (B. Oswald)	109
6.8 Extreme Magnetic Fields (H. Lohnert)	111
6.9 Magnetic-Field Measuring Technique (A. Kellerbauer, P. Krüger)	111
7. <u>Vacuum and Technology Group</u> (H. Häglsperger)	111
7.1 Vacuum Technique	111
7.2 Low-Temperature Technique	112
7.3 Technology	113
7.4 Glass Technique (F. Zitzmann, K. Fritsch, W. Landgraf, R. Ehrlich)	114
8. <u>Installation Group</u> (M. Kottmair)	114
8.1 200-kV Accelerator of Dr. von Gierke's Department (M. Kottmair)	114
8.2 Chargers for Capacitor Banks 8-70 μ F, 20 kV and 4-8 μ F, 40 kV (M. Kottmair, W. Jakobus)	114
8.3 Rectifier 1000 V, 450 A for MPI, Institut für Extraterrestrische Physik (M. Kottmair)	115

	Page
9. <u>Special Physico-technical Group (E. Berkl)</u>	115
9.1 Symposium 1964 (E. Berkl)	115
9.2 Hard Superconductors (W. Amenda, E. Berkl)	115
9.3 Helium Liquefier (E. Berkl)	116
9.4 Random Sampling (R. Klockenkämper)	116
9.5 Frequency Modulation of Laser Light (E. Berkl, R. Klockenkämper)	116
10. <u>Chemistry Group (H. Weichselgartner)</u>	117
10.1 General and Routine Work (H. Weichselgartner, H.-J. Wittich)	117
10.2 Special Electroplating Processes (H. Weichselgartner, H.-J. Wittich)	117
10.3 General Material Testing (H. Weichselgartner)	117
10.4 Growing of Large Monocrystals (H. Weichselgartner)	117
11. <u>Central Workshop Group (H. Stoll)</u>	118
11.1 Mechanical Workshops (H. Stoll)	118
11.2 Carpentry Shop (W. Kaehs)	119
12. <u>Central Electrical and Electronics Workshops (J. Asenkerschbaumer, E. Hecht A. Simon)</u>	119
 <u>MANAGEMENT AND ADMINISTRATION</u>	
1. <u>Personnel Development</u>	121
2. <u>Construction Work</u>	121
3. <u>Organizational and Financial Development</u>	125
<u>Laboratory Reports</u>	129
<u>Publications</u>	133

EXPERIMENTAL PLASMA PHYSICS 1 (PROF. DR. FÜNFER)

1. Summary

a) Theta Pinch

In 1964 the Department concentrated attention more than ever on the field of the linear theta pinch. Available in addition to a few small banks used mainly for diagnostic purposes were two banks with energies of 30 kJ and 80 kJ respectively. At the present time the 1.5/2.6-megajoule bank is still at the technical testing stage.

Experiments with the 30-kJ bank served first of all for providing comparisons with calculations obtained by the three-fluid theory. Previous measurements of electron density and magnetic-field distribution do not afford any satisfactory conclusion as to the suitability of this model and were supplemented by spectroscopic temperature determinations from line intensities of additional components. Moreover, the electron density and temperature were established from light scattering measurements with a pulsed 5-MW ruby laser. Within the relatively wide, experimental margins of error agreement was satisfactory. In order to provide a further comparison with theory an experiment was conducted to find the ion temperature by measuring the line profiles of additional components. For this purpose a special installation comprising monochromator and Fabry-Perot interferometer with a system of concentric ring mirrors was used.

With antiparallel, trapped magnetic fields macroinstabilities were observed. These consisted in the plasma cylinder breaking up into separate rings. These instabilities are particularly pronounced when perturbations, such as are caused by probes, probe ports and the like, are present in the discharge vessel. If the wall of the discharge vessel is smooth the formation of water films on the wall as a result of previous discharges is responsible for the break-up. With appropriate treatment beforehand this effect could largely be eliminated. The rates of growth of these instabilities could be better accounted for in terms of resistive diffusion than in terms of the times postulated in theory for tearing-mode instabilities.

With the appreciably faster 80-kJ bank it was possible at initial pressures as low as 3μ to reach relatively high ion temperatures. With antiparallel fields neutron bursts were mostly symmetrical to the field distribution. With $B_0 = 0$ the neutron maximum precedes the maximum of the compressing field. This premature decrease was probably due to end losses since the plasma was macroscopically stable. Estimates of the ion temperatures were obtained by three methods: from the total neutron emission, from the equilibrium radius and from the kinetic energy of the ions on the first compression, assuming a subsequent adiabatic compression. Values of 1 - 2 keV were obtained for T_i . Electron temperatures of between 100 and 400 eV were determined from absorption measurements of the soft X-radiation and from continuum measurements with an X-ray spectrometer in the region of $8 - 14 \text{ \AA}$. With antiparallel fields in particular, a rotation of the plasma with a frequency of a few Mc/s was found towards the end of the half-cycle. Even with no trapped field a rotation of even higher frequency was occasionally observed.

Preionization with the aid of a fast theta pinch discharge showed remarkable behaviour as a function of the filling pressure. In a certain pressure range the plasma cylinder oscillates in phase with the magnetic field, which results in periodic contact with the wall and thus gives rise to impurities. In other pressure ranges the plasma cannot follow the time variation of the force and with approximately constant diameter remains clear of the wall, the result being a lower percentage of impurities.

Construction of the 1.5/2.6-megajoule bank was sufficiently far advanced to allow a start on technical tests toward the end of the year. The properties of the z-pinch preionization had previously been investigated in the original discharge vessel.

The three-fluid model was improved in several respects. Cases with antiparallel fields and fieldless plasma can now be calculated as well. Moreover, much better constancy of the total mass of the plasma was attained. In addition, the degree of ionization was calculated more accurately and the influence of impurities investigated. Detailed treatment of the energy contributions, i.e. the kinetic energy of the plasma and the thermal energy of ions and electrons, showed that up to the first compression the influence of impurities and radiation losses on kinetic and thermal energy is remarkably small.

Theoretical consideration was given to the extent to which the kinetic energy of particles can be raised by reducing the initial particle density n in the theta pinch. The various pinch models all show an increase in the particle energy of $1/\sqrt{n}$. This still does not take into account the question of thermalization. Theoretical and experimental results with the turbulence heating investigated by Babykin et al. would seem to indicate, however, that thermalization may be expected in a collisionless plasma as well. It is thereby assumed that, as a result of two-stream instabilities, waves are excited which enter into non-linear interaction and on being absorbed raise the thermal energy of the plasma. An attempt is being made to transfer these results to the case of the theta pinch with very low initial density. In this connection experiments were conducted to try and verify ideas on space-charge coupled electron and ion oscillations of a low-density non-diamagnetic plasma.

In order to devise ways of reducing end losses, a start was made to calculating vacuum cusp fields at the ends of the linear theta pinch.

b) Preionization Methods for the Theta Pinch

Due consideration was given to the decisive role of good preionization in the case of the theta pinch by investigating a series of preionization methods. First a fast theta pinch predischARGE was investigated, then a linear z-pinch discharge and finally plasma injection with conical z and theta pinches. Work was also begun on photoionization by means of the UV radiation from gas discharges. A z-pinch preionization was chosen for the megajoule experiment also because it breaks down right to the lowest initial pressures.

c) Other Plasma Configurations

Theoretical considerations of the magnetohydrodynamic equilibrium between an external magnetic field and a field-free plasma for plane geometries were concluded. For the special case of the two-dimensional M+S torus, the so-called Quasilimus, analytical solutions were obtained and compared with experimental results.

An antipinch for producing shock waves was constructed and the distribution of the electron density gradient in the shock front investigated with a differential interferometer. This yielded appreciably higher density gradients than those measured with magnetic-field probes.

d) Diagnostics

Substantial progress was achieved by further development of the light scattering method. By introducing a multiple slit comprising glass-fibre bundles it was possible to carry out simultaneous measurement from 7 wavelengths of a scattered-light spectrum. In the transition region between Thomson scattering and the region where collective effects are encountered the occurrence of satellite lines could be shown for the first time. It was also possible

to verify the central line, but without spectral resolution. An apparatus enabling the spectrally resolved central line to be measured for very small scattering angles has been developed and is to be used for measuring the ion temperature.

With the aid of the Doppler effect in a travelling-wave Kerr cell it was possible to shift the frequency of the ruby laser line so as to put the difference frequency in the range of the plasma frequencies.

Progress was made in the construction and testing of differential interferometers, electric double probes, piezoelectric probes, detectors for infra-red radiation, methods of measuring line profiles with image converter and multiplier, spectroscopic measuring devices, pulsed neutron sources and electronic measuring devices.

In 1964 there were 21 regular scientific staff members, 3 guests from abroad, 8 doctorate candidates and 6 diploma candidates.

2. Theta Pinch

2.1 Theta Pinch I (H. Herold, G. Decker, M. Kornherr, F.L. Ribe⁺, H. Röhr)

Data of installation:

Bank for bias magnetic field:

$$C = 200 \mu\text{F}, U_o \text{ max} = 10 \text{ kV}, T = 55 \mu\text{sec}, \text{ crowbar in field maximum.}$$

Bank for preionization (across the theta pinch coil):

$$C = 1.6 \mu\text{F} (3.2 \mu\text{F}), U_o = 25 \text{ kV}, T = 1.7 \mu\text{sec}, \text{ additional RF cable discharge}$$

Main bank:

$$E = 80 \text{ kJ}, U_o = 40 \text{ kV}, B_{\text{max}} = 100 \text{ kG}, T = 5.3 \mu\text{sec.}$$

Coil:

30 cm long, 7.1 cm in diam.

In the discharge vessel a base pressure of about $5 \cdot 10^{-8}$ torr can be achieved after baking. At the beginning of the discharges the degree of impurity of the filling gas due to the leak rate and the filling time is $< 5 \cdot 10^{-4}$ (vol/vol) at 10μ filling pressure. After the first half-cycle a vacuum switch in parallel with the coil takes roughly half of the total current. In this way the stress on the discharge vessel in the following half-cycles is appreciably reduced.

The installation was put into service in the middle of the year. The results of investigations so far can be summarized as follows: success was achieved in producing a hot, neutron-emitting deuterium plasma ($10^6 - 10^7$ neutrons per discharge) which is stable at least over the greatest part of the half-cycle. The electron temperatures lie between 100 and 400 eV, depending on the experimental conditions, and the ion temperatures are estimated at between 1 - 2 keV. The degree of purity of the plasma is still unsatisfactory.

Below are a few details relating to the measurements:

a) A few properties of the preionization discharge were investigated. Measured from the ratio of continuum to $D\beta$ line intensity, the electron temperature is about 0.5 eV at 20 and 60μ filling pressure. The concentration of oxygen impurities as measured from O II line intensities by the addition of oxygen and by extrapolation was a minimum of about 0.35 %. Noteworthy is the dynamic behaviour of the predischage as a function of pressure and bias field. End-on streak photographs and the observation of O II line intensities indicate the following interpretation: in certain pressure ranges (e.g. 20 - 40μ , D_2) the plasma cylinder oscillates roughly in phase with the sinusoidally decreasing magnetic field or in phase with every second half-cycle (Fig. 1 c and 1 b). Because of successive contacts with the wall this gives rise to strong impurity concentrations. In other cases (e.g. at 60μ and $B_o = 0$) the plasma cannot follow the time variation of the force and remains confined in a plasma cylinder of approximately constant diameter, clear of the vessel walls (Fig. 1 a). Impurities are therefore not so pronounced. Accordingly, the properties of such frequently applied radio-frequency predischarges vary intensely with pressure and appropriately modify the behaviour of the main discharge.

⁺ Guest from Los Alamos, USA

b) The purity of the main discharge was determined from time-integrated spectra and observations of line intensities. The time-integrated spectrum shows only oxygen and silicon lines. No carbon lines could be detected. The oxygen content of the discharge was mostly 1 % and with antiparallel bias field ($B_o = 1k$) was greater than for $B_o = 0$. The observations were conducted on an O II line (4075 \AA) and with an X-ray spectrometer on an O VIII line (15.18 \AA). On addition of O_2 the intensities of both lines varied in proportion.

c) Neutron emission was established both for $B_o = 1k$ and $B_o = 0$ in the first half-cycle of the main discharge. In both cases the yields attain a maximum at relatively low pressures (Fig. 2). Fig. 3 shows the dependence of the mean neutron yield on various bias fields. The neutron burst commences on the 2nd - 3rd compression of the plasma and for $B_o = 0$ attains its maximum prior to the maximum of the compressing field. For $B_o = -2 k\Gamma$ the burst is mostly symmetrical to the field. As streak photographs of the plasma at $B_o = 0$ usually show a macroscopically stable plasma column, the early decline of the neutron burst at $B_o = 0$ can be explained in terms of end losses. No displacement of the burst maximum at various pressures ($3 - 60 \mu$, D_2) and $B_o = 0$ could be detected. The resulting assumption that the rates of loss are independent of the filling pressure is to be checked by interferometric investigations.

d) At $B_o = 1k$ streak photographs show (stereoscopically as well) in the last third of the half-cycle a rotation of the plasma with a frequency of 4.5 to $2 \cdot 10^6$ c/s. At $B_o = 0$ as well a rotation of higher frequency (about $6 \cdot 10^6$ c/s) can occasionally be detected.

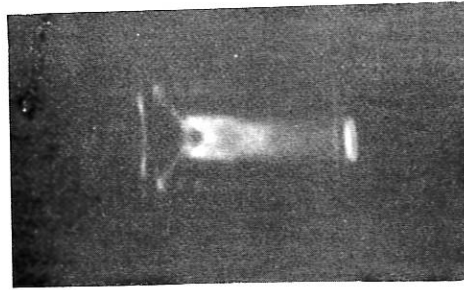
e) An X-ray spectrometer was used in end-on observation at 40μ , D_2 and $B_o = -2 k\Gamma$, with and without oxygen added. A KAP crystal ($2d = 26.56 \text{ \AA}$) was used as analyser crystal and a plastic scintillator as detector. The continuum radiation was measured in the interval from $8 - 14 \text{ \AA}$. The measurements without oxygen added gave values of 360 eV for T_e , while with 10 % oxygen added a value of 155 eV was obtained (Fig. 4). An O VIII line (L_{γ} at 15.177 \AA) was measured. With the given resolution of the spectrometer, which is determined by the Soller collimator, it is not possible to establish the true line width at the ion temperature concerned.

f) An estimate of the ion temperature was made for the cases $B_o = -4 k\Gamma$, $p_o = 60 \mu$, D_2 and $B_o = 0$, $p_o = 10 \mu$, D_2 by three different methods: from the equilibrium radius at the time of the field maximum (assuming $\beta = 1$), from the neutron yield and from the kinetic energy of the ions at the first compression, assuming the succeeding compression to be adiabatic. The estimate gives for T_i values between 1 and 2 keV.

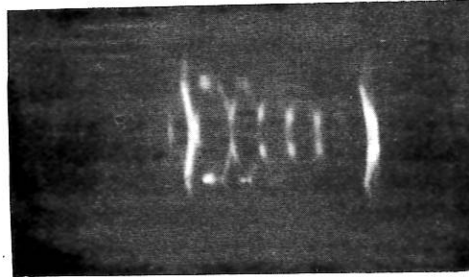
g) With a laser beam of approx. 1-MW radiation power pulsed by a Kerr cell, scattering measurements were carried out at 90° to the direction of incidence. At low filling pressure (10μ) there was definite evidence of a scattering signal. The poor reproducibility of the scattering signal, however, does not allow a spectrum to be measured point by point in successive discharges. At higher filling pressures (up to 60μ D_2) there was no longer definite evidence of the scattering signal. This is due to the bremsstrahlung of the plasma which increases with n^2 (scattered light $\sim n$). That is, the ratio of scattered light to plasma light is appreciably poorer at higher electron densities.

MAIN DISCHARGE

a) $P_o = 60 \mu$
 $B_o = 0$



b) 20μ
 $B_o = -2k \Gamma$



c) 10μ
 $B_o = 0$

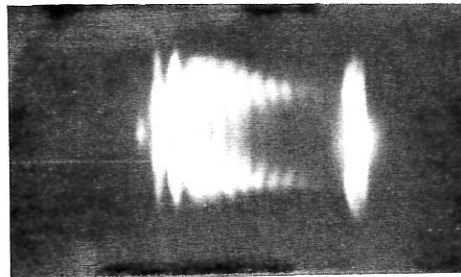


Fig. 1: End-on streak photographs of the predischARGE

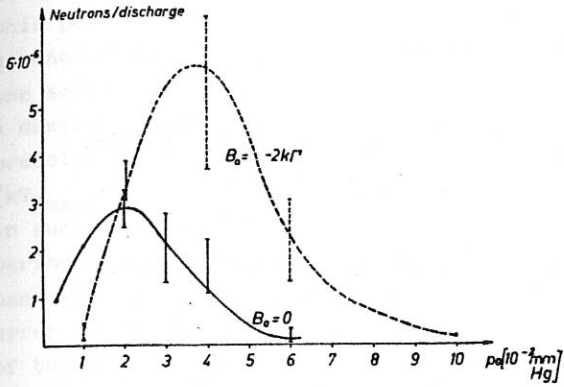


Fig. 2 Neutron yield as function of filling pressure

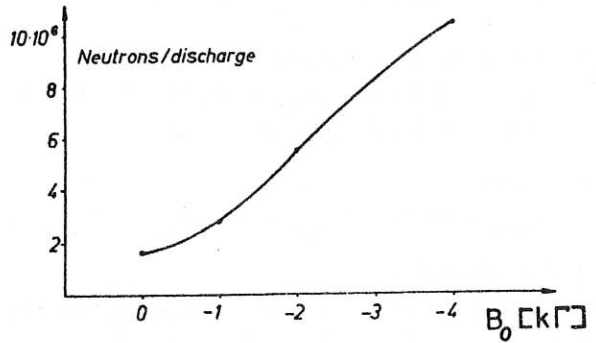


Fig. 3 Neutron yield (mean values) with various antiparallel bias fields - B_0 , $p_0 = 4 \cdot 10^{-2}$ mm Hg, D_2

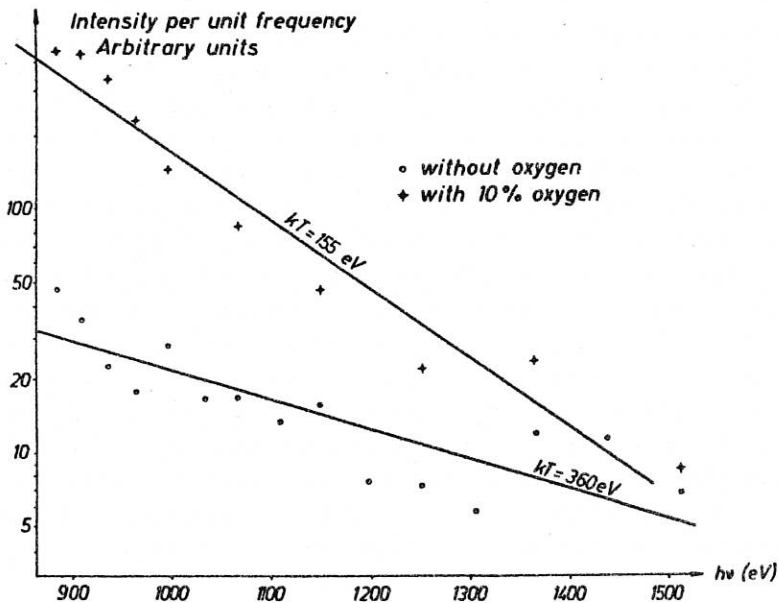


Fig. 4 Spectral dependence of the continuum with and without oxygen

2.2 Theta Pinch II (A.Eberhagen, M.Bernstein, H.Glaser, H.Griem⁺)

Data of installation:

Bank for quasi-stationary magnetic field:

$$W_{\max} = 8.1 \text{ kJ}, U_{\text{omax}} = 2.5 \text{ kV}, T = 260 \mu\text{sec}, 0 \leq B_{\text{omax}} \leq 7 \text{ kG}.$$

Bank for preionization:

$$W_{\max} = 0.6 \text{ kJ}, U_{\text{omax}} = 25 \text{ kV}, T = 2.0 \mu\text{sec}, B_{\max} = 6.7 \text{ kG}, dB/dt = 2.2 \cdot 10^{10} \text{ G/sec.}$$

additional RF cable discharge.

Main bank:

$$W_{\max} = 41 \text{ kJ}, U_{\text{omax}} = 50 \text{ kV}, T = 6.4 \mu\text{sec}, B_{\max} = 68 \text{ kG}, dB/dt = 6.7 \cdot 10^{10} \text{ G/sec.}$$

Theta pinch coil:

$$\text{Length} = 30 \text{ cm}, \text{minor diameter} = 5.4 \text{ cm.}$$

After critical examination it turned out that the results of the measurements of electron density distribution and magnetic-field distributions described in the annual report of the IPP for 1963 do not justify on their own any conclusions as to whether the three-fluid theory developed describes adequately the behaviour of the plasma in the main discharge of a theta pinch. No statement on this point will be forthcoming until additional measurements of the plasma temperature have been completed. Attempts were therefore made to obtain experimental data on this subject in the three ways indicated in the first three sections following. The last three sections then proceed to describe investigations of the behaviour of the entire plasma column - particularly with antiparallel, trapped magnetic fields - , the search for causes of macroinstabilities encountered also being of major importance.

a) Spectroscopic temperature determination by measuring line intensities.

For the temperature ranges to be expected with the present theta pinch discharge this method relies on the emission lines of components added to the hydrogen plasma. Carbon, less than 0.03 % of which is contained in pure H plasma, is particularly well suited as a temperature indicator for such measurements since it has emission lines of higher ionization levels in the wavelength range between 2200 Å - 2600 Å, still relatively feasible from the experimental standpoint. An estimate of the occurrence of these emission lines showed, however, that their relaxation times at the beginning of the discharge are comparable with or greater than the variations with time of the plasma parameters (kT_e and n_e). At the earlier stages of the discharge, especially during the implosion phase, it is therefore no longer possible to determine the temperature distribution by simple means from the line intensities obtained. The three-fluid model was therefore extended by the addition of carbon, whereupon it afforded also the spatial occurrence of carbon lines at the various times (v. 2.4). These were to be compared with the C line distributions obtained experimentally. With 0.7 % carbon added the intensity distributions of the following C lines were measured: CII (2509 Å + 2512 Å), CIII (2297 Å), CIV (2524 Å), CV (2271 Å). The said comparison of these lines with the statements of the three-fluid theory has not yet been concluded.

For the later times ($t \approx 0.7 \mu\text{sec}$) the determination of the plasma temperature from the line intensities in the case investigated: $p_{\text{H}_2} = 0.15 \text{ torr}$, $B_{z0} = 0.8 \text{ kG}$ is simplified as a result of the simultaneous occurrence of the CIV (2524 Å) and the CV (2271 Å) lines and by the fact that the plasma parameters (kT_e and n_e) vary more slowly here than the relaxation times of these lines. Because of the uncertainties involved in the cross sections used, however, the range of error for the temperature data thus obtained (Fig.5) for these later times extends roughly from + 100 % to - 35 %.

+ Guest from the University of Maryland

b) Local determination of the plasma temperature with a laser.

In order to provide temperature data for the earlier times as well, profile measurements of the laser light scattered at 90° were conducted on the theta pinch discharge. For this purpose a pulsed ruby laser (output 5 Mwatt, pulse duration 30 nsec) was used, while a monochromator with glass-fibre bundle wavelength resolution (v. 6.1) served to record the scattered light profile. The results were as follows: 1) At the first maximum compression a maximum electron temperature of 20 - 25 eV was obtained; 2) At the second maximum compression $(kT)_{\max} = 25 - 30$ eV; 3) At the moment of maximum plasma temperature ($t = 1.4 \mu\text{sec}$): $(kT)_{\max} = 50$ eV (Fig. 5) [44]. It was possible here to obtain the radial temperature profile in successive discharges by focusing the laser beam on a volume in the region of 0.5 mm^3 at various distances from the discharge axis. Because the radiation power of the laser beam used was relatively weak for the purposes of the present investigation, the experimental error for a single temperature determination was approximately $\pm 50\%$. For the later times of the theta pinch discharge, for which temperature data from both spectroscopic measurements and measurements of scattered laser light are now available, the values in each case fall within the common range of error.

In these measurements it was possible, moreover, to obtain data on the electron density distribution from the profile of the scattered laser light, in addition to data on the radial temperature distribution. Satisfactory agreement with previous spectroscopic results was achieved here as well within the experimental margin of error.

c) Measurements of line profiles.

With regard to the comparison with the three-fluid theory it appeared desirable to supplement the experimentally obtained electron temperature distributions with data on the ion temperature. This is to be done by determining the profiles of those emission lines of additional components for which the pressure broadening in the case of the present plasma parameters is less than the Doppler broadening. The measuring equipment designed for this profile determination makes use of a monochromator for the spectral pre-selection and then a Fabry-Perot interferometer for producing the line profile. At the suggestion of J.G. Hirschberg spectral separation of the resulting interference fringe into individual rings was undertaken for the purpose of separate, photoelectric recording by a system of concentric ring mirrors. In the process the major diameter of each single mirror joins up with the minor diameter of the next and by means of alternating alignment of its normal in relation to the optical axis: Fabry-Perot to interference fringe, each individual ring mirror reflects in a different direction the spectral amount of the total profile impinging on it. Concave mirrors then serve to focus the intensity quantities on the individual photomultipliers. The selection of emission lines of additional components used hitherto for these investigations: CIV (5801.5 \AA), NV (4603 \AA), OVI (3811 \AA) made possible during the discharge a profile measurement from about the time of the first maximum compression ($0.4 \mu\text{sec}$) up to $t \approx 1.0 \mu\text{sec}$. In general, the line profiles obtained were not only determined by the thermal Doppler broadening, but also broadened to a great extent by directed velocity components of the plasma. More exact evaluation of measurements thus far available is being carried out at present.

d) Observations of macroinstabilities in the theta pinch.

Previous investigations have already shown that with antiparallel, trapped magnetic fields the plasma column tends to break up along the discharge axis into separate rings. In order to establish possible causes of such macroinstabilities, a discharge coil of perforated sheet copper was used and the axial behaviour of the plasma column observed with a streak image converter [20; IPP 1/27]. In this way the following causes of macroinstabilities

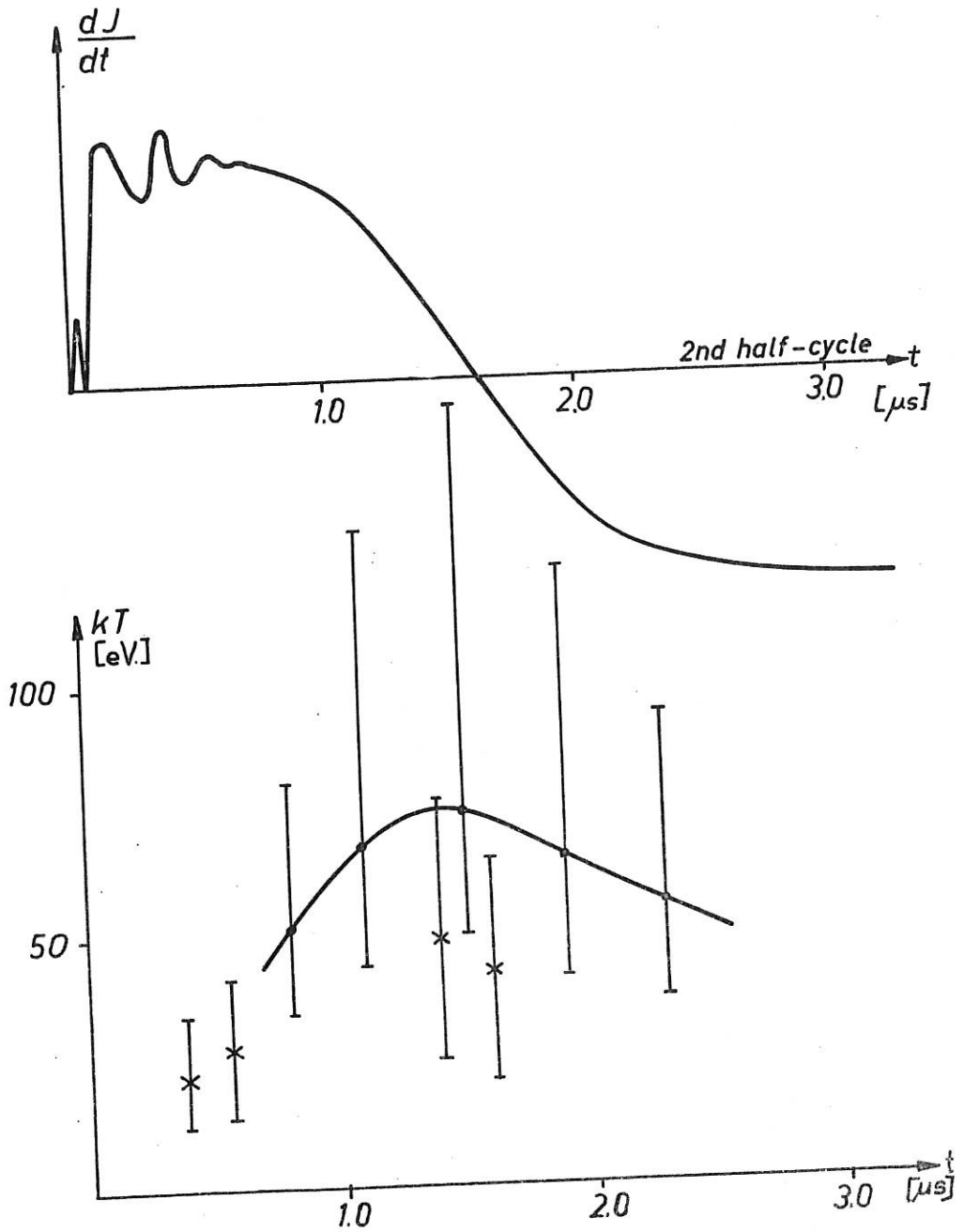


Fig. 5: Temperature measurements on Theta Pinch II
($B_{z0} = 0.8 \text{ kG}$, $p_{H_2} = 0.15 \text{ torr}$)

- a) From emission lines CIV (2524 Å) and CV (2271 Å) : ———
b) From profile measurements of scattered laser light: x

were found: a) If a port of quartz glass, such as is used, for instance, in magnetic-field measurements for protecting the probe coil, projects into the plasma, the plasma column breaks up into two parts at the point of perturbation immediately after the first maximum compression. b) A similarly pronounced break-up of the plasma column was also detected when the quartz port projecting into the plasma was replaced by a side pocket projecting from the discharge vessel. c) When smooth discharge vessels were used individual plasma rings did not form till later, their number and place of origin varying from discharge to discharge. It was also possible to eliminate these macroinstabilities, namely by means of a preceding discharge with parallel, trapped magnetic field. It was found that this after-effect of a discharge on the following one was caused by the formation of water as a result of the reaction of the hot plasma with the oxygen from the SiO_2 structure of the vessel wall. By simple pumping this water could be removed only partially from the walls and was absorbed again as an impurity by the plasma of the next discharge. By means of the said pretreatment it was possible to produce a plasma with antiparallel, trapped magnetic field that was macroscopically stable up to the maximum B_z field. In these investigations the times up to the break-up of the plasma column into separate rings could be better accounted for by resistive diffusion times than by the tearing-mode resistive instability times according to the theory of H.P. Furth, J. Killeen and M.N. Rosenbluth.

e) Measurement of electron density distribution along the discharge axis.

The behaviour of the plasma column was determined qualitatively by means of streak photographs and at the same time measurements were made of the electron density along the discharge axis. As described in the annual report of the IPP for 1963, radially resolved measurements of continuum intensities were made for the purpose, but this time through observation slits at various distances from the midplane of the coil and outside the actual discharge coil. Measurements were made both with parallel ($B_{z0} = 0.8 \text{ kG}$, $p_{\text{H}_2} = 0.15 \text{ torr}$) and antiparallel ($B_{z0} = -2.3 \text{ kG}$, $p_{\text{H}_2} = 0.10 \text{ torr}$), trapped magnetic fields. Evaluation of the extensive measurement data is at present being done on the IBM 7090 in collaboration with the Data Processing Group. The latter was also responsible for compiling the necessary computing programmes for the further processing of measurement values obtained, computing the profile across the discharge cross section from the signals of the individual photomultipliers, approximating this stepped intensity distribution by smooth curves, solving the Abel-type integral equation and converting the radial continuum distribution into electron densities. In this connection tables for evaluating intensity measurements of hydrogen plasmas were also compiled [IPP 1/23; IPP 6/20].

2.3 Theta Pinch 1.5 / 2.6 MJ (C. Andelfinger, A. Eberhagen, M. Ulrich, R. Wunderlich)

In the course of the year the collector system for the large theta pinch (150-cm coil length at 180 kG) was completed by the Engineering Department. After a sixth of the collector was installed in summer initial attempts were made to put into service one-sixth of the bank operating at a voltage of 30 kV. It was then found necessary to make minor changes on the spark gaps, which then gave the desired maximum scattering time of 30 nsec for the spark gaps. Moreover, the Hall probes, the purpose of which is to monitor the installation, had to be taken out of the bank and removed to a room at some distance because their signals were being subjected to interference caused by the magnetization of metal parts in the installation. In the week preceding Christmas attempts to put sections of the installation into service were resumed.

Meanwhile, investigations on the preionization were set in progress. The continuum and $H\beta$ intensities were measured, resolved in time and space. In initial experiments with a 3-m long z-pinch, which was short-circuited at the time of the first maximum compression, an ionization level of approx. 15 % and an electron temperature of approx. 0.5 eV were obtained. More recent experiments with the original discharge vessel and preionization bank point to a higher degree of ionization, particularly at lower pressures ($< 10^{-1}$ torr). Precise evaluation is now in progress.

In the meantime, various diagnostic instruments have been prepared for the experiments to be conducted on the device.

2.4 Pinch Dynamics (D. Düchs)

a) Numerical methods used in the evaluation of the three-fluid model for pinch dynamics have now been improved to such an extent that cases of antiparallel, trapped B fields or the case without trapped B field can also be calculated. Moreover, the total mass remains constant at less than 0.5 % during the calculation. (Previous numerical methods involved deviations of 20 - 30 %)

b) The practice hitherto has been to use ionization and recombination coefficients derived on the assumption that the plasma is optically thin for all excitation lines. For the Lyman α line at least, however, the plasma is practically always optically thick. With the collaboration of Prof. H.R. Griem the degree of ionization in the three-fluid programme was therefore calculated more accurately.

c) The influence of oxygen and carbon impurities was investigated, again in collaboration with Prof. H.R. Griem. For this purpose the differential equations for determining the individual degrees of ionization had to be calculated together with those of the three-fluid model.

Detailed consideration of the energy contributions (kinetic energy of the plasma, thermal energy of the ions and electrons) shows that up to the first compression not only the kinetic, but also the thermal energy of the plasma is influenced relatively little by ionization of impurities and radiation losses.

d) Comparisons of calculation results from the three-fluid model with those from simpler models, such as the snowplough, afford an estimate of the quantitative usefulness of these simple models.

An account of work in progress was given in Jülich, February 1964 and in Varenna, October 1964.

2.5 Theoretical Studies of the Behaviour of a Theta Pinch at Extremely Low Plasma Density

(R. Chodura)

a) Breakdown mechanism of a theta pinch discharge

Taking as a basis the mechanism, dealt with briefly in the last annual report, of the space-charge coupled motion of electrons and ions in a time-varying magnetic field, ionization in a theta pinch discharge was discussed for various time dependences of the magnetic field. An account of the results was given at conferences of the Group de Liaison, Jülich, February 1964 and of the Fachausschuss für Plasmaphysik of the Deutsche Physikalische Gesellschaft,

Karlsruhe, March 1964, and these were published along with previous results relating to ionization at fairly low electron densities [16; IPP 1/21].

b) Coupled electron-ion oscillations of a collisionless, cylindrical plasma column in an axial magnetic field.

The object here was to verify in a separate experiment the non-linear oscillations mentioned in a) by measuring with the aid of a microwave interferometer the density changes occurring. For this purpose calculations were made to find the most favourable dimensions for the experiment.

c) Heating a collisionless plasma in the theta pinch

Simple models of magnetic compression in the theta pinch show that both the kinetic energy per particle of the azimuthal electron current W_e and the kinetic energy per ion W_i of the radial motion at the time of the first compression is of the order

$$W_e \sim W_i \sim \sqrt{\frac{m_i}{n}} \cdot E,$$

where m_i stands for the ion mass, n for the initial density of the plasma and E for the azimuthal field strength at the boundary of the evacuated vessel. A decrease in the initial density n of the plasma would accordingly cause an increase in the particle energy. More recent investigations by M.V. Babykin and colleagues of so-called "turbulence heating" have shown that it should be possible to thermalize such directed particle energies quickly and effectively in a collisionless plasma as well. The theoretical explanation for this turbulence heating assumes that electron plasma oscillations increasing exponentially with time as a result of the directed electron motion (two-stream instability) are excited. These enter into non-linear interaction giving rise to new oscillations, which may in some cases be stable and can in turn be absorbed by the plasma particles owing to Landau damping. The time scale of thermalization should be given roughly by $(m_i/m_e)^{1/3} \omega_{pe}^{-1}$, (ω_{pe} = electron plasma frequency), its efficiency being given experimentally as ~ 0.2 .

With regard to this possibility of thermalization the production of the directed particle energy was investigated in various density ranges, namely for the coupled or uncoupled motion of ions and electrons in a homogeneous magnetic field increasing with time and for compression with conservation of magnetic flux in the plasma, according to the free-particle and snowplough models. Moreover, a start was made to investigations of the collisionless compression of the plasma in more general conditions by numerical treatment of the relevant magnetohydrodynamic equations.

d) Resistive instabilities in the theta pinch

In connection with observations of the break-up of the plasma column in theta pinch discharges with antiparallel, trapped magnetic fields, it was discussed whether these phenomena can be interpreted as tearing-mode instabilities according to the theory of Furth, Killeen and Rosenbluth. The experimental data and data of the said theory are compared in the laboratory report [IPP 1/27].

2.6 Experimental Investigations of the Collisionless Compression of a Low-Density Theta Pinch Plasma (P. Igenbergs)

As part of these investigations it was attempted to verify theoretical results relating to the space-charge coupled electron and ion oscillations in a low-density non-diamagnetic plasma by measuring with the aid of microwaves the density fluctuations involved.

Experimental conditions:

- a) The neutral-gas density has to be so low that during the measurement time the charged particles do not collide. This gives as condition for the density $n < 1.5 \cdot 10^{11} / \text{cm}^3$.
- b) The magnetic field within the coil should be homogeneous.
- c) The plasma should be "cold" and homogeneously distributed at the start of the theta pinch discharge.

Hitherto, two methods have been adopted for ionizing the H_2 gas, a) by means of theta pinches of various electrical data, b) by means of a z-pinch. With theta pinches it was found that in the pressure range specified above the pinches do not break down ($p_0 < 4 \cdot 10^{-3}$ torr).

The use of a z-pinch for ionization made it possible to lower the pressure range appreciably. In order to curtail the breakdown delay, auxiliary electrodes were introduced into the vessel which generate a spark in front of the z-pinch by point discharge. Investigations with the z-pinch have not yet been concluded.

2.7 Vacuum Magnetic Field in Theta Pinch Coils and Cusped Geometries (F. Pohl)

Current distribution and magnetic field in theta pinch coils of finite length with an observation slit perpendicular to the coil axis were calculated numerically. Only azimuthal surface currents were taken into account; under these conditions the magnetic flux through the coil is constant and the coil behaves like a bunch of insulated wire rings whose inductances bring about the current distribution

The magnetic field was calculated from the current distribution; results are given in [IPP 1/31].

In addition, current distribution and magnetic field were calculated for the following systems:

1. Two identical coils separated by a slot for the following two cases:
 - 1a. when one of the coils is short-circuited and
 - 1b. when the voltages in the two coils are equal but opposite (cusped geometries).
2. A coil separated from a disc by a slot
 - 2a. Added to geometry 2. are two coaxial DC-carrying rings, whereby a cusped magnetic-field configuration is attained in the half-cycle when the coil current flows antiparallel to the current in the rings.

2.8 Brightness Distribution along the Axis of a Theta Pinch with Unperturbed Coil

Geometry (E. Glock, K. Hübner)

In end-on observations on the theta pinch results are integrated over the entire coil length. In order to observe the axial distribution it is a frequent practice to use coils which are slotted or perforated, but these give rise to uncontrollable field distortions. The use of a plate-type light conductor in the collector slot enabled the coil axis to be reproduced on the slit of the spectrograph and its spectra to be recorded with an image converter shutter.

Electrical data:

$$C = 17.6 \mu\text{F}, U_0 = 24 \text{ kV}, \tau = 6.5 \mu\text{sec.}$$

Data of the coil:

$$L = 100 \text{ mm, diam.} = 50 \text{ mm, filling gas being } N_2 \text{ with } p_0 = 300 \mu.$$

The photographs were taken in the first half-cycle and show that

- the plasma remains a few cm short of the ends of the coil,
- the N III lines (2 - 5 eV) occur only in the middle quarter of the coil, the N II line (1 - 3 eV) only in the middle half and the brightness along these lengths is uniform,
- the continuum is luminous only during the most powerful compression and then only unevenly along the middle quarter of the coil.

The experiments are being continued.

2.9 Preionization in the Theta Pinch

2.9.1 z-Pinch Preionization (R. Wunderlich)

As of May the spectroscopic measurements on the long z-pinch (preionization for 2.5-MJ theta pinch) were continued. Image converter photographs had shown at which times the bank, depending on the filling pressure in the vessel, has to be crowbarred in order to produce a fairly stable homogeneous plasma. Electron density and electron temperature should then be measured in the conditions thus obtained. The intensity of the $D\beta$ line (4861 Å) and of the continuum in an adjacent wavelength band (4976 Å) was measured, resolved in time. Observations for this purpose were made axially at three different radii ($r = 0$, $r = 1.5$ cm, $r = 3.5$ cm). Such small values ($T_e < 0.5$ eV, $N_e < 5 \cdot 10^{14} \text{ cm}^{-3}$) for temperature and density were obtained on evaluation that the assumptions (local thermal equilibrium) used as a basis are no longer valid. For calculating the degree of ionization consideration has to be given rather to the primary processes of ionization and recombination. The relevant calculations are now in progress.

Finally, some comment should be made on the degree of impurity. In side-on observation a time-integrated spectrum showed impurity lines of O_2 , Cu, Zn, C and Si.

Time-resolved observations gave no indication of axial diffusion of electrode material. The impurities are released from the wall surface and excited immediately after breakdown.

2.9.2 Conical z-Pinch as Preionization Method (C. Andelfinger, E. Glock, R. Wunderlich)

A conical z-pinch comprising a plate and a ring electrode and operated with 38.5 μF at 18 kV with an 8 μsec cycle propels a plasma cloud into a tube 1000 mm long and 100 mm in diam. The turbulence of the resulting flow does not allow reliable spectroscopic determination of temperature and density and excludes this as a method of preionizing a theta pinch.

This flow was examined by photographing helium discharges with narrow-band filters and image converter shutter in the light of HeI (4471.48 Å) and of HeII (4685.75 Å). Superimposed on the measurement values of the flow velocity was a statistical component, which was eliminated by averaging out.

Variation of the pressure and loading capacity and also assessment of the photographs gave the following results:

- a) The tendency toward turbulent flow increases with the electric energy and decreases with rising initial pressure.
- b) A shock wave does not occur in the investigated range $p_0 = 80 + 300 \mu\text{He}$. The front boundary of the plasma has the form of a paraboloid, the hottest point being the tip.
- c) The flow in the tube is produced solely by the first compression of the pinch. Its velocity is proportional to $[dJ/dt]_{\text{max}} \cdot M^{-1/4}$ ($M = \text{mass density}$).

The investigations were discontinued at this stage.

2.9.3 Preionization by UV Radiation (G. Hofmann)

For heating experiments on the theta pinch it is intended to produce by photoionization a fieldless initial plasma which is as homogeneous and highly ionized as possible.

As the photoionization cross section of hydrogen decreases rapidly at $1/\omega^3$, from the longwave limit (800 Å), and the cold plasma thus produced recombines within a very few microseconds, it is necessary to produce within a time not exceeding this recombination time a very intensive radiation pulse just below 800 Å. For this wavelength band there are no practicable windows and so the separation of the UV source from the hydrogen volume to be ionized should be performed dynamically.

In a first phase the discharge vessel of a z-pinch is filled for a short time with a suitable luminous material of high density; in a second phase a fast high-voltage z-pinch heats the luminous material (data of the z-pinch: 120 kV, 6 kJ, $f \approx 500$ kc/s). The hydrogen volume to be ionized is contained in a tubular attachment perpendicular to the z-pinch.

With inductance being kept to a minimum, the high-voltage pinch was set up together with a switch consisting of a dielectric foil. The compact construction necessary for this purpose caused flashover, which has so far prevented the full charging voltage from being attained.

From various models estimates were made as to the degree of ionization possible with the present installation.

3. Antipinch

(W. Engelhardt, W. Köppendörfer, P. Merkel)

Further to the orientating experiments with an antipinch in the preceding year, a new, improved device for producing and observing shock waves in plasma was constructed.

Data of installation:

$$W = 60 \text{ kJ}, U_0 = 40 \text{ kV}, T = 16 \mu\text{sec}$$

Discharge vessel:

$$\text{Hollow cylinder } D = 45 \text{ cm}, d = 16 \text{ cm}, L = 50 \text{ cm (25 cm)}$$

Predischarge:

$$W_v = 3 \text{ kJ}$$

The large vessel was chosen so as to obtain an approximately plane wave travelling radially outwards from the centre.

The velocity and steepness of the shock front are observed with a differential interferometer which enables electron density gradients to be measured. The streak interference photographs of the 13-cm long, observable path show a constant velocity of the magnetic piston of $8 \cdot 10^6$ cm/sec at $5 \cdot 10^{-2}$ torr D_2 filling pressure. Although it has not yet been possible to assess the photographs exactly, it is already evident that the density gradients involved are very much greater than could be established from the magnetic-field probe measurements in the preliminary experiments. In the subsequent course of the experiments it is intended to obtain information on the velocity and structure of the shock front as a function of the degree of ionization or the particle density. It is intended to superimpose an axial magnetic field for varying the velocity of sound and also to compare the differential interferometer measurements with magnetic-field probe measurements.

4. z-Pinch

4.1 X-Radiation in the Linear z-Pinch (J. Sommer)

The experimental investigations on the mechanism causing a hard X-radiation pulse observed just before the first contraction of the plasma column were supplemented by solving numerically the system comprising four coupled differential equations, namely the three motion equations of the electron as a single particle and the motion equation of the plasma column. The calculations confirmed the experimentally established influence of the inhomogeneity of the external stabilizing field on the hardness of the X-radiation. Furthermore, with regard to the acceleration mechanism itself new knowledge assigning a major role to the external axial electric field was obtained.

4.2 Electron Density Measurements with Microwaves (H. Hermansdorfer)

Electron density measurements were carried out with an 8-mm microwave reflection probe on a fast linear z-pinch discharge without preionization and without B_z field. In successive discharges the density distribution in time at various distances from the axis was measured.

Reflection measurement with a microwave probe is a new way of measuring dense plasmas locally; the plasma frequency exceeds the measurement frequency. In principle, electron density and electron collision frequency can be determined by measuring the transition to metallic reflection with increasing electron density. It was possible to measure densities between a few 10^{13} cm^{-3} and a few 10^{16} cm^{-3} by using an 8-mm interferometer of high time resolution which was developed here and which afforded an angle accuracy of approx. 3° and an amplitude accuracy of approx. 5 %.

5. Fieldless Plasma Configurations in Equilibrium with Plane Magnetic Fields (P. Merkel)

The magnetohydrostatic equilibrium between an external magnetic field and a fieldless plasma was investigated in the case of "plane" geometries. The latter term is used to refer to linear, infinitely long configurations in which all currents flow parallel or antiparallel to a defined direction. For this two-dimensional problem of potential theory a function-theoretical method providing simple solutions can be found, if the conductors for the external currents are wires and the complex potential has therefore only isolated, logarithmic singularities.

Besides the general treatment of the problem, analytical solutions were given for the two-dimensional analogon of the M+S torus ("Quasilimus"), which is a cylindrical, doubly connected plasma, and for the linear cusp and picket fence device, which are singly connected plasma configurations.

Part of the results were announced at the 10th MEETING OF THE EUROPEAN STUDY GROUP ON FUSION in May 1964 in Jülich.

6. Measuring Methods

6.1 Use of the Laser in Plasma Diagnostics

(B. Kronast, H.-J. Kunze, H. Röhr, G. Weiser, H. Zietemann)

a) Further development of the 90° light scattering method

Investigations of the light scattered in a plasma make it possible, as is already known, to determine local plasma parameters such as electron density, electron temperature and ion temperature.

After light scattered at 90° was found for the first time in a theta pinch plasma, as announced in the annual report for 1963, investigations of scattered light were continued this year. The measuring equipment was improved; among other things, a multiple slit consisting of glass-fibre bundles now allows 7 wavelengths of a scattered light spectrum to be measured simultaneously. The entire measuring device can, moreover, be wheeled to any other installation. Serving as light source is a giant pulse laser operated by a Kerr cell [IPP 1/26].

This method was tested by conducting light scattering measurements at 90° on a small theta pinch installation of 7.5 kJ for the time being. In addition to spectra which have a virtually Gaussian profile with a half-width corresponding to the electron temperature,

the main concern was to measure those spectra in the transition region in which correlation effects between the plasma particles begin to modify the spectrum: the occurrence of so-called satellite lines could be shown here for the first time [45]. Electron density and electron temperature are hereby obtained from the spectrum alone. Further improvements even made it possible to show the simultaneous presence of the central line [IPP 1/30], which, however, could not be spectrally resolved. The results were completed by absolute measurements of the intensities. A detailed discussion of the problems, method and results of the 90° scattering is contained in [IPP 1/30], second part in [43].

This method was used finally on a 26-kJ theta pinch for measuring the radial distributions of electron density and electron temperature [44], (v. 2.2). As the laser output of 5 MW is too low for this purpose, however, the data obtained involve a mean error of roughly 50 %. Attempts are therefore in progress to use two ruby lasers already available as a combined oscillator-amplifier and thus to increase the output. It has already been possible to intensify the output of the laser oscillator fivefold.

b) Measurement of the ion temperature of a plasma

At scattering angles θ , for which the parameter $\alpha = \frac{\lambda}{4\pi \cdot D \cdot \sin\theta/2} \geq 1$ (λ = light wavelength, D = Debye length), the scattered-light spectrum consists of a narrow central line and two satellite lines symmetrical to it (v. [IPP 6/21], p. 49/50). If α is not very large in relation to 1 the central line will be broadened mainly by the ion motion, and this affords the possibility of determining mean ion velocities.

In the case of plasmas with a temperature of a few 100 eV the scattering angle θ for $\alpha > 1$ will be really small, even with electron densities of 10^{17} cm^{-3} . An apparatus which can absorb light scattered at small angles from defined volume ranges and convey it without great losses into a high-resolution monochromator has been tested and the final version constructed. The high-resolution monochromator with multiple glass-fibre slit was developed by E. Glock (v. 6.10.b) and is also under construction.

c) Light scattering measurements on a theta pinch plasma of high electron temperature were conducted on Theta Pinch I, the results being included under that heading.

d) Measurements of the second harmonic, produced in the plasma, of laser radiation

One major difficulty encountered here was the harmonic-free penetration of unavoidable windows and the harmonic-free separation of the primary beam from the beam to be measured. Both requirements could be satisfied by widening as much as possible the primary-beam bundle at the location of the window and filters and by using fluid filters, the result being that the power of the harmonic in the beam to be measured was less than 10^{-12} of the primary radiation. The final experiments with plasma did not materialize, however, because more accurate calculations completed in the meantime by W.H. Kegel (Theory) pointed to a harmonic yield from the plasma substantially smaller than 10^{-14} and both laser and measuring apparatus were inadequate in this case.

e) Modulation of laser light

Work on this aspect was concluded, the results being summarized in [IPP 1/26] and [73].

6.2 Frequency Shifting of Laser Radiation by the Doppler Effect (F. P. Küpper)

Two experiments for shifting the frequency of ruby laser light by means of the Doppler effect were conducted.

1. By enlisting fields with extremely short rise times ($dE/dt \sim 5 \cdot 10^{14}$ V/cm·sec) in nitrobenzene it was possible to effect a time variation of the optical path, the result being a frequency shift of more than 20 \AA . This shift could not be verified, however, as the field rise had an exponential time behaviour.

2. With the use of a Kerr cable (60 cm long) the time variation of the optical path was effected by an electric wave passing into the Kerr cable. With a constant field the extent of the frequency shift is dependent here only on the velocity of the electric wave. In this way a time constancy of the displaced laser frequency is obtained. It was possible to measure this shift spectroscopically. For an electric wave of $\approx 2 \cdot 10^5$ V/cm it amounts to $\approx 2 \text{ \AA}$.

6.3 Laser Light Source for the Interferometer (R. Beck)

A laser light source was developed for the Mach-Zehnder interferometer. With a powerful pumping capacity and a high-grade resonator it was possible to achieve constant emission from the total laser surface for $20 \mu\text{sec}$. This light source is used for taking high-speed photographs of the distribution of the interference fringes with more than 300 fringes. Moreover, by means of framing photographs it could be shown that the laser developed oscillates reproducibly in oscillation modes of type TEM_{pp} .

6.4 Differential Interferometer (A. Heiss)

In the case of plasmas over 1 m long the Mach-Zehnder interferometer can no longer be used because with large density gradients ($dn/dr \geq 10^{17} \text{ cm}^{-4}$) the beam is bent. For interferometric measurements the measuring range can be extended by means of a differential interferometer. In this way the gradient of the electron density can be measured perpendicular to the direction of observation. A differential interferometer was tested on a fast preionization theta pinch. In this connection streak photographs and snapshots over the entire discharge cross section were taken. The rotational symmetry of the discharge was ensured by means of schlieren photographs, since only the density changes perpendicular to the direction of the interference fringes can be ascertained with the differential interferometer.

Preparations are in progress for using the differential interferometer on the large theta pinch experiment.

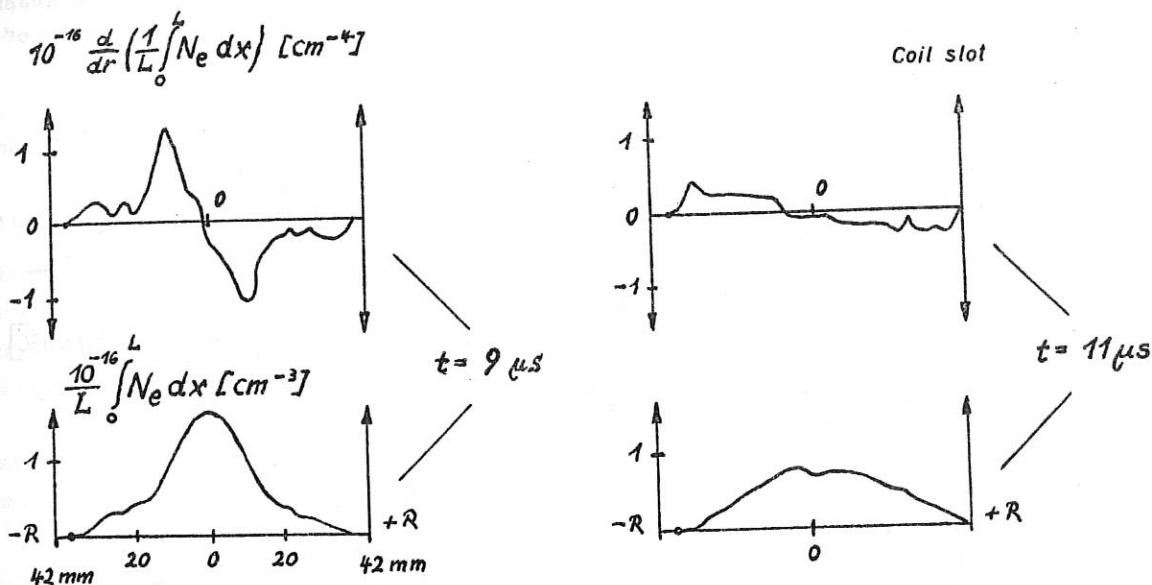


Fig. 6 Radial electron density distribution in a theta pinch, measured with differential interferometer.

6.5 Testing Electric Double Probes in Hot Plasmas (D. Combecker)

On a 7.5-kJ theta pinch density measurements by electric double probes were compared quantitatively with interferometric measurements. At the same time the emission of spectral lines from the probe material was observed spectroscopically.

The radial density distribution of the discharge was measured with a Mach-Zehnder interferometer which integrates over the axial density distribution. The time resolution was obtained by streak photographs. The electric probe was introduced radially and imaged on the slit of the streak camera in order to obtain with the interferometer at the same time the plasma density distribution at the probe location. Measurement of the probe current was done with a microwave transmitter (v. [34]).

From the light emitted by the evaporating probe a monochromator isolated oxygen, silicon and iron lines, which were recorded by a multiplier. The results showed close qualitative agreement between the densities measured by the probe and those measured by the interferometer. With regard to quantity the probe measurements gave a density value smaller by a factor of about 5. The cause is still unknown.

The probe evaporation is fairly strong. It begins about 0.5 μsec after the first breakdown of the plasma and reaches its maximum when dJ/dt passes through zero. The light emitted by the vapours at the location of the probe is roughly 1000 times greater than the inherent plasma luminosity without probe.

The fact that sometimes no probe signal occurs on the first breakdown of the plasma seems to indicate that radial insertion of the probe prevents breakdown.

The comparative measurement should be interpreted with caution since the probe measures at a particular point while the interferometer integrates over the entire length of the tube.

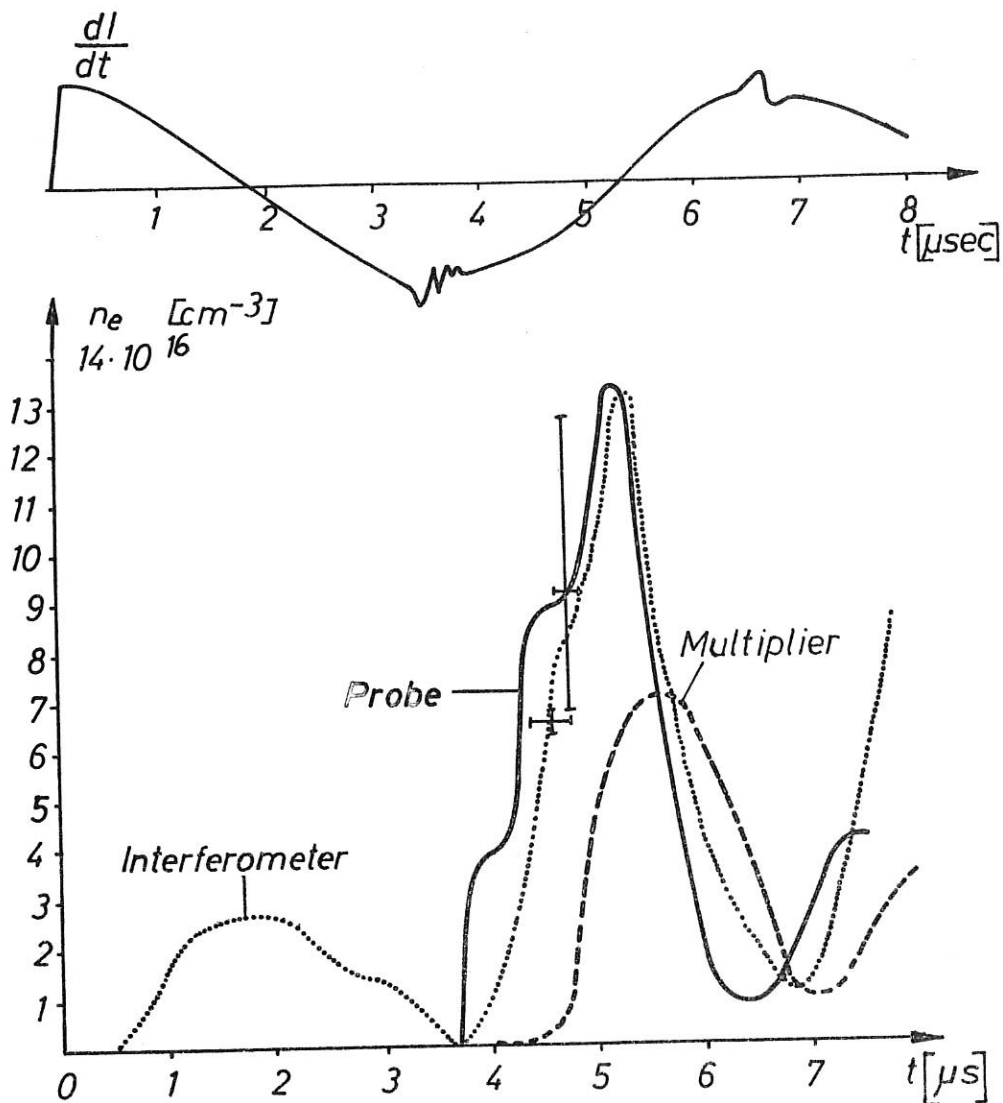


Fig. 7 0.07 mm hydrogen; probe location: centre of coil; probe in the axis
 - - - Intensity of a Si line (5056 Å) at the probe location
 The indeterminacy of the density obtained with the probe is due to the indeterminacy of the electron temperature, which enters into the measurements as the root and is estimated roughly. The probe signal was enlarged by a factor of about 5.

Development of Piezoelectric Probes for Pressure Measurement in Very Fast

Discharges (W. Katsaros)

was endeavoured to reduce to a minimum the limitations of previous pressure probes.

exploiting every technical possibility:

the time resolution was improved by a factor of 3,
the sensitivity was increased by a factor of 2,
accurate reproduction of the pressure profiles to be measured was achieved,
the calibrating accuracy was raised to $\pm 10\%$.

With these improved probes pressure measurements are now to be carried out on very fast discharges.

7 Infra-red Radiation of Plasma (D. Gross)

For frequencies equivalent to $\lambda = 100 \mu$ which still exceed the plasma frequency at electron densities of 10^{16} to 10^{17} cm^{-3} the bremsstrahlung continuum is optically dense up to a few 100 eV at radiation distances of 0.1 - 1 mm, and so the electron temperature can be determined from an absolute intensity measurement. The independence of Doppler effects means that measuring is uninfluenced by local perturbations of density and temperature and by macroscopic velocities of the plasma.

He-cooled germanium monocrystal doped with Sb was tested on an IR calibration source in stationary operation which was constructed for this purpose, and calibration curves were then recorded for various filters.

8 Infra-red Radiation in an Inhomogeneous Cylindrical Plasma Column in an Axial Magnetic Field (H. Gratzl)

The infra-red bremsstrahlung was determined for an inhomogeneous cylindrical plasma and evaluated numerically for theta pinch values calculated by Duchs. The neutral-gas component of the discharge can practically be ignored here.

At the observation frequency is not much smaller than the maximum plasma frequency the intensity of the thermal radiation is almost attained, but with much lower or higher frequencies this is no longer the case.

Due to the influence of the magnetic field in the geometrical optics and the local thermal equilibrium any appreciable intensity change (at least several percent) would occur only at frequencies smaller than about five times the gyrofrequency. At these frequencies the locally variable electron temperature can be replaced to close approximation by the temperature at the point where the radiation is reflected almost totally. Because of the geometrical dimensions, however, the geometrical optics ceases to be a good approximation at these frequencies with this pinch. The question as to whether a radiation maximum of the ordinary polarization, to be expected in theory and produced by the magnetic field, can be measured properly in the meridian plane at a certain angle of observation depends particularly on whether this polarization can be separated experimentally from the extraordinary polarization.

6.9 Recording of Rapidly Varying Optical Line Profiles with Image Converter and Multiplier (W. Nässl)

The principle of the method is described in the annual report for 1962. Work has now been concluded with the construction of an efficient tube, which was tested with photographically produced phantom profiles at recording times of a few 10^{-7} sec. A luminous flux of about 10^{-5} watts was required for a reproduction accuracy of 10 % in the profile maximum. Determination of the electron-optical unsharpness gave, with reference to the photocathode, a width of 50μ for the reproduction system used. The test profiles recorded were wide in comparison.

Full particulars of the accuracy of the reproduction of the profile as a function of various parameters (ratio of slit width to half-width, luminous flux, quantum efficiency of the photocathode, band width of the electronic system) are contained in the laboratory report [IPP 1/29].

6.10 Spectroscopic Measuring Devices (E. Glock)

Because of the wide variety of measurement conditions the use of conventional equipment with fixed data entails a good deal of difficulty and expense. By way of experiment two flexible units have now been designed:

a) A rotating-mirror spectrograph which can be used alternatively with the following data:

Streak speed:	Streak length:	Rel. aperture:
0.4 mm/ μ sec	3 mm	1 : 1
2.5 mm/ μ sec	20 mm	1 : 6.8

Intermediate values are possible, depending on the optical systems available. The calibrating system for wavelength and intensity are built in.

b) A monochromator in a Littrow arrangement, with slight aberration for line profile measurements. $f = 150$ to $f = 2250$ mm; rel. aperture 1 : 1.5 to 1 : 20, depending on the optical system available.

6.11 Further Development of a Neutron Source (H.-J. Schneider-Muntau)

The high voltage pulse generator required for boosting neutron yield was constructed. It was developed as a low-inductance, 10-stage Marx-type generator with cables as energy stores, specially for an extremely high-speed pulsed neutron source. The pulse lasts 100 nsec at a terminal resistance of 54Ω and the maximum open-circuit voltage is 300 kV.

In order to measure the time distribution of the voltage, a differentiating, capacitative voltage divider with following integrator was designed, but has not been tested so far.

In addition, the vacuum apparatus necessary for the neutron source was set up.

6.12 Electronic Systems (F. Lindenberger, M. Ulrich)

Completion of the light-dividing monochromator attachment begun the previous year.

Development and construction of a coaxial voltage divider for voltages of up to 15 kV and 2 μ sec pulse duration, 60 Ω input resistance and a divider ratio of 20 and 100 and also a coaxial spark gap which can be adjusted when live.

Development and construction of a 14-kV pulse generator with unearthed output. Cables and capacitors can be used as stores.

Development and construction of a trigger separator. This prevents premature breakdown of the 14-kV thyratron by the anode. (A certain improvement in this respect can be achieved simply by incorporating a separator spark gap) In conjunction with this device a low-scatter pulse transformer with four ring cores was developed.

Development and construction of a generator for pulsing a Hg lamp; $I_{\max} = 100$ A. The length of the square wave is infinitely variable up to 100 μ sec. The principle can be used for longer times and at higher currents as well.

Construction of two neutron counters with amplifier.

Design of a monochromator attachment for 10 multipliers with light divider in accordance with British specifications.

Development and construction of an electronic attachment for measuring the revolution frequency of a turbine drum camera.

Development and construction of pulsed power supply system for a 40-kV double Kerr cell.

To eliminate the necessity of working with multipliers directly on the cable wave resistance an emitter repeater was developed which was screwed on to the existing multiplier attachments on the signal bush. The power supply for the emitter repeater is obtained from the calibration signal of an oscillograph, the signal cable itself serving as power lead.

Design of a screening box for the leads through the floor, with flexible plug-in tubes for the megajoule bank.

Construction of a device for measuring the magnetic field in the megajoule bank.

Electrical installations for screened rooms.

EXPERIMENTAL PLASMA PHYSICS 2 (DR. G. VON GIERKE)

1. Summary

At the beginning of the year it was decided to shift the emphasis in the "Interactions" Group slightly by ceasing to regard the interaction phenomena as such as the sole object of experiments and using them directly instead for the production of high-temperature plasmas. This raised the question of a stable confinement. This problem was solved by choosing mirror machines with minimum-B configurations. The ensuing HELIOS and HELIOSIS projects were adopted as the main programme of the group, and the experiments still in progress are to be concluded as soon as possible. Such experiments include primarily those no longer directly connected with the new programme of the group, such as, for example, diffusion and oscillation investigations on the CABINET I apparatus. On the other hand, it proved possible to set up from existing components an ion beam interaction experiment (JO-JO) with which a few preliminary investigations for HELIOSIS can be conducted.

The instability found two years ago in the WW I apparatus during electron beam and plasma interaction has now been investigated more closely. The experiment will probably be concluded in the course of 1965.

The diffusion experiments on CABINET III are being concentrated more and more on the wall problem, which, as is well known, occupies a decisive role in the case of finite plasmas (e.g. instabilities in mirror machines).

In the Microwave Group the previous work in the field of measurement technique was rounded off and concluded. Preliminary experiments for producing an electron cyclotron resonance plasma are under preparation, for which purpose the now vacant CABINET I apparatus is being used.

This year various investigations were conducted on the plasma of the HOKE hollow-cathode discharge, this plasma being originally intended for ion cyclotron resonance experiments. The plasma diameter was raised to 3 cm. This plasma still seems to provide a suitable basis for I.C.R. experiments, although somewhat overshadowed by the confidence placed in the E.C.R. plasma. The HOKE plasma has been investigated by various diagnostic methods, whereby the Whistler mode propagation seems to stand out as a reliable method of measuring plasma densities.

In the course of the year operation of the helium liquefier was taken over completely by the Engineering Department.

In the "Thermal Plasmas and Probe Diagnostics" Group the experiments on the radio-frequency probe were concluded. The new experiments are concerned primarily with wave propagation in thermal plasmas. In addition, the particle losses of a caesium column in straight and curved magnetic field were examined. These experiments showed that in the previous geometries and with the investigation methods applied no statement can be made on the prevailing loss mechanism at low densities.

Investigations of the wall problem in the "Ultra-high Vacuum" Group were continued according to plan.

The size of the staff showed an increase on the previous year. Working temporarily in the Department as guests were: Dr. N. D'Angelo (Princeton), Prof. R.W. Gould (Pasadena) [25], [24] and Dr. R.S. Harp (Stanford). Dr. K.H. Wöhler was granted leave of absence (Monterey).

2. High-Temperature Plasmas

(F. Boeschoten)

2.1 Proposed Method for Producing High-Temperature Plasmas (HELIOS and HELIOSIS)

(F. Boeschoten, A. Borer, G. Cattanei, H. Grawe, W. Herrmann, G. Lisitano, G. Siller, K.H. Wöhler)

This year it was suggested that an electron cyclotron resonance plasma might be an excellent initial plasma for the larger interaction experiments planned. It was therefore proposed that a stationary (or semi-stationary) E.C.R. deuterium plasma be produced with the aid of a microwave transmitter (40 KW, 20 Gc/s C.W.). In this way it should be possible to produce 10 to 20 litres of plasma (density $n_e \approx 10^{12} \text{ cm}^{-3}$; electron temperature $T_e \approx 100 \text{ keV}$). The deuterons of this plasma were to be heated afterwards on the ion cyclotron resonance principle, namely with the transmitter (1.5 MW, 2 msec, 5.5 Mc/s) supplied at the end of the year (HELIOS), or high-energy deuterons were to be injected with the ion beam (100 keV, 0.5 A) being developed (HELIOSIS). The plasma was to be confined in a minimum-B field configuration [5].

In experiments conducted recently at Oak Ridge, however, it was found that there are also many cold electrons ($T_e \approx 10 \text{ eV}$) present in the E.C.R. plasma (n_e also $\approx 10^{12} \text{ cm}^{-3}$). Their presence is undesirable because they take away the energy of the heated ions. Investigations of the E.C.R. plasma should therefore be directed primarily at avoiding the cold electrons and minimizing the neutral-particle density ($\approx 2 \cdot 10^9 \text{ cm}^{-3}$).

For coupling the ion cyclotron wave into the plasma, capacitive coupling seems to be the most feasible proposition. The problems which may arise at the electrodes do not appear to be insuperable. As an alternative it was suggested that the microwaves be modulated with the I.C.R. frequency; the extent to which the plasma can act as a demodulator has still to be investigated.

Taking into account as well the latest experiments in Livermore, it seems that a hexapole field is the most suitable for ensuring stable confinement of the plasma.

The projects were discussed at length but no final decision has been reached so far.

The ion beam experiments were concerned primarily with the extraction and focusing of the highest possible ion currents. As yet it has not been possible to obtain a high extraction current and good focusing at the same time. Currents of over 100 mA were extracted with energies of up to 40 kV; by means of a diaphragm 3 cm in diameter at a distance of 1.85 m from the source about 70 mA could be focused with up to 70 kV. An energy analyser for investigating the energy distribution of the beam particles was constructed. In the final quarter of the year operations were interrupted as it was discovered that without suitable overload protection damage to the electrode system caused by breakdown is inevitable. An overload protective device (triode) for voltages of up to 100 kV is being constructed.

2.2 WW I (W. Herrmann)

Measurements on the electron beam plasma were continued [33]. These were concerned primarily with the energy losses of the beam. With instability present the energy losses reached values of roughly 30 % of the injection energy. The energy losses are dependent primarily on the pressure. They are greatest just above the critical pressure. They increase slightly as the current increases. The absolute energy losses ΔE rise as the injection energy E . The relative losses $\frac{\Delta E}{E}$ remain constant.

The electron beam was also injected into a mirror field. With intense magnetic fields (approx. 2500 gauss in the mirror) gamma radiation with an energy $E > 50$ keV is found in the region just above the critical pressure. The radiation originates at the collector. The injection energy was only 4 keV.

Oscillation measurements were conducted primarily in the low-frequency range. Oscillations of high amplitude in the kc/s range seem to accompany a rotation of the beam. Furthermore, with instability present outside the beam oscillations were detected at a few 100 kc/s. For these oscillations three to six harmonics could be found. The frequency of these oscillations does not depend on the radius, but varies roughly in inverse proportion to the magnetic field and pressure.

2.3 Ion Beam Interaction (JO-JO) (A. Borer)

Interaction between beams of charged particles, i.e. the conversion of kinetic energy into oscillation energy, already ensues theoretically from the simple model of a plasma that consists of a large finite number of cold components drifting against one another. Preliminary theoretical work on the basis of this model yielded information on the order of magnitude of the effects anticipated¹⁾. JO-JO is intended as an experiment which should conform to this simple model as far as possible: two ion beams of a few mA with energies of up to 10 keV, neutralized by electrons produced in the residual gas, are fired at one another in a magnetic field of up to 4 kG. Density and energy modulation of the beams make it possible to record the frequency properties of the system.

2.4 CABINET I (F. Boeschoten, K. Geissler, G. Siller)

At the beginning of the year the diffusion measurements on the CABINET I apparatus were concluded and the findings compiled in a laboratory report [IPP 2/35]; [6]. The survey of diffusion measurements in a magnetic field which was announced in the last annual report was published [4]. The oscillation measurements on the beam were also terminated this year, partly in collaboration with R.W. Gould.

2.5 CABINET III (K. Geissler)

Hitherto the influence of boundary conditions on the diffusion of a plasma in a magnetic field has not been understood very well [IPP 2/35]; [6]. A decaying plasma affords good scope for investigating this influence. For this purpose a plasma (neutral-gas pressure 10^{-3} to 10^{-1} torr, magnetic field 0 to 4000 gauss) is produced in a metal cylinder

1) Internal reports: "Anregung von elektrostatischen Schwingungen in einem System von zwei entgegengesetzt gerichteten Ionenstrahlen mit strahlenparallelem Magnetfeld" (April 1964), "Elektrostatische Schwingungen in einem System von zwei entgegengesetzt gerichteten Ionenstrahlen" (August 1964).

(L = 70 cm, D = 16 cm) with the aid of a pulsed electron beam, and the decay of the plasma due to diffusion is observed. The wall and ends of the metal cylinder are split up into 17 rings insulated from one another so that the wall currents produced by the non-ambipolar diffusion mechanism can be measured directly (cf., for instance, the "short-circuit effect")¹⁾. The apparatus enables the wall currents to be measured in the interval from 10^{-3} to 10^{-11} A for every cm^2 of the wall, i.e. the plasma decay can be kept track of over a correspondingly wide density range.

2.6 Microwaves (G. Lisitano)

In a concluding internal report²⁾ on the work performed in the field of microwave measuring methods the systems developed and the measurement results from plasma experiments were described. This paper was submitted without the section on plasma diagnostics to the TH Munich as a doctorate thesis [48].

Further attention was devoted in particular to the measuring system for the automatic indication of the impedance transformation of a quadrupole in the mm wave range. A report on the subject was submitted for publication.

In the case of the dual interferometer measuring system the technical principles were formulated and a detailed investigation of possible measurement errors conducted [49].

In connection with a diploma work (M. Michaelis) the following developments were realised:
1. Frequency doubling from a 4-mm klystron; 2. Comparison between 2-mm Philipps detectors and standard IN-53/4-mm crystals; 3. Microwave optical system with Teflon lenses; 4. Comparison between the following four interferometric methods in the 2.5-mm wave range: phase bridge system, amplitude modulation system, Michelson interferometer, frequency modulation interferometer with "Polar" and "Fringe" display; 5. Construction of an interferometer for three wavelengths (8, 4 and 2.5 mm).

2.7 Hoke (K. Weinhardt)

First of all the experiments for increasing the arc diameter were continued. Ta cathodes with internal diameters of up to 30 mm and arc currents of up to 400 A were used. The influence of the separating walls on the neutral-gas pressure was investigated. A water-cooled, hollow anode and conical cathodes were prepared. In the external plasma n_e and T_e were determined with a spherical probe and oscillations investigated. A start was made on spectroscopic measurements in helium. The mean density and the mean diameter of the arc core were determined by means of 4-mm transmission measurements.

A Dicke radiometer was used without success to find at the harmonics of the electron cyclotron frequency the same radiation observed by COCOLI in a similar discharge. Comparison of the B-dependence of the inherent noise seems to indicate that Hoke is too "quiet" for the emission of cyclotron harmonics.

With two pin antennae forming a system similar to a double probe which is forced through the arc by a lever mechanism, electromagnetic waves which propagate quite definitely in accordance with the Whistler mode were excited in the plasma and verified. At present the

1) A. Simon, Phys. Rev. 98, 317 (1955)

2) G. Lisitano, "Ein Messverfahren zur direkten Anzeige des Übertragungs- und Reflexionsfaktors im mm-Wellenbereich (mit plasmadiagnostischer Anwendung)", Nov. 1964

coupling between antenna and plasma is being investigated in order to create the conditions for quantitative measurements.

3. Thermal Plasmas and Probe Diagnostics

(G. Müller)

3.1 Particle Losses of a Cs Plasma Column in Straight and Curved Magnetic Fields

(E. Guilino, in collaboration with the "Wendelstein" Group, MPI)

See under Experimental Department (Plasma Physics) of the MPI, "Wendelstein" Group, of the present report.

3.2 Excitation and Propagation of Plasma Oscillations

3.2.1 Bernstein Waves and Self-Excitation of Plasma Oscillations in the Vicinity of the Electron Cyclotron Harmonics (R.S. Harp, G. Müller)

These investigations were begun in the summer of this year after the radio-frequency resonance probe measurements were completed. The self-excitation of plasma oscillations at the electron cyclotron frequency and its harmonics was verified to the 12th order both in the thermal Cs plasma of the ALMA II apparatus and in an Ar low-pressure discharge with a Helmholtz coil system in the region of 100 to 400 Mc/s (0 to 150 gauss). The oscillations were recorded with electric RF probes located inside the plasma column. With normal operation of the discharge both the oscillation amplitudes and the order of the excited cyclotron harmonics decreased as the neutral-gas pressure increased and vanished at approx. $4 \cdot 10^{-4}$ torr. In the presence of superthermal electrons these oscillations were excited at higher gas pressures of up to approx. 10^{-3} torr as well.

In the Ar low-pressure discharge with large column diameter of approx. 4 cm it was also possible with probes at an oscillation frequency of 400 Mc/s and a plasma frequency ≥ 400 Mc/s to excite longitudinal electron waves perpendicular to the magnetic field, so-called Bernstein waves, and carry out transmission measurements. In a magnetic field region between the fundamental and first harmonics of the electron cyclotron frequency wavelengths from 1 mm to 2 cm were measured and the theoretical dispersion relation for Bernstein waves verified. Waves between the higher harmonics were measured as well, the wave propagation coming to an abrupt end each time at the higher harmonic. Hitherto it has not been possible to measure these wavelengths because of their appreciably lower amplitude.

3.2.2 Low-Frequency Electrostatic Ion Oscillations (k // B) (E. Guilino)

In the second half of the report year preparations were initiated for an experiment to investigate electrostatic ion waves. With the aid of grids traversed by the plasma column excitation is effected in such a way that a plane wave propagates along the axis parallel to the magnetic field. In the contact ionization plasma of the ALMA II apparatus the frequency range to be investigated, which is below and close to the ion cyclotron frequency and below the ion plasma frequency, lies between a few kc/s and 100 kc/s. In the collisionless plasma the wave is subjected axially to strong Landau damping.

Towards the end of the year the experiment apparatus was completed but for a few minor improvements still to be attended to. It was possible to verify ion oscillations of the desired kind.

The following investigations are planned:

- a) Absolute measurement of the wave amplitude in the plasma. Comparison between a theory of R.W. Gould [24] and the experiment.
- b) An attempt is to be made to measure the phase velocity of the wave more accurately by suppressing the plasma drift; on the other hand, if the phase velocity is known the drift velocity of the plasma can be determined. In any other way the phase velocity is difficult to measure in the Cs plasma, but it influences the evaluation of probe measurements and provides valuable information on the emitter sheath.
- c) Measurement of the transition from Landau damping to collisional damping by raising the impact frequency (admixing neutral gas). Transition from Landau damping amplification by distortion of the velocity distribution of the ions. Later, dependence of the damping on the temperature ratio T_e/T_i by additional heating of the Cs plasma.

In order to obtain a more pronounced plasma column (steeper radial density gradient at the column boundary) and a higher cyclotron frequency, it is necessary to have a more intense confining magnetic field. In collaboration with the Engineering Department (B. Oswald) a new coil system producing a magnetic field of 13 kG was designed and commissioned.

A new, radially expanded vacuum vessel will also allow the introduction of axial probes in double-ended operation (in collaboration with the MPI Design Office - P. Meyer, Allgeyer, Melchior).

3.3 Probe Diagnostics

3.3.1 Investigation of the Velocity Distribution of the Electrons in a Hg Low-Pressure Discharge (M. Troppmann)

The principle of the experiment was described in the previous annual report (section III.3.1). Meanwhile the constriction of the plasma in dependence on the gas pressure, discharge current and constriction voltage was measured. The discharge was constricted to approx. 1/50 of the original cross section at voltages of up to 1000 V, the operating voltage increasing as a result by up to 15 V. Moreover, the plasma apparatus was improved in several respects and the electronic system for recording the energy distribution was completed so that a start can now be made on the actual investigations.

In addition, theoretical studies were made of the electron energy distribution in the plasma constriction and in the plasma at the anode end and also of the influence of the electron drift on the probe characteristic.

3.3.2 Investigations of Ion Current with a Grid Probe (V. Joshi)

Investigations of the ion current from the plasma to a probe with the aid of grid probes were discontinued in May this year when V. Joshi left the Institute. Unlike measurements in low-pressure discharges, measurements in the Cs plasma of the ALMA I apparatus (annual

report for 1963) showed an exponential rise in the ion current and a pronounced ion saturation current. In the absence of magnetic fields the ion temperatures determined were approx. 30 % above the electron temperature, which was also measured with probes. Increasingly flatter ion current characteristics were found as the magnetic field increased, from which it might be concluded that the ion temperature rises as the magnetic field. This conclusion, however, would have to be checked first by further experiments. The ratio of electron to ion saturation current - measured with the grid probe - agrees satisfactorily with the theoretical value $\sqrt{M_+/m_-}$, unlike the value obtained with Langmuir probes.

3.3.3 RF Plasma Resonance Probe (G. Müller, W. Ott, G. Peter)

The problem of DC resonance was clarified already in the experiments conducted last year on the RF resonance probe (annual report for 1963) [62]. A further publication in the report year [23] deals with the influence of boundary sheaths on resonance behaviour.

3.3.3.1 Influence of the Geometry of Probes and Plasma Boundary Sheath on the Resonance Frequency

Calculations on the influence of the probe geometry on the resonance frequency were confirmed by comparative measurements with plane, cylindrical and spherical probes of various sizes [58].

3.3.3.2 Influence of RF Voltage on Resonance Behaviour

The resonance frequency showed definite dependence on the RF amplitude δV . Like the quasi static direct current (at lower frequencies), the resonance direct current is proportional to the square of the RF voltage for $e \cdot \delta V \ll kT_e$. Compared with the quasi-static direct current, however, the resonance current rises more rapidly at $(\delta V)^2$, the more negative the probe bias. At higher RF amplitudes these laws are subject to deviations which are due essentially to the form of the probe characteristic.

3.3.3.3 Measurements of the RF Current of the Resonance Probe

Investigations hitherto have shown that the resonance of RF current and direct current coincide only if either the resonance damping or the capacitance of the conductors to the probe can be neglected. If, as in the practical case, this does not apply the RF current resonance is always below the DC resonance frequency. If capacitance and damping can be ignored the RF current minimum coincides with the plasma frequency and shifts with increasing capacitance to lower frequencies. Measurements on an equivalent circuit for resonance probe and plasma (plasma simulator) showed analogous behaviour. Investigations are to be concluded soon.

3.3.3.4 Ion Resonance

According to a short paper by KATO et al.¹⁾ it was suggested that in addition to the electron resonance in the vicinity of the electron plasma frequency there should be a DC resonance at the ion plasma frequency $f_i = (\frac{e^2 n_i}{M_i \pi})^{1/2}$. In experiments on the Cs plasma of the ALMA I apparatus in the ion density range from 10^7 to 10^{10} cm⁻³ no

1) Kato, Ogawa, Yoseli, Shimahara, J. Phys. Soc. Japan 19, 1849 (1963)

resonance of the ion direct current to the RF probe was found at frequencies of 50 kc/s to 5 Mc/s and even with high RF amplitudes of up to 25 V.

3.3.3.5 Resonance Probe in a Magnetic Field

If the lines of electric force are perpendicular to the lines of magnetic force, resonance should occur according to the MAYER sheath model¹⁾ at a single frequency, namely at the hybrid frequency $\sqrt{\omega_s^2 + \omega_{ce}^2}$ (ω_s = resonance frequency in the corresponding case without magnetic field, ω_{ce} = electron gyrofrequency). In the experiments in the frequency range between 10 and 50 Mc/s and at electron densities $\leq 3 \cdot 10^8 \text{ cm}^{-3}$ in the Cs plasma of the ALMA II apparatus there occurred, however, in addition to the hybrid frequency a whole series of other resonance frequencies. These vary in characteristic manner as the other parameters and raise serious doubt as to whether the resonance probe in a magnetic field can be enlisted for plasma diagnostics. The experiment was discontinued for the time being. It is intended to resume this investigation if the experiments at present in progress lead to a better understanding of the propagation of electron oscillations perpendicular and parallel to the magnetic field (v. sect. 3.2.1, for example).

3.3.4 Plasma Boundary Sheaths (Electron Beam Probe) (W. Ott)

The studies on the static sheath announced in the last annual report were concluded [IPP 2/34]. The new electron beam apparatus was constructed in the course of the year and initial measurements made on a Cs plasma. Of particular importance was the fact that the deflection sensitivity of the electron beam was raised from an original 20 V/cm to 5 V/cm at a beam voltage of 60 kV by incorporating two magnetic lenses, the one for beam focusing and the other for angular magnification. Sensitivity is to be increased even more by means of an improved aligning system. Equipment for automatic measurement of the spatial field strength distribution are nearing completion. A further new development was a moveable emitter which makes it possible to measure, in addition to the fields in the sheath next to a passive wall, the fields next to an emitter under various operating conditions. This experiment is particularly important for investigations on the particle balance of a plasma column (v. sect. 3.1)

3.3.5 Comparative Density and Temperature Measurements with Probes and Spectroscopic Methods (A. van Oordt)

In the course of the year the photoelectric spectroscopic measuring device was finished. With the aid of a periodic light beam cut-off system (frequency approx. 370 c/s; phase-sensitive rectification) the band width of the noise signal is reduced to approx. 0.5 c/s at a time constant of 1 sec. At room temperature the noise signal of the photocathode at the output end of the multiplier corresponds to a photoelectric current of approx. 10^{-10} A. Photoelectric currents of up to $2 \cdot 10^{-10}$ A can therefore still be detected, which is equivalent to a luminous flux of approx. 10^4 photons/sec at 4000 Å. By cooling the photocathode - the components required for this purpose are at present being made - this sensitivity can be increased by at least two orders. This high sensitivity is necessary for the following two experiments to be conducted with the said device:

- a) Measurement of the density and temperature in the region of $10^{11} < n < 10^{13} \text{ cm}^{-3}$ - for comparison with the results of probe measurements in a magnetic field - at the arc plasma source II in He, the density being determined from the merging of the high series lines and the temperature from line intensities.

1) Internal Institute Report: W. Ott, "Zur Resonanzsonde im Magnetfeld" (Feb. 1964)

b) Measurement of the density in the region of $10^9 < n < 10^{11} \text{ cm}^{-3}$ - for comparison with the results of probe measurements in a magnetic field - in a Ba contact ionization plasma, the density being determined from the scattering of the resonance radiation of the Ba ion.

Initial results of experiment a) show He series, merging of the series lines being clearly identified in the 20th order. Construction of the apparatus for experiment b) is still not complete owing to various delays. These experiments help to account for, among other things, questions relating to the particle balance in the plasma column (v. sect. 3.1).

4. Ultra-high Vacuum

(E.W. Blauth)

Investigation of the wall problem involved various fields:

1. Sputtering of solid material with high-energy hydrogen ions from an accelerator and with ions of lower energy in the field emission microscope,
2. Development of mass spectrometers for the UHV,
3. Special problems of UHV physics.

4.1 Surfaces

4.1.1 Sputtering of Solid Material (R. Behrisch)

In the course of the year the 150-kV UHV accelerator was improved to such an extent that there are prospects of having it fully operational at the beginning of 1965. Besides completion of the vacuum system the modifications affect the ion extraction system and ion post-acceleration system.

A report summarizing the sputtering of solid materials by ion bombardment was published [3].

4.1.2 Investigations of Field Emission (H. Vernickel)

A field emission microscope was used to begin measurements concerned with the influence of ion bombardment on the tip surface and with subsequent gas absorption (systems: tungsten-oxygen; ions: Ar^+ and Xe^+ with an energy of roughly 4 keV). Results to date: ion bombardment causes pronounced roughening of the surface. Details of the crystalline order are destroyed, while the basic characteristics of the crystal structure are preserved. The amount of change in work function is the same for tempered and bombarded tips. Details of the adsorption kinetics and the surface defects caused by bombardment will have to be investigated more accurately.

Further improvements were made in the method for measuring the work function by simultaneous determination of the DC resistance and the differential AC resistance of the field emission path.

Preliminary experiments on the desorption of adsorption layers by ion bombardment showed that an apparatus with separate ion source will have to be constructed for this purpose.

4.2 Mass Spectrometers (E.W. Blauth, H. Hötzl, E.H. Meyer)

Measurements on the new linearly periodic time-of-flight spectrometer (Tempitron) were continued. By energy analyses it was verified that hitherto the ion signal consisted mainly of reflected ions. The system was converted accordingly. With new measurements it is now intended to clarify whether higher resolution and sensitivity can be attained.

Work on the design of a unit-composed four-pole spectrometer in UHV technique was continued and the result submitted at the end of the year to the Engineering Department for clarification of technological details and final construction.

4.3 UHV Measurements

4.3.1 Oil Flow in the UHV (H.E. Schulze)

Further improvements were made in the method for measuring layers, forming on the walls in the UHV, with the aid of the frequency variation of piezoelectric quartz crystals. It is now possible to make measurements with quartz cooled to the temperature of liquid N_2 . The method using low-temperature quartz is to be used for carrying out vapour pressure measurements in an effusion cell.

The back-streaming products of an oil diffusion pump were caught in a trap cooled to low temperature which can be shut off and after thawing analysed with the Farvitron up to mass 400. Mainly CO_2 occurred. An oil diffusion pump cannot be used therefore as vapour source for conductance measurements with oil vapour.

4.3.2 Initial Flow (B.M.U. Scherzer)

a) The problem of initial molecular flow was formulated mathematically in collaboration with R. Gorenflo (Theory Dept.) on account of its significance in determining the mean sojourn of the gas molecules on the wall. So far no analytical solution has been found. For this reason M.G. Pacco (Theory Dept.) and R. Gorenflo set up a Monte Carlo programme with which special initial phenomena can be simulated. This programme also serves to check the approximation on which the diffusion equation is based.

b) Blears effect: Closer observation of the molecular flow of oil and its crack products resulted in a new explanation of the Blears effect [67].

4.3.3 Base Pressures of Hg Diffusion Pumps (B.M.U. Scherzer)

It was possible to show that the base pressure of Hg diffusion pumps depends to a great extent on the preliminary vacuum and its composition. Pressures $< 10^{-13}$ torr were obtained in suitable systems.

4.3.4 Ion-Electron Converter (B.M.U. Scherzer)

In order to detect the smallest ion currents a converter according to F. Bernhard, Berlin, was constructed for the UHV. The experience gained led to a new design.

4.3.5 Two-Chamber Ionization Gauge (G. Venus)

A two-chamber gauge with improved mechanical properties was constructed. Electric perturbations occurring were investigated and (where technically feasible) reduced. Calibration was carried out with helium in the region of 10^{-7} to 10^{-10} torr. The gauge is now to be used in oil vapour atmospheres (Blears effect).

EXPERIMENTAL DEPARTMENT (PLASMA PHYSICS) OF THE MAX-PLANCK-INSTITUT
FÜR PHYSIK UND ASTROPHYSIK, MUNICH (DR. G. VON GIERKE)

1. Summary

It was possible to produce a quasi-stationary discharge with magnetic-field stabilization (Hourglass) up to axial temperatures of at least 200 000 °K. A better understanding of the discharge was gained by using models the results of which are in agreement with the experiments. Substantial progress was made with the investigations on toroidal confinement.

For small values of β (Wendelstein) consistent observation of the behaviour of alkali plasmas in magnetic fields affords results which indicate a new approach not only to the question of equilibrium in stellarator geometry, but also in confinement in linear geometry with end plates.

In the case of large values of β it was possible to observe an extension of the confinement times, with increasing approximation to the M+S profile predicted in theory. At higher temperatures, however, the equilibrium state becomes increasingly difficult to achieve. Investigation was therefore made of additional stabilizing mechanism. Initial results were obtained primarily with additional " φ current".

The work of the Diagnostics Group was continued on the same lines as hitherto. Of particular interest is the work on line broadening and transition probabilities. The Dr. Boldt Group (Vacuum UV) becomes part of the Institut für Extraterrestrische Physik at the turn of the year, since its activities are assuming increasing importance for astrophysical purposes.

The size of the staff remained more or less the same. In 1964 the Department included the following guests: Dr. W.S. Cooper III (Berkeley), Dr. N. Kaiser (application of microwaves), Dr. E.H. Pinnington (Hamilton), Dr. F.W. Hofmann (Princeton), Dr. K.A. Uo (Kyoto, Princeton), Dr. R.L. Barger (Boulder), D. Müller (Zagreb). Leave of absence was granted to Dr. J.H. Mayer (to Boulder).

2. Hourglass

(P. Grassmann, O. Klüber, H. Wulff)

As efforts in the preceding report year to stabilize a He plasma with a strong external magnetic field (up to 80 kG) were successful, the main emphasis of the work shifted to the measurement of state variables. By combining measurements of the electrical resistance of the plasma using probes with spectroscopic temperature measurements in the boundary zones of the plasma it was possible to establish that the axial temperature is $\geq 200\,000$ °K. Measurement of the Faraday effect in a linearly polarized laser beam showed that the electron density on the axis was a good deal greater than 10^{16} particles per cc. These measurements were made with a relatively small power input, i.e. ≈ 8 kW per cm length of plasma. At higher inputs the plasma is unstationary and so the methods employed are useless. (The cross section of the unstationary plasma is only slightly larger compared with that of the stationary plasma, and so plasma and wall remain separated.) Studies based on magnetohydrodynamic theory were made and these helped to clarify the unstationariness. It was possible to confirm by experiment the prediction that longer configurations are conducive to stationariness of

the plasma. Future investigations are therefore to be conducted on configurations with magnetic-field coils 60 cm long. In order to allow spectroscopic temperature determinations in areas other than the boundary zones, preparations were made for measurements in the vacuum UV spectral region.

Efforts to achieve an energy balance for the wall-stabilized plasma revealed that at the present temperatures a substantial part of the power input is lost because of the resonance radiation of the He ion emitted from layers which are not optically thin. As this loss mechanism cannot be treated quantitatively, measurements on the wall-stabilized Hourglass were abandoned and work with a similar objective initiated on the field-stabilized configuration. This involves first of all investigation of the extent to which magnetohydrodynamic theory reproduces the plasma properties correctly. Within the scope of these experiments it is also possible to comment on the magnetic behaviour of the plasma. The result so far has been a preponderance of diamagnetic effects. The deviation from the external field was between 10^{-4} and 10^{-3} .

3. Wendelstein

(D. Eckhartt, G. Grieger, M. Hashmi, H.P. Zehrfeld)
(Engineers: C. Freudenberger, J. Kolos, M. Zippe)

The Wendelstein Group is investigating the confinement of plasmas in toroidal magnetic-field configurations under the condition $\beta \ll 1$. It was already shown in the preceding year that thermal alkali plasmas can be used to advantage for this purpose.

The experiments were continued and the results discussed.

Towards the end of the report year the stellarator W1a with helical windings of type 1 = 3 was replaced by the W1b, which features helical windings of type 1 = 2. Stellarator W11 (with discharge tube diameter enlarged four times in relation to W1) was completed but for the helical windings of type 1 = 2.

3.1 Particle Losses of a Cs plasma in a Stellarator

The results of the stellarator experiments¹⁾ were again discussed. In this connection the equilibrium of a plasma of finite conductivity in a stellarator was dealt with in a simple model (the results obtained agree with those already indicated by Pfirsch and Schlüter²⁾). The main emphasis was placed on the balancing mass flux parallel to the magnetic field necessary for producing a stationary state, this flux requiring as driving force a non-vanishing component of the pressure gradient parallel to the magnetic field. This means that the magnetic surfaces are satisfactory approximations of surfaces of constant pressure only when the velocity of the balancing mass flux is small in comparison with the thermal velocity of the ions. This condition was used for defining a parameter of similarity which allows discharges in H_2 and Cs to be compared with one another.

Experimental results in respect of Cs plasmas are available for density ranges in which the theoretical velocity of the balancing mass flux is high and also for others in which it is low in comparison with the thermal velocity of the ion. In the second case - disregarding losses due to the finite conductivity of the plasma - equilibrium can be expected, but not in the first case.

1) N. D'Angelo, D. Dimock, J. Fujita, G. Grieger, M. Hashmi, W. Stodiek, International Conference on Ionization Phenomena in Gases, Paris 1963 (paper III c, 9).

2) D. Pfirsch, A. Schlüter, Laboratory Report MPI-PA-7/62

No change of the plasma state is observed experimentally, however, on transition from the one density range to the other. Instead, the observed density profile is in no case rotational symmetric and consequently the areas of constant pressure are in each case very much different from the magnetic surface. Rather do the density profiles bear out the assumption that the balancing currents flow through the conductive wall of the vacuum vessel, instead of through the plasma parallel to the magnetic surface [MPI-PA-29/64; 21].

This hypothesis suggests the following experiments:

1. Replacing the conductive wall by an insulating one,
2. Increasing the radius of the vacuum tube and thus the distance of the plasma from the wall,
3. Repeating the measurements with a rotational transform of type 1 = 2.

3.2 Particle Losses of a Cs Plasma in a Magnetic Field with Variable Curvature

(experiments on ALMA II in collaboration with E. Guilino, IPP)

To enable the influence of curvature of the magnetic field on the extent of plasma losses to be studied an experiment was started with ALMA II. In this experiment, the particle production rate being kept constant, the resulting particle density (and thus the rate of loss) was determined as a function of the curvature of the magnetic field. Langmuir probes were used for the density measurement. These experiments were concluded in the report year. They showed that on transition from the homogeneous to the curved magnetic field the plasma losses increased by a factor of less than 2 [MPI-PA-20/64]. With curvature of the lines of magnetic force, a slight rise in particle losses is expected, however, as a result of violation of the plasma equilibrium in the curved magnetic field [MPI-PA-12/64] or of geometrical asymmetries in the experiment apparatus which are hard to avoid. On the other hand, an increase in particle losses of several orders of magnitude was estimated from the results of the stellarator experiment on transition from the straight to the curved magnetic field. The condition for this was that the plasma is in thermal equilibrium with the end plates and thus, in the case of the straight field, the particle losses are caused only by collisional diffusion and end plate recombination. This discrepancy was clarified by measuring in a further experiment the particle losses in the case of the straight field. It was thereby found - as described below - that it was not possible in the given apparatus to produce in a homogeneous magnetic field a Cs plasma in which the particle losses were sufficiently small compared with those occurring in the stellarator experiment.

3.3 Particle Losses of a Cs Plasma in a Homogeneous Magnetic Field

In the stationary case the total flux of the particles lost by the plasma volume has to be equal to the total flux of the particles produced at the end plates. Taken as criterion of the plasma losses is the mean lifetime of the particles, i.e. the ratio of the total number of particles to the total input flux. In the density range $10^9 - 10^{12} \text{ cm}^{-3}$ and with a magnetic field of 1.7 kG measurements of the particle density n_0 (Langmuir probe) and of the ion flux Φ (plate) show that the particle flux Φ is proportional to n_0 and the mean lifetime is thus independent of n_0 [MPI-PA-21/64]. Assuming thermal equilibrium with the end plates and an electron layer at the end plates, Φ should, however, be proportional to n_0^2 . In order to account for this behaviour, the influence of the form of the radial density profiles [MPI-PA-13/64], the end plate recombination [MPI-PA-14/64] and the end plate diffusion [MPI-PA-15/64], on the particle loss rate was investigated. The experimental results could not be described, however, until the assumption of thermal equilibrium was abandoned, since at low densities the collision frequency is too small to keep at a sufficiently low level perturbations of the distribution function resulting from diffusion losses and the presence of Langmuir probes [MPI-PA-16/64; 28].

3.4 Equilibrium in Toroidally Closed Configurations

a) "Scallops" (D. Dimock, Princeton)

In toroidal devices in which the strength and direction of curvature of the magnetic field varies periodically in a suitable manner there exists a flux tube of infinitesimally small cross section along which the balancing currents compensate over a spatial field period. Theoretical treatment of the problem in two-dimensional geometry has shown that the balancing currents that do not vanish in the vicinity of this flux tube can be minimized [MPI-PA-18/64]. The calculations are to be extended to the three-dimensional case.

b) $V'' < 0$ Configuration

Toroidal devices were considered in which the confining magnetic field has the property $V'' < 0$ (the condition $V'' < 0$ is identical with the requirement $\nabla_p \cdot \nabla \oint \frac{dl}{B} > 0$, whereby the integral is to be taken along a closed line of force, i.e. $\oint \frac{dl}{B}$ should be a maximum for $p = p_{\max}$). Of particular interest in this respect are those devices in which the current distributions producing the vacuum magnetic field include components which, considered alone, lead to conventional stellarator fields. This affords a simple way of comparing the two devices. Calculations are in progress.

3.5 Ba Plasma

(in collaboration with F.W. Hofmann, Princeton, and A. van Oordt, IPP)

At very low particle densities perturbations of the plasma due to the presence of Langmuir probes can no longer be neglected. The measurements made hitherto in Cs plasmas are therefore to be supplemented by others made in Ba plasmas which enable the particle density to be determined by spectroscopic methods using resonance fluorescence.

3.6 "Ambipol" (F. Karger)

In the Ambipol experimental device investigations into the behaviour of a positive column in a curved magnetic field are being carried out.

a) Theoretical part

In place of the equation describing the problem exactly an approximation was solved analytically first of all. The result shows that the drift motion of the plasma in the curved magnetic field alone causes the particle losses to pass through a minimum as the magnetic field increases, without its being necessary to assume helical instability.

b) Experimental part

The coil systems for producing the magnetic field were completed and installed. Teflon glass sealing for inserting the radial probes was tested, and for introducing the centre conductor (rotational transform) an insulating, extremely thin-walled high-vacuum sealing (sandwich comprising glass, Teflon, stainless steel and ceramic) was designed. Development of a device for blocking the discharge from the pump leads was completed [39]. Towards the end of the report year a start was made to investigating the plasma losses by measuring the longitudinal electric field as a function of the magnetic field.

4. Theta Pinch in Toroidal Magnetic-Field Configurations (M+S)

(H. Bialas, J. Junker, W. Lotz, F. Rau, E. Remy, K.I. Uo⁺, H. Wobig, G.H. Wolf)
(Engineers: H. Finkelmeyer, F. Hartz, H. Schubäck, D. Seewald)

The behaviour of plasmas with high β in toroidal equilibrium configurations was investigated in closed (M+S) and non-closed field configurations (hexapole cusp). The plasmas were produced by toroidal theta pinch discharges (hydrogen, filling pressure 10, 20, 40, 100 μ , temperature in the order of 10 eV, densities of a few 10^{16} cm^{-3}). A purely toroidal and a linear theta pinch were used for comparison purposes [MPI-PA-10/64; 63; 51; 53; 50; 29; 52].

4.1 Theory

4.1.1 Numerical Calculation of the Magnetic Field in the Space Outside a M+S Plasma

Further work was performed on a computing programme for the analytical extension of the magnetic field on a M+S surface into the space outside. This programme is now at the testing stage.

4.1.2 New M+S Surfaces

A more general differential equation enables new M+S surfaces to be calculated, e.g. those with corrugated external contours or else with surfaces unsymmetric in relation to the z coordinate. It is possible to furnish statements on exchange instabilities.

A mechanical simulator ("Matte") for new M+S surfaces was prepared in order to test, for example, the possibility of a rotational transform for M+S.

4.2 Experiments

4.2.1 "Drehfeld" Measuring Station - up to 16 kJ

In order to improve the accuracy and mechanical strength of the coils, the winding technique used in the "Kronen" torus (16-turn uncorrugated theta pinch coil with additional windings for producing the M+S field) was abandoned. A new collector divides the torus circumference into 16 periods, with 12 current bows in parallel connection for each period. This technique was enlisted in the following experiments:

4.2.1.1 "Lupus N" - 4 kJ

This is an ordinary torus (purely toroidal magnetic field) which was used for testing the new bow technique and the collector. Drift velocity (approx. 1 $\text{cm}/\mu\text{s}$) and time-integrated spectrum are comparable with previous results at 4 kJ.

4.2.1.2 "M+S Lupus" ("First Approximation") - 4 to 16 kJ

As "First Approximation" in the M+S lupus programme a glass vessel is used whose surface possesses M+S geometry, so that the plasma is in an equilibrium configuration at the moment of breakdown. With the bows positioned equidistant it was possible in the first half-cycle to observe an extension of the confinement time by a factor of about 3 compared with Lupus N.

+ Guest from the University of Kyoto, Japan

A change in the geometrical arrangement of the bows did not bring any improvement on this result. In the second half-cycle the plasma was pressed at the "neck" against the inner wall of the torus directly after compression; in relation to an ordinary torus the confinement time in this case was extended by a factor of about 5.

In ringing discharges time-integrated spectra showed (faintly) lines of $O\ V$ ($5606/5608\ \text{\AA}$). Under otherwise identical conditions these lines could not be observed in the ordinary torus, but they were in the "Lintus" (cf. 4.2.3.2).

4.2.1.3 "Schalenlupus" ("First Approximation") - 4 to 16 kJ

Probe measurements showed that a significant part of the lines of magnetic force emerged between the bows at the "neck". In order to create a flux tube, the bows were replaced by shaped copper shells. This coil configuration results, however, in excessive ripple of the magnetic field. Immediately after breakdown the plasma contacts the inside of the vessel wall at the "neck" then splits up into several (up to 3) tubes each of which retains its position independently of the others for some time (approx. 4 - 6 μs) before drifting outward. Various modifications on the shells did not result in any improvement.

4.2.1.4 "Schalenlupus" ("First Approximation") - or "Bügelupus" ("First Approximation") with Ψ currents

Induced Ψ currents showed at $40\ \mu$ filling pressure no improvement of the confining efficiency of the said configurations. At $10\ \mu$ filling pressure, however, Ψ currents prevented the above-mentioned splitting. The plasma also showed in this case a greater integral light emission (higher temperature ?) for a period of $10\ \mu\text{s}$, then for a further $10\ \mu\text{s}$ it remained inactive in the middle of the vessel with gradually decreasing brightness. Contact of the plasma with the wall on the inside of the vessel at the "neck" no longer appears to take place. This means that an extension of the confinement time by a factor of about 8 in relation to the purely toroidal theta pinch has probably been achieved.

4.2.1.5 "M+S Lupus" ("Second Approximation") - 4 to 16 kJ (under construction)

The glass vessel for the "Second Approximation", in the M+S Lupus programme, is less corrugated than that of the "First Approximation". The dimensions of this vessel were selected on the basis of an already compressed plasma with M+S configuration; the vessel surface is at a constant distance from the theoretical plasma surface. The field is prevented from escaping by replacing the current bows with copper discs.

4.2.1.6 "Über M+S" (planned)

The M+S contour used hitherto involves unfavourable curvature over the entire outside. Investigation is to be made as to whether the zones of "good" curvature produced by having a wavy effect on the outer contour as well exert a stabilizing influence. This calls for a more pronounced corrugation of the inner contour of the M+S surface. Pathological configurations are prevented by increasing (by approx. 1 m) the major radius of the torus. Since the plasma volume is to remain unchanged, a torus sector is planned. The influence of end losses will be discussed separately.

4.2.1.7 Standard Torus - 4 kJ, with hexapole field - 4 kJ

This non-closed field configuration is a stable equilibrium configuration. Compared with a linear theta pinch (Lintus, cf. 4.2.3.2) it gave a shorter confinement time, which fact can be deduced from the amount of diffusion due to line cusp losses predominant in the present temperature range.

4.2.2 "Zwilling" Measuring Station

4.2.2.1 "Zwilling" Standard Torus - 4 kJ

The investigations of the various magnetic-field probes were concluded and special plasma configurations (trapped fields) measured (for evaluation cf. 4.4.2).

4.2.2.2 "Spinne" - 50 kJ, convertible to 50 kJ + 50 kJ hexapole field

In autumn 1964 the "Zwilling" was dismantled and the reliable capacitor units (Bosch capacitor with "cooled" ignitrons) used to start construction on the "Spinne" 50-kJ apparatus (first as a standard torus with solid single-turn coil).

It was particularly difficult to insulate the collector.

The Spinne apparatus can be put into service at the beginning of 1965. The planned production of shaped M+S coils was not put into effect since the results of the "Second Approximation" have to be awaited.

The incorporation of Joffe wires for hexapole stabilization is still at the planning stage. At the moment it is obvious that the technical difficulties will be immense.

4.2.3 "Quickly" Measuring Station - 4 kJ

4.2.3.1 "Quickly" Standard Torus - 4 kJ (four-turn)

In January 1964 capacitor units with spark gaps (Engineering Department IPP) were again incorporated. These units were not a success and have now been replaced by units with cooled ignitrons. As the winding technique can no longer be used at higher bank energies, Quickly has been abandoned.

4.2.3.2 "Lintus" - 4 kJ

In place of Quickly a linear theta pinch ("Lintus") was installed. At the same volume and with the same discharge conditions this "linear torus" allows a comparison between the linear and toroidal theta pinch (in open field configurations as well). For this purpose spatial mean values of electron density and electron temperature are determined spectroscopically as a function of the time.

4.2.4 Measuring Station T-2 - 4 to 16 kJ

On the T-2 standard torus - first of all with a bank energy of 4 kJ - the distributions in space and time of electron density and electron temperature were determined spectroscopically. (Method: absolute intensity of the continuum at 5000 Å, ratio of the intensities of $H\beta$ to

the continuum). With a filling pressure of 40μ at time $t = 2.5 \mu s$ maximum values $n_{e \text{ max}} = 1.2 \cdot 10^{16} \text{ cm}^{-3}$, $T_{e \text{ max}} = 8 \text{ eV}$ were obtained. The measuring method thus devised is to be used on a standard torus with and without hexapole system (up to $16 + 16 \text{ kJ}$) and on a M+S Lupus as well.

4.2.5 "Limpus" - 380 kJ ? (planned)

Independent of the equilibrium problem, the question arises as to whether exchange instabilities can occur in a plasma in M+S configuration and how high their rates of growth are. For the keV range (Larmor radius stabilization) a linear theta pinch with periodically corrugated "Limpus" coil is therefore planned.

4.2.6 "Copper Plasma"

The plasma is simulated by a copper body in M+S configuration; the outer coil consists of copper discs in parallel with different bores and at various distances from the collector. By varying the coil geometry the condition $|B| = \text{const}$ was optimized on the surface of the copper body. For the best configuration a measuring accuracy of $|\delta B|/|B| \approx 1.3\%$ was obtained. The resulting confinement time of a real plasma would be less than that observed in the M+S Lupus.

4.3 Technical Aspects

4.3.1 "Capacitor Unit with Ignitrons" Fatigue Test

The service life of Bosch MP capacitors (made in 1964) showed an increase by a factor of 10 on those of 1960. This is comparable with that of BICC capacitors, but the latter have a higher internal ohmic resistance.

The ignitron GL 7703 (cooling-water temperature 20°C) withstands an average of 42 000 discharges.

4.3.2 "Spark Gaps" Fatigue Test

In comparison with ignitrons spark gaps have the advantage of more rapid voltage rise and smaller jitter. On the other hand, they have the disadvantage of a very much smaller ignition range. Pressure spark gaps supplied by the Cooke Engineering Company, USA, failed to give satisfactory performance in a fatigue test. The knowledge gained was used for designing new spark gaps for the preionization capacitors in which it is important to minimize jitter.

It has not been possible so far to perform a fatigue test on a spark gap for the main discharge as no apparatus has been available for this purpose in the last few months.

4.3.3 Short-circuiting Device

For reasons of safety capacitors have to be short-circuited when not in use. A short-circuiting device (testing voltage 40 kV, service life $> 10^4$ switching operations under normal conditions) was developed which enables up to 12 electrically separate capacitors to be short-circuited simultaneously.

4.4 Data Processing

Attempts are being made on an increasing scale to process in the IBM 7090 the information gained in experiments. Available for the evaluation of oscillograph curves is a compound table with measuring microscope to which an electronic counter is connected. Data can be issued on 5-bit punched tapes or alternatively on IBM cards.

4.4.1 Preliminary Programme

This programme is intended for punched tapes on the G3 computer and punched cards (under preparation) on the IBM 7090 and provides for rotation of the coordinate system, determination of the time and amplitude zeros, the interpolation of data in a selectable number of equidistant steps and also the issue of interpolated values.

4.4.2 Probe Measurements

The signals of magnetic-field probes enable the distribution in time and space of current, electron temperature and electron density to be calculated (in progress).

4.4.3 Spectroscopy

4.4.3.1 Dispersion Curve

The dispersion curve of the Zeiss 3 prism spectrograph is approximated by a family of overlapping hyperbolae. Wavelengths of unknown lines (e.g. impurities) can be determined.

4.4.3.2 Establishing Electron Density and Electron Temperature from Measurements on the Duochromator

With due allowance for the necessary calibration and correction values, the spatial mean values of electron density and electron temperature are determined by interpolation from the evaluation tables compiled by A. Eberhagen and W. Lünow [IPP 1/23 = IPP 6/20, 1964].

5. Spectroscopy

(K. Bergstedt, C.-R. Vidal)

Measurement of the He I and He II line profiles at electron densities between 10^{16} and 10^{17} cm^{-3} was concluded. As yet it has not been possible to decide whether further evaluation adds to existing knowledge on this score.

Work on the stationary RF discharge was continued by C.-R. Vidal [70; 71]. First the photoelectric measuring technique for recording line profiles was extended to the quartz ultraviolet and the infra-red spectral region. On the one hand, the accuracy was here increased by means of a new recording unit and, on the other, the sensitivity was substantially improved. The improved technique is used for measuring the merging and for recording the infra-red profiles of H and He. Furthermore, preliminary work was concluded which enables the line profiles of both elements in a H - He mixture to be determined simultaneously.

6. RF Plasma Interaction

(H.M. Mayer)

Before H.M. Mayer took leave of absence his work on sheath behaviour in the case of the wide-band probe was described in two laboratory reports [MPI-PA-24/64; MPI-PA-25/64].

7. Vacuum Spectroscopy

(G. Boldt)

The Vacuum Spectroscopy Group under G. Boldt is withdrawing from the Institut für Physik at the turn of the year. Its work is to be continued in the Institut für Extraterrestrische Physik along the same lines but with wider objectives.

7.1 NI Oscillator Strengths in the Region of $1000 < \lambda < 1800 \text{ \AA}$ (F. Labuhn)

The NI absorption oscillator strengths are determined by emission measurements, the connection between "equivalent width", population of the lower state and absorption oscillator strength, referred to as the "growth curve", being used. Serving as light source is a cascade arc operated in defined argon-nitrogen mixtures. The normal intensities required for determining the equivalent widths are produced in the form of black-body radiation with the aid of the same arc. The population is obtained for the NI particle density. The latter in turn is determined by a method which ignores the assumption of constancy in the mixture ratio of argon to nitrogen and also knowledge of any transition probabilities.

This work was terminated last year. The result is absorption oscillator strengths of 35 NI multiplets in the wavelength region of 1000 to 1800 \AA [46; 8].

7.2 Si I, II Oscillator Strengths in the Region of $1100 < \lambda < 2000 \text{ \AA}$ (W. Hofmann)

The original intention was to measure the oscillator strengths of alkali earth ions. For this purpose an apparatus was constructed for defined introduction of alkaline earth into the arc plasma. This was accomplished by heating alkali earth halides to 1000 - 1100°C (with a constancy of $\pm 1^\circ \text{C}$), the ensuing vapour being carried off by argon flowing past on top. When a start could be made on spectroscopic measurements in the cascade arc, it was shown that no observable part of the alkaline earth introduced stays put along the arc axis. Nor would it be any different if the alkaline-earth input were to be increased by an order of magnitude. Since the influence of this unexpectedly powerful "separation effect" can be prevented only by radial modification of the measuring method, the experiment was discontinued in the middle of the year and a start made instead on investigation of silicon.

The introduction of silicon into the arc is performed in principle in much the same way as alkaline earth. Argon passes through a container filled with SiCl_4 and kept at constant (room) temperature, taking the vapour along with it into the arc. The separation effect is not so pronounced here as in the case of alkaline earth, and so lines can be observed in the arc axis. It was found, however, that silicon and solid silicon compounds are deposited on the arc wall. This upsets the constancy of the measurements, limits as a result the maximum quantity of SiCl_4 that can be introduced per second and causes, moreover, a decrease in the silicon concentration along the arc column. Attempts are being made at present to compensate for this drop in concentration by introducing the SiCl_4 vapour in suitable doses at various points in the arc channel.

7.3 Line Wing Profile of the Hydrogen Line Lyman α (G. Boldt, W.S. Cooper)

Measurement of the pressure broadening effect in the hydrogen line Lyman α (at 1216 Å), already mentioned in the last annual report, was concluded. This was done at an electron density of $8.4 \cdot 10^{16} \text{ cm}^{-3}$ and a temperature of 12 200 °K up to a distance of 20 Å from the line centre, and the result was then compared with the various theories available at present. Furthermore, it was possible to detect an asymmetry of the line profile, probably due to Stark effect of quite a high order [MPI-PA-6/64; 9; 7].

7.4 H₂ Oscillator Strengths in the Region of 900 < λ < 1100 Å (G. Boldt, E.H. Pinnington)

Towards the end of this year preparations for measuring H₂ oscillator strengths were begun. A knowledge of these oscillator strengths is a prior condition for the planned extra-terrestrial measurements of the interstellar H₂ density.

7.5 Comparison of Various Intensity Normals in the Vacuum UV Spectral Range

(G. Boldt, F.W. Hofmann)

The two methods of absolute intensity calibration in the vacuum UV range developed a few years ago at the MPI and Princeton are to be compared with one another. Preparations toward this end have already been started.

7.6 Intermittence Effect on Various Photographic Emulsions (K.H. Stephan)

After investigation of the behaviour of emulsion in respect of the Schwarzschild exponent under extreme exposure time conditions and intensity conditions [MPI-PA-19/63] the influence of intermittent exposures was measured with a special polygonal rotating-mirror device.

Tests were conducted as to the dependence of the developed blackening S on the dark-bright time ratio

$$V = \frac{t_D}{t_H}$$

of the light pulse train with constant impinging total energy at various frequencies corresponding to

$$1.2 \cdot 10^{-3} \text{ sec} > t_H > 0.9 \cdot 10^{-5} \text{ sec}$$

and various intensities as parameters in the wavelength range

$$3500 \text{ Å} \leq \lambda \leq 7000 \text{ Å}$$

for the plates:

Perutz Spektral 450/550/680
Perutz Perseno
Perutz Peromnia
Perutz Superomnia
Ilford HPS
Ilford HP3
Ferrania 7200

Experimental work was concluded. An attempt is to be made to combine the results of the two investigations so as to provide a statement on the mechanism of the photographic elementary process.

8. Microwaves

(U. Hopf, F. Klan, G. Landauer, B. O'Brien, M. Tutter)

8.1 Longitudinal Waves (M. Tutter)

a) Experiments were continued with the short waves found at the end of last year in a homogeneously magnetized plasma cylinder. The wave number k was recorded as a function of ω_p/ω and ω_e/ω . The wave modes proved to be rotational symmetric in relation to the tube axis. The onset of the propagation at $\omega_e/\omega = 1$ and the refractive index, which increases as the plasma density decreases, could not be reconciled with any of the known theories. The experiments were therefore abandoned and an improved, more flexible apparatus set up.

b) For the above experiments, on the one hand, and for the Whistler measurements on the theta pinch torus, on the other, certain ideas were put forward and summarized in a laboratory report [MPI-PA-19/64].

c) An experimental device for exciting plasma waves by means of electromagnetic waves in an inhomogeneously magnetized plasma was almost completed. The geometry of the device approximates to that stipulated in the calculation given in the laboratory report [MPI-PA-15/63].

8.2 Resonance Experiment on a Low-Pressure Discharge (B. O'Brien)

Investigations of Tonks-Dattner resonances and plasma cable propagation were carried out on a low-pressure mercury discharge. Calculations based on a simple model agree closely with the experimental results.

8.3 PIG I (G. Landauer)

Of all the discharge types in which the emission of the harmonics of the electron cyclotron frequency of non-relativistic electrons has been observed to date, the Penning discharge has shown the most intense excitation of the spectrum up to high harmonics $n = \frac{\omega}{\omega_e} \approx 45$. Investigations on PIG I were therefore continued.

The field distribution of the static magnetic field was varied by altering the arrangement of the excitation coils. As the inhomogeneity of the magnetic field increases line broadening takes place, but there occurs at the same time a perturbation of the line symmetry which consists in one of the flanks having a less steep rise. If the deviation of the field from homogeneous distribution has roughly the structure of a magnetic bottle (field minimum in the middle of the vessel), each individual line has a flattened flank on the side of higher frequency $f > f_0$ (f_0 = frequency of the line maximum). When the field maximum is in the centre of the vessel and reduction of the field occurs toward the ends of the vessel, the asymmetry seems to shift to lower frequencies ($f < f_0$). This observation was made in measurements of the radiation perpendicular and parallel to the magnetic field and led to the conclusion that the radiation is emitted principally from a zone of the discharge vessel which, viewed axially, is central.

The discharge was operated with disc-shaped and ring-shaped cold cathodes of various diameters (a departure from the previous cathode 80 mm in diam.). This involves changes in the potential condition inside the discharge. Within certain limits these result in

variations in current, voltage and pressure and also influence the spectrum of the harmonics. The principal results are (gas : helium):

- a) More intense excitation of higher harmonics with small cathode diameters, approx. 40 mm (anode diam. : cathode diam. $\approx 4 : 1$).
- b) Decrease in line width as cathode diameter is reduced (limitation of the radiating zone to a smaller area with increased field homogeneity).
- c) Pressure-dependence of the line width could be observed for the first time with several cathodes. The relative line width $\frac{\Delta B}{B} = \frac{\Delta f}{f}$ could be reduced to 1.0 - 1.2 % in the pressure range 10 μ to 40 μ , starting approx. at 2 %.
- d) The pressure-dependence of the entire spectrum could be determined more accurately. At low pressure (approx. 5 μ) harmonics of fairly high number n with very weak intensity are observed first, these being grouped around $n = 12$ as a relative maximum. Then, as the pressure rises, the intensity of the spectrum increases and passes through a maximum, as is already known. At the same time the relative maximum of the intensity distribution shifts continuously from $n = 12$ to $n \leq 5$ at high pressure ($> 30 \mu$) (cathode diam. 110 mm).
- e) As already observed on several occasions, the Penning discharge includes various discharge states whose appearance depends on, among other factors, the operating temperature of the cathodes. The discharge state with the lowest electrode voltage at a given current appears to be most conducive to excitation of the harmonics. Here it is not possible to establish the influence of the cathode temperature on the intensity of the spectrum during operation.

A cathode of the discharge vessel was put on anode potential, thus creating a discharge corresponding to the positive-column type. In the frequency range 10 Gc/s the harmonics $n = 2, 3, 4$ were here measured with intensity which was weaker in comparison with the Penning discharge.

8.4 PIG III (F. Klan)

In microwave measurements on PIG II the occurrence of emission lines at the harmonics of the electron cyclotron frequency was detected at the end of 1963. After a time, however, it was found that it is difficult to obtain reproducible results with the given device. One of the main problems was caused by the strong cathode sputtering, which also rendered it difficult to make headway with one of the major objectives of the glass apparatus, namely measurement of the angular distribution of the radiation. For this reason and several others, the apparatus was modified. Efforts were made to provide for the following:

1. Reliability and reproducibility of the discharge at high currents as well.
2. Reduction of cathode sputtering and the resulting impurities on the vessel wall.
3. Simple cleaning of the vessel.
4. Straightforward installation and dismantling of the vessel and all auxiliary equipment.
5. Limited bakeability (up to 200 °C).
6. Highly homogeneous magnetic field.

In order to accomplish these objectives the following measures were adopted:

1. Viton sealing used instead of metal.
2. Design of a water-cooled cathode system with exchangeable cathodes.
3. Design of mobile magnetic coils.
4. Incorporation of a more powerful pump system.
5. Changeover to short-time operation of the discharge (pulsing).
6. Alteration of the potential distribution in the discharge region.
7. Use as cathodes of materials that do not readily sputter.

All of these measures have been initiated, a large part being already finished. The cathode system, for instance, has been successfully tested in the new discharge vessel, the discharge operating reliably and with good reproducibility at currents of up to 4 A. It is expected that conversion will be complete before the end of 1964.

The following experiments were prepared in the course of this year and are to be implemented in the very near future:

1. Investigation of the dependence of microwave emission on the potential distribution in the discharge region.
2. Measurements involving extremely homogeneous magnetic fields.
3. Transmission measurements.
4. Investigation of radiation with 4-mm radiometer.

8.5 Miscellaneous (U. Hopf)

1. A new type of microwave generator (Laddertron) was put into service and its output determined (5 to 15 watts in the 35-Gc/s band).
2. The millimetre wave measurements on Hoke II were continued.
3. Two new devices with special antennae and lenses for measurements on the RF-excited plasma were constructed; the antennae and lenses were investigated with a reflection method at 35 Gc/s.
4. Diffraction phenomena at metal strips of various widths (8 - 62 mm) were measured at 70 Gc/s. The results agreed closely with M. Tutter's calculations.

8.6 Use of Microwave Technique on Physico-chemical and Biochemical Problems

(N. Kaiser as guest)

It was possible to improve considerably the recording stability of the previously described bridge method with highly sensitive detector (B. O'Brien). The reflection method (N. Kaiser Report 1962) also already described was modified by M. Tutter with regard to its evaluation and programmed by Miss Bock in such a way that this method can be used for small quantities of substances with low damping.

Besides measuring the absolute values of the damping and the phase relationship, the bridge method was also used for effecting the continuous, simultaneous and highly sensitive recording on the change in these values in various measuring subjects of interest. The result of measurement of the viscosity change of pure water in dependence of the temperature, already announced in the annual report for 1963, could be improved in accuracy. Moreover, the photochemical effect of the UV irradiation of trans-dichlorethylene was recorded. What is involved here is probably a polymerization process. In the biochemical field the change

in the measurement values during the conversion of gelatin solutions from the sol to the gel state was determined. Measurement of the changes in value involved in the metabolic process caused by coagulation of citrate blood during a heparin tolerance test was just as feasible as the attempt to follow the coagulation process of pure blood in vitro, which was carried out under largely physiological conditions and practically completely sealed off from the air.

After measurement of the relevant reflection values the dielectric values of the measuring subjects and the changes in them during the above-described reaction were determined.

9. Electronic Workshop

(K. Moustafa, J. Machate, H. Utzat)

The following are some of the devices developed and constructed:

The appropriate logical circuit was produced for transferring the measurement results of the Ferranti counter to an IBM card punch (026b). The system developed is also suitable for tape punch operation. The unit was provided with a card-counting device.

For the Drehfeld torus a rapid two-channel differential integrator with Nuvistors was developed for magnetic field probe measurements. Moreover, several auxiliary electronic devices were constructed for field measurements involving special plasma profiles (H. Bialas).

A high-voltage trigger device with a time lag of 60 nsec altogether was built for the spark chamber. In addition, logical circuits for synchronizing the spark chamber with the camera as well as rapid counters and control devices were designed and put into service. A high-voltage trigger device fitted with semiconductors is being developed.

A calibrator with an accuracy of 1 % was designed and built for high-precision measurement of the pulsed field in the bubble chamber with the aid of the rapid integrators and analogue digital converters supplied by Adage.

Also developed for field measurements were a high-grade rapid 10-channel pulse height meter with adjustable thresholds and also a calibration generator (accuracy 2 %). The accuracy of this meter is better than 1 %. In addition, an integrator and symmetry converter were made for measurements with Rogowski coils.

In order to synchronize the bubble chamber with the proton-synchrotron in Saclay a timer was constructed and put into operation.

A screening system was developed for use when operating photomultipliers in the vicinity of high pulsed fields.

Also designed and constructed for the bubble chamber were a temperature indicator, a voltage and resistance converter with servo motor and also various timing and delaying units.

For the Microwave Group 1 and 100-kc/s quartz-stabilized oscillators with synchronous time signal outputs were developed. In order to balance various microwave measuring units a noise indicator was constructed. Also produced were a 100-kc/s amplifier, a square-wave generator and also various power units for supplying intermediate-frequency amplifiers.

For the Hourglass a double coincidence circuit for operation with frequency counters was developed. A quadruple coincidence circuit is being developed.

EXPERIMENTAL PLASMA PHYSICS 3 (PROF. DR. R. WIENECKE)

1. Summary

The experiments involving the ohmic heating of a stationary plasma in which the thermal-conductivity losses are reduced by an axial magnetic field were continued in the report year. The first partial objective, a stationary H_2 arc with an axial temperature of $\sim 10^5$ °K, was achieved. Efforts were directed principally toward verifying and supporting provisional results by using various measuring methods. Comparison with theoretical results generally showed most satisfactory agreement. - In the case of the helium arc the radiation transport phenomena exerted such an influence not only on the energy balance and temperature profile, but also on the measuring methods for the temperature, that at present it is not worthwhile continuing with the He experiments. Also considered were ways of achieving a further rise in temperature, since ohmic heating leads to temperatures of only a few 10^5 °K owing to the increasing electric conductivity.

Another set of problems was concerned with the magnetohydrodynamic conversion of energy. The crux of the problem here is to obtain as high an electric conductivity as possible at the lowest possible temperatures of the gas sample, as are possible for instance, in a nuclear reactor. Interesting possibilities are afforded by a stream of rare gas injected with an alkali metal (concentration ≈ 1 %). Since the collisions between electrons and the heavy atoms are almost exclusively of an elastic nature, the efficiency with which the thermally produced electrons lose their energy gained in the electric field of the generator is poor because of the large difference in mass. This brings about a rise in the electron temperature T_e and thus a higher degree of ionization as well as higher electric conductivity. Measurements of this effect actually showed an increase in T_e when a power source was connected to the generator from outside and no magnetic field was present. The existence of a magnetic field gives rise to complications, which can probably be attributed to inhomogeneities and boundary effects. Various individual aspects were investigated both theoretically and experimentally. With a device of greater flow cross section a better version of the temperature rise effect is to be expected.

The work of the third group is concerned with the interaction of shock waves and magnetic fields and is closely connected with problems of energy conversion. Experiments with T tubes provided the initial basis for these experiments. In the past, however, it was found that the plasmas thus produced are unsuitable for the purpose intended here. Final measurements with a Mach-Zehnder interferometer and microwave reflectometer provided very interesting information on the physical behaviour of electromagnetically produced shock waves. This confirms the experience which we have had in past years. Interactions with magnetic fields, magnetoplasma dynamic energy conversion in particular being given prominence, are much easier to follow when carried out with shock waves set up by a diaphragm shock tube. Theoretical studies on the reflection and passage of shock waves through spatially limited magnetic fields indicate a wide range of possibilities for such investigations. The diaphragm tube complete with magnetic field has been constructed and tested, and so measurements can be started in the near future. The work will proceed in close conjunction with the stationary conversion investigations and will afford a worthwhile supplement.

In the report year work on the interior of the laboratory block L 5 and the rectifier centre L 5 E was completed. Some of the office facilities could be occupied by the middle of December.

The size of the staff in the Department did not increase in the report year to any appreciable extent. Working in the Department as guests were: Z. Celinski (Warsaw), Dr. R. Hodgson (Vancouver). Accepting an invitation from Stanford University, California Prof. Wienecke was absent from March till October.

2. Stationary Heating of High-Density Plasmas

(S. Witkowski)

2.1 Helium Arc in a Magnetic Field (C. Mahn, S. Witkowski)

Electron density and temperature were determined first of all from the intensities of a He I and a He II line (annual report for 1963) in a helium arc, already described in previous annual reports (400 amperes, approx. 1 cm in diam., 10 - 20 cm long), in an axial magnetic field of $23 \text{ k}\Gamma$. With the Saha equation minimum values of temperature and density are obtained, with the corona formula maximum values. In the absence of information on the entire radiation field of the arc this method did not provide more accurate data.

It was therefore decided to try and determine the temperature from the intensities of two carbon ion lines (C III and C IV) for which the corona formula would be valid with close approximation. For this purpose a few percent of a gaseous carbon compound (methan, acetylene) was admixed with the helium. However, perturbing impurities appeared, the cause of which could not be explained. The arc temperature, moreover, was influenced beyond control by the carbon added and in the end no C IV line occurred so that this method did not achieve its object either.

As the contribution of the radiation to the energy transport in the case of a helium plasma in our range would complicate the energy balance to an extraordinary degree and probably make determination of the thermal conductivity impossible, even if an exact temperature profile were available, the experiments with helium were discontinued for the time being. The apparatus was converted for hydrogen operation and fitted with a ring anode of higher capacity. This now allows operation of a hydrogen arc of 1000 A in a magnetic field of $32 \text{ k}\Gamma$.

2.2 Hydrogen Arc in a Magnetic Field (C. Mahn, H. Ringler, G. Zankl)

Investigation of the hydrogen arc (2000 amperes, approx. 3 cm in diam., approx. 10 cm long) in an axial magnetic field of $10 \text{ k}\Gamma$ was continued. The temperatures calculated from the line intensities of the "thermometer" helium on the basis of the Saha-Boltzmann equation are certainly too low. Owing to the low He concentration rather does the corona formula represent here a closer approximation. Axial temperatures of roughly $90\,000 \text{ }^\circ\text{K}$ are obtained with it.

Assuming the validity of the corona formula, more exact values for the axial temperature should be obtained from the ratio of the intensities of a C III and a C IV line. In order to produce these lines a small quantity of methane was admixed with the hydrogen. Besides the photographic method used hitherto, a photoelectric method of recording the spatial intensity distribution of spectral lines was tested.

The Doppler shifts of the lines of added argon and nitrogen, which, as already stated in the annual report for 1963, point to rotations of the arc column, led to azimuthal velocities of a maximum $3 \cdot 10^6$ cm/sec. Image converter photographs and the time dependence of the intensity of spectral lines - recorded with monochromator and multiplier - in various parts of the arc show that no spiral-like structure is present, but that the arc rotates as a cylinder about its axis.

The spatial distribution of the potential was measured with tungsten probes fired at high speed through the arc. The thus determined axial component of the electric field strength is 2.5 V/cm, while the radial component is up to 200 V/cm. The surprisingly high value of the radial field strength agrees closely with the value of the "induced" field strength $[\underline{v} \times \underline{B}]_r$, calculated from the measured azimuthal velocity and axial magnetic field.

After many setbacks another apparatus in which an arc is operated at magnetic fields of up to 30 kG and in which the arc profile can be observed at various distances from the cathode now works reliably. Spectroscopic measurements are so far available (owing to the absence of an adequate power supply) only for a magnetic field of 16 kG and an arc current of 1200 A.

For the purpose of further heating, work is proceeding on preliminary experiments aimed at reducing the pressure in the experiment vessel while the pressure in the arc is roughly constant. This involves introducing the gas through a hole in the tungsten cathode. The main portion of the gas leaving through the anode is pumped off (at high pressure) separately from the quantity which leaves the arc as a result of diffusion in a radial direction.

2.3 Calculation of the Characteristic of a Hydrogen Arc in a Magnetic Field with Due Allowance for the Radiation (U. Heidrich)

In respect of a cylindrically symmetric hydrogen arc on which a strong homogeneous magnetic field is superimposed in the axial direction, the current-voltage characteristic and the radial temperature profile were obtained by numerically integrating the energy balance. Three different models were calculated, varying significance being attached to the radiation losses.

The results show that for fully ionized plasma the amount of electric power required per unit column length for axial temperatures exceeding approx. $2 \cdot 10^4$ °K is substantially reduced owing to the lowering of the thermal conductivity perpendicular to the magnetic field. For an arc in hydrogen atmosphere, for instance, with a pressure of $5 \cdot 10^4$ dyn/cm², a radius of 2 cm, a superimposed magnetic field of 20 kG and an axial temperature of 10^5 °K a power input of approx. 3.5 kW/cm is required, the energy loss due to radiation being approx. 0.5 kW/cm. Without an external magnetic field, on the other hand, the power requirement is approx. 200 kW/cm.

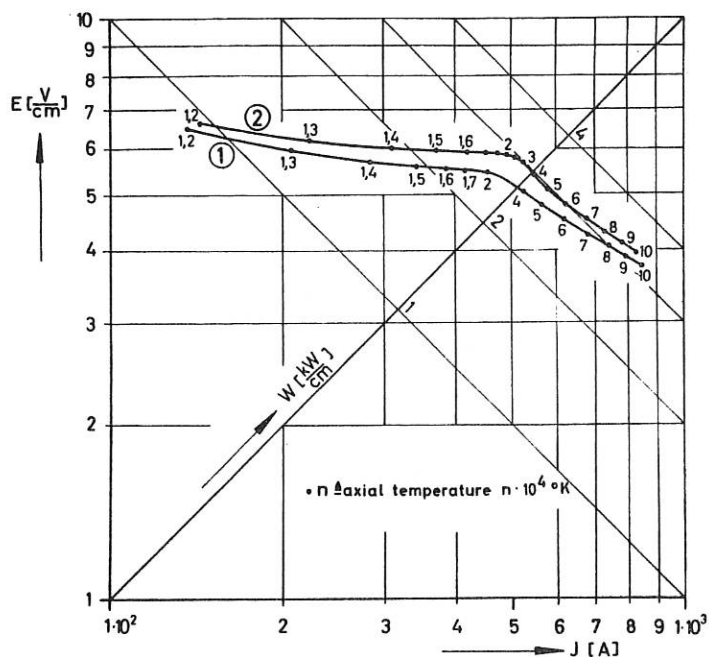


Fig. 1 Current-voltage characteristic of a hydrogen arc in a magnetic field with (2) and without (1) regard to the radiation losses. $B = 20 \text{ k}\Gamma$, $p_a = 5 \cdot 10^4 \text{ dyne/cm}^2$.

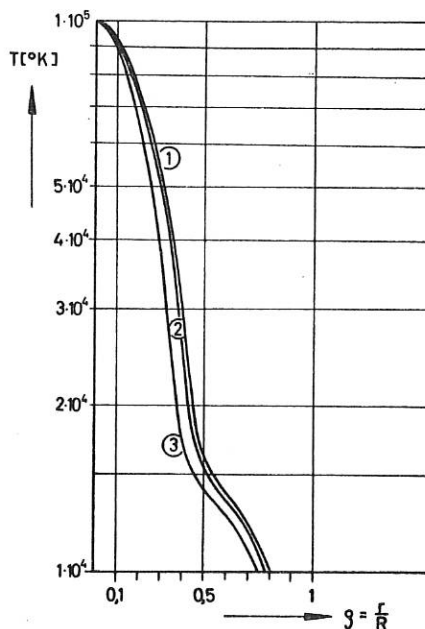


Fig. 2 Temperature profiles of hydrogen arcs in a magnetic field with ((2) $R = 1 \text{ cm}$, (3) $R = 2 \text{ cm}$) and without (1) regard to the radiation losses. ($R = \text{arc radius}$), $B = 20 \text{ k}\Gamma$, $p_a = 5 \cdot 10^4 \text{ dyne/cm}^2$.

2.4 Doppler Temperature Measurement (K. Büchl)

For determining the ion temperature from the Doppler width of suitable spectral lines with the aid of a Fabry-Perot interferometer an apparatus was constructed which enables the interference fringes to be recorded with photomultipliers. As yet the results of the temperature measurements are not available.

2.5 Experimental Investigations of the Pressure Profile in a Hydrogen Arc with Superimposed Magnetic Field (H.F. Döbele, S. Witkowski)

This work serves as experimental confirmation of the pressure rise in a hydrogen arc with superimposed axial magnetic field which was calculated by R. Wienecke. Between a tungsten cathode and a water-cooled copper anode a 10-cm long hydrogen arc is run at a current of 200 A. The pressure in the discharge chamber outside the arc is 7.5 or 15 torr, the magnetic field 8 to 12.5 k Γ (Fig. 3).

The temperature and electron density profiles were measured. The results obtained by various methods agree with one another within the measuring accuracy. For various distances from the arc axis the pressure was determined with a mercury gauge connected to a small boring in the anode.

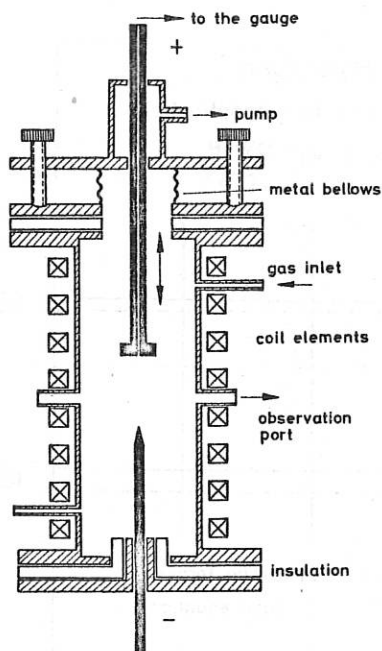


Fig. 3 Principle of the experiment for measuring the pressure profile in a hydrogen arc.

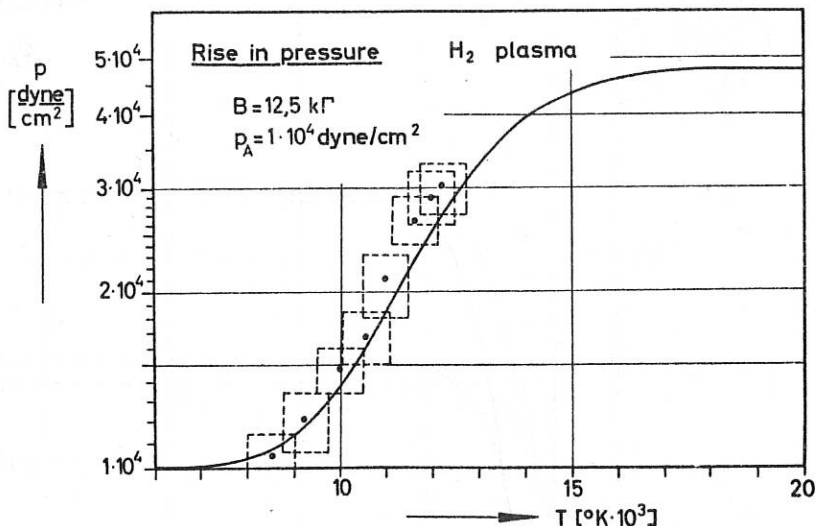


Fig. 4 Calculated and measured pressure profile in a hydrogen arc with magnetic field.

Fig. 4 represents the pressure profile calculated for the parameters $p_A = 7.5$ torr, $B_A = 12.5$ kΓ in comparison with the measured values. For other parameter values as well the measured data agree closely with those calculated.

2.6 Consideration of the Pressure Increase in an Arc Column with Superimposed Axial Magnetic Field (S. Witkowski)

In the annual report for 1962 an account was given of calculations of the pressure profile in a cylindrical arc column with superimposed axial magnetic field. The condition for these was local thermal equilibrium (validity of the Saha equation). At low pressure this assumption will often not be valid. For the other limiting case, namely validity of the corona formula, appropriate calculations were therefore made [IPP 3/23]. As ionization takes place later than in the case of the Saha formula the pressure does not rise till higher temperatures are attained. In both cases, however, the maximum pressure increase is about the same.

In Fig. 5 calculations with the corona and Saha formulae were compared for an external pressure $p_A = 1 \cdot 10^4$ dyne/cm² and magnetic fields of 10 kΓ and 50 kΓ.

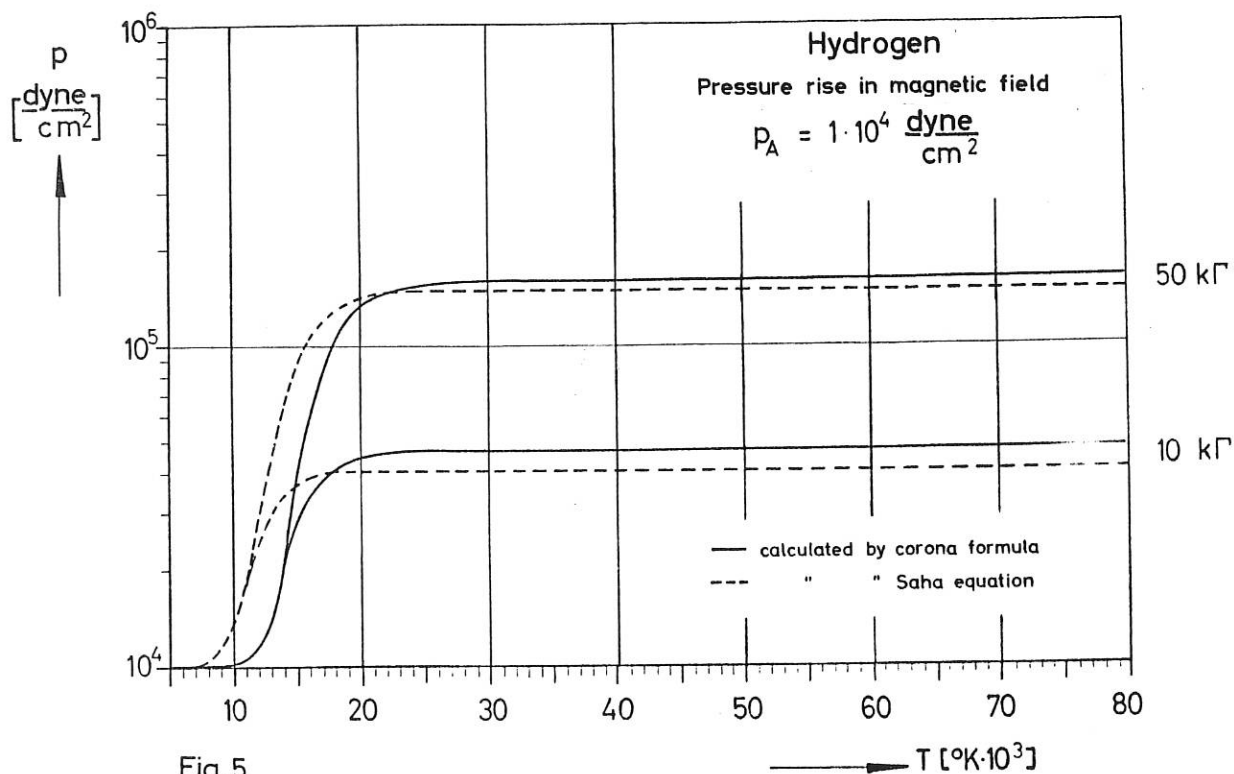


Fig. 5

25/14

Fig. 5 Comparisons between the results obtained by the Saha and corona formulae.

2.7 Velocity Measurement by "Colouring" a Plasma Beam (H. Salzmann, G. Zankl)

Experiments with the method described in the annual report for 1963 were continued. It was found that chromium which was electro-deposited on a tungsten wire and suddenly evaporated by a capacitor discharge made a suitable "colour". In the light of the Cr resonance line (4250 Å) highly reproducible multiplier signals were obtained which could be assigned to a sharply defined sheath moving at a velocity of about 50 m/sec. The velocity is almost constant in a wide area around the axis of the beam and does not drop till the boundary of the (luminous) beam is reached. Streak photographs with a drum camera showed, however, in addition to this photoelectrically observed sheath other luminous fronts in the plasma which are propagated at different velocities altogether. At present attempts are being made to explain the causes of this phenomenon.

2.8 Population of Energy Levels with Due Allowance for the Radiation Field (S. Ramer)

In treating this problem it was necessary to confine attention first of all to hydrogen. In this simplest of cases the intention is to investigate the interaction between the population of the discrete levels and the radiation field and to devise a method for simultaneous solution of the relevant equations. The basic idea is as follows: First of all the radiation field of the most important lines is calculated by integrating the radiation transport equations, reasonable population of the energy levels being assumed (e.g. according to Saha-Boltzmann). With the radiation field obtained in this way the solution is then improved iteratively.

So far a computing programme has been developed for calculating the population at known radiation intensities. For a few special cases the population was calculated with this programme under, among other conditions, those for the radiation assumed by McWhirter et al., but with newer, more reliable values for the collision cross sections. In keeping with the smaller values of these collision cross sections the deviations from the Boltzmann distribution are greater than those obtained by McWhirter.

The computing programme is kept so flexible that atoms other than those of hydrogen can be treated as well, if the relevant collision cross sections and transition probabilities are known.

3. Magnetoplasmdynamics

(M. Salvat)

3.1 Theoretical Studies on Raising the Electron Temperature in a Rare-Gas Alkali Generator

(M. Salvat, G. Brederlow, W. Ohlendorf)

Direct conversion of nuclear energy into electric energy is in principle possible with the aid of a MHD generator. In order to achieve adequate electric conductivity at temperatures which are technically feasible in nuclear reactors, however, the electron temperature T_e has to be raised above the gas temperature. As is already known, this is possible in rare-gas alkali plasmas of low temperature because the energy gained by the electrons in the effective electric field is lost again very inefficiently when they are involved in elastic collisions with neutral atoms.

In order to appreciate the possibilities of raising T_e in rare-gas alkali generators, basic consideration was given first of all to this mechanism and these ideas were applied to various generator configurations. Since the measurements described in 3.2.1 did not agree with these theoretical results, a microscopic theory of T_e increase was devised (with the assistance of Dr. Feix, Theory Dept.). Apart from minor deviations, however, the result was the same as in the macroscopic approach.

Also investigated was the possibility of attaining sufficient electric conductivity in a generator operated with a pure stream of rare gas without alkali injection. A preliminary ionization requires an auxiliary discharge which prior to the entry of the working gas into the generator yields a sufficient number of electrons. The temperature of the electrons is then raised in the effective electric field of the generator, thus enabling them to increase the degree of ionization. The calculations have not yet been completed, but already they indicate the possibility of such a process.

In the generators with a channel cross section of 1 - 1.5 cm² operated hitherto, perturbations as a result of wall effects became noticeable up to distances of 1.5 - 2 mm from the wall. For this reason it is necessary to construct a generator with a cross section of ≈ 5 cm² and a start has now been made to preliminary planning. At a flow velocity of 660 m/sec. the gas flow rate should be about 100 g/sec. For reasons of cost it is necessary to have a closed cycle. The gas should be heated by a plasma jet with an output of 150 kW.

3.2 Measurements of Electron Temperature and Conductivity in the Argon-Potassium Plasma of a MHD Generator (G. Brederlow)

In order to test the theory of T_e increase in an argon-potassium plasma stream, T_e was determined both spectroscopically by the line reversal method and by measurement of the conductivity. The generator described in the annual report for 1963 was used for the measurements.

3.2.1 Measurements of the Electron Temperature in an Electric Field without Magnetic Field (G. Brederlow, W. Riedmüller)

If an external electric field was set up between the electrodes without the magnetic field being brought into operation, measurements at current densities in excess of 1 amp./cm² showed an electron temperature rise agreeing with the theory. At current densities of less than 1 amp./cm² the increase was substantially smaller than expected in theory. The measured electron temperature and the electron temperature calculated from the conductivity were in agreement over the entire current density range. Moreover, the influence of contamination of the argon-alkali plasma by N₂ on the rise in electron temperature was investigated. Since energy transfer from electrons to neutral-gas molecules is highly effective in inelastic collisions with impurity molecules, a substantially smaller rise in electron temperature can be expected whenever a small amount of N₂ is added. The measurement results showed a more pronounced drop in electron temperature than calculated.

3.2.2 Measurements of the Electron Temperature and Electric Conductivity in a MHD Generator and with Applied Crossed Electric and Magnetic Fields (G. Brederlow, R. Hodgson)

Owing to the limited $[\underline{v} \times \underline{B}]$ e.m.f. it was possible to achieve a maximum current density of 0.4 amp./cm² in the MHD generator channel. No increase in the electron temperature was recorded, however, although the measurements described in 3.2.1 point to a rise of 10 %. The cause of the discrepancy can be attributed to short-circuit currents in the plasma and distortions in the current distribution. The voltage drop at the electrodes can also be increased by the magnetic field with the result that the effective field in the plasma is reduced. In order to eliminate or clarify these sources of perturbation, the geometry of the measuring system was altered and an adjustable external field set up in addition to the $[\underline{v} \times \underline{B}]$ e.m.f. At the same time probes could be used to determine the potential distribution in the channel. It was now possible to cover a current density range of up to 10 amp./cm². Measurements showed that at the same current densities the conductivity rise and thus the electron temperature rise as well decreases as the magnetic field increases (Fig. 6). This behaviour is unexpected and so far unaccounted for. The probe measurements showed an increase in the voltage drop at the cathode as the magnetic field increased. Initial results were dealt with in conference papers.

3.2.3 Electron Temperature Distribution in a Segmented Argon-Potassium MHD Generator (F. Fischer)

From the electron temperature distribution in the generator channel it is possible to determine the current density distribution. If the electron temperature distribution is known short-circuit currents in the plasma and the distortions in the current distribution can therefore be established on the basis of the high $\omega \tau$ values.

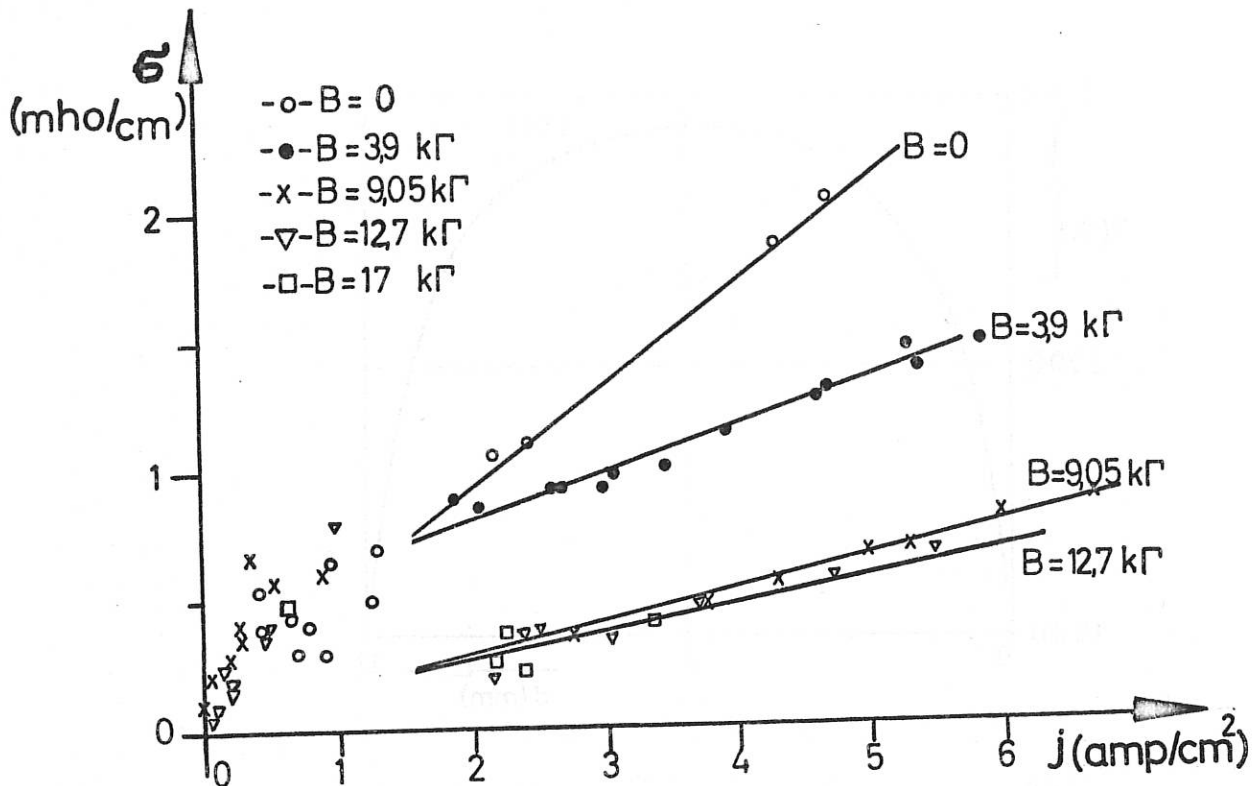


Fig. 6 Conductivity as a function of the current density for various magnetic-field strengths.

Construction of the MHD generator and measuring device is in progress.

3.3 Measurements of the Temperature and Velocity Profiles in a MHD Generator (Z. Celinski)

In a generator completed at the beginning of the year the spatial distribution of the $[\underline{v} \times \underline{B}]$ e.m.f. induced in the magnetic field was measured with probes and, \underline{B} being known, the flow profile was determined accordingly. The measurements showed a steep drop in the flow velocity near the wall within a region of less than 1 mm. Moreover, in the same device with W-Rh thermocouples it was possible to measure the temperature profile. In Fig. 7 the temperature and velocity profiles are plotted against the width of the channel. It can be seen that the influence of the wall on the velocity distribution is much smaller than on the T profile, this being due partly to the relatively poor thermal insulation of the channel walls.

3.4 Vector Representation and Analysis of the Principle of Various MHD Generator Types (Z. Celinski)

With the aid of a vector diagram representation the principle of the three known types of generator (continuous and segmented electrodes, Hall generator) was examined more closely. The Hall coefficient $\beta_e = \omega_e \tau_e$, the load factor K and a geometry factor are the parameters. For any generator, electric conductivity being assumed, it was a simple matter to represent geometrically the relationship between the electric field present in the generator and the current density [IPP 3/19, 3/20, 3/21].

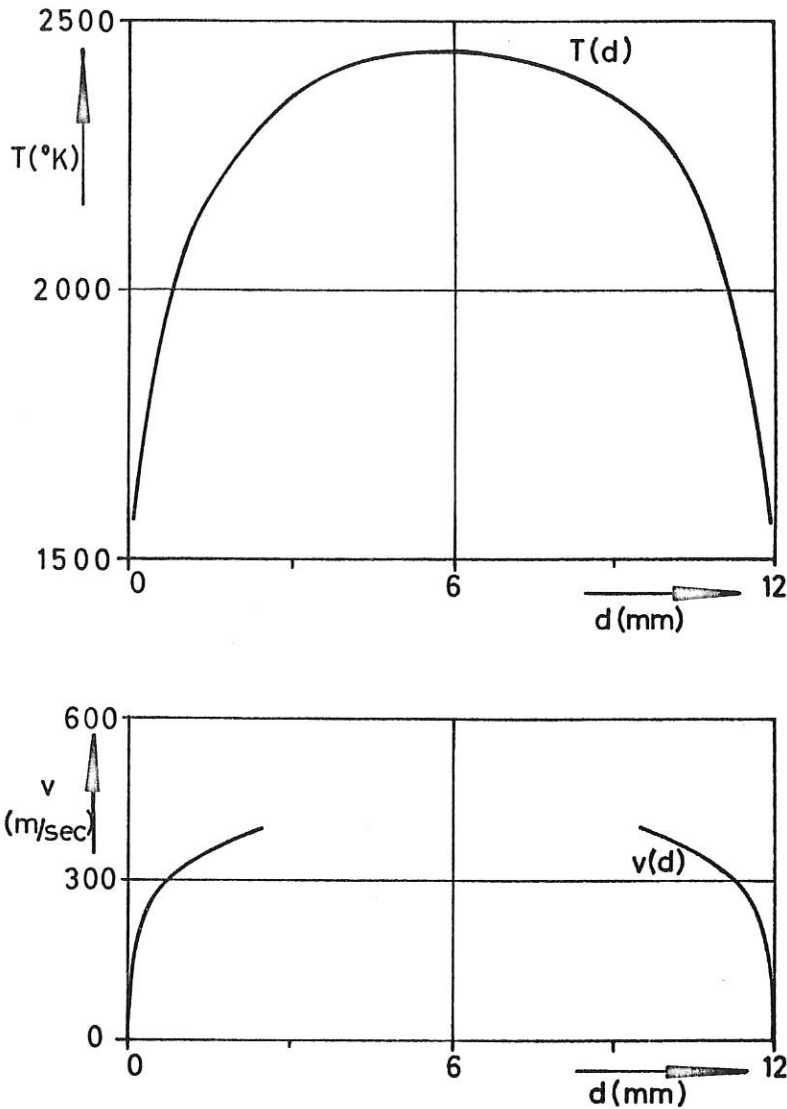


Fig. 7 Measured temperature and velocity profiles in the MHD channel.

3.5 Two-Dimensional Analysis of the MHD Generator with Segmented Electrodes

(Z. Celinski, M. Fischer)

Proceeding from the fundamental equations, the local current density and the potential field were calculated with the aid of the IBM 7090 for a generator with segmented electrodes. Included in the calculation as parameters are the geometric quantities and the Hall coefficient β . It was possible to illustrate the result in many individual representations. So far calculations have been made on the assumption of constant temperature and thus of electric conductivity as well. It is planned to extend calculations to allow for the process of increase in T_e .

3.6 Calculation of the Transport Properties of Weakly Ionized Rare-Gas Alkali Plasmas

(R.T. Hodgson)

The transport properties of an argon-potassium or argon-caesium plasma can be derived from the Boltzmann equation if a slight perturbation is observed which is superimposed on the equilibrium case of the Maxwell energy distribution (for the electrons). For the IBM 7090 a programme was compiled which gives the mobility tensor of such a plasma as a function of the electron temperature and pressure, potassium atom concentration and the magnetic field. The cross section for momentum transfer between electrons and argon or electrons and alkali atoms were taken from the literature. In addition, use was made of an expression of Frost¹⁾ which gives the collision frequency between electrons and ions.

3.7 MHD Generator with Non-thermal Radio-Frequency Ionization (W. Ohlendorf)

Last year it was attempted with the aid of a capacity-coupled RF energy to ionize a cold, flowing gas so as to produce adequate conductivity and thus to make energy conversion possible. With a suitable choice of RF parameters it is possible to maintain a stable homogeneous discharge in the entire generator at pressures up to about 0.1 atm. and with magnetic fields of up to $\approx 20 \text{ kG}$. The flow velocity was as high as 300 m/sec; the RF generator was operated at a frequency of 100 Mc/s. The discharge can be maintained up to atmospheric pressure, but above 0.1 atm. increasing pressure causes instability and inhomogeneity. In the region of 1 atm. the generator is no longer completely filled by the discharge. The instability and inhomogeneity of the discharge at high pressure seem to be caused by the non-thermally emitting electrodes.

During operation the RF plasma produces at the MHD electrodes DC voltages in the order of the $[\mathbf{v} \times \mathbf{B}]$ e.m.f. which depend in an indeterminable way on the gas pressure, gas velocity and magnetic field. The reason for this is the uneven heating of walls and electrodes.

As the e.m.f. of the generator with segmented electrodes is extremely small, only a Hall generator, whose open-circuit voltage may be in the order of 10^3 volts, can be considered for practical use.

3.8 Plasma Acceleration (G. Hahn, M. Salvat)

In the $\mathbf{j} \times \mathbf{B}$ acceleration of a plasma beam issuing from a plasma jet it was possible to measure from the $[\mathbf{v} \times \mathbf{B}]$ e.m.f. by means of two tungsten probes introduced laterally the velocity field of the beam. Difficulties were encountered with the acceleration itself as the accelerating electrodes do not afford adequate electron emission and the transverse discharge changed into an undesired arc discharge even at relatively low currents. This can probably be overcome by electrodes of thoriated tungsten [IPP 3/22]. The experiment had to be interrupted in early summer as G. Hahn returned to France to do his military service.

1) L.S. Frost, J. Appl. Phys. 32, 2029 (1961)

4. Shock Wave Experiments and Problems of Non-stationary MHD Conversion

(H. Muntenbruch)

4.1 Investigations of a Rail Spark Gap (L. Liebing)

Experimental investigations of this problem could be concluded as early as 1963 (v. annual report for 1963). Theoretical evaluation of the measurement results was continued. The tilted position of the current sheath in the spark gap is due to the Hall effect. The inclination of the current sheath toward the electrodes results in the gas initially at rest being accelerated in the direction of the cathode on entering the sheath. This in turn results in the accumulated gas being able to get behind the current sheath by "rebounding" from the cathode without penetrating the sheath itself. A balance of energy, momentum and mass affords close agreement with results arrived at by various measuring methods.

4.2 Investigation on T Tubes

4.2.1 Interferometric Measurements (H. Brinkschulte)

Whereas in 1963 technical considerations limited observations to a narrow range at a distance of 50 cm from the discharge gap, it has meanwhile proved possible to extend the scope of interference figures to practically the entire T tube and thus to record the time dependence ($x = x(t)$) of the shock wave [IPP 3/24]. This was realized by using rectangular tubes made from glass plates of sufficient optical quality. In this way an entire cross section of the discharge tube could be observed at the same time.

Further to the statements made in the annual report for 1963 evaluation of the streak interferograms showed the following:

- a) The shock wave is reproducible (!) but not the discharge plasma behind it.
- b) The density discontinuity in the front corresponds to that calculated from the discontinuity conditions, dissociation and ionization being allowed for.
- c) The refraction index of atomic hydrogen was measured and corresponds to that calculated quantum mechanically.
- d) Behind the shock front equilibrium sets in immediately (H_2 , $p_0 = 5$ torr, $5 < M < 20$), and the Saha equation is applicable.
- e) At the higher velocities the discharge plasma forces its way right to the shock front. At the lower velocities it remains well behind the shock front. The distance between shock front and luminous front cannot be derived from a "piston model".
- f) In the vicinity of the spark gap electrons ($n_e > 10^{17} \text{ cm}^{-3}$) occur in the shock front, but soon the index of refraction is determined by the heavy particles.
- g) In an oscillating discharge the succeeding half-cycles also set up shock waves, which then interact with the first one in a way that is not evident from the luminous phenomena.
- h) The streak photographs perpendicular to the direction of flow reveal that the shock fronts are slightly curved and have a radius corresponding to the distance from the spark gap (spherical waves). With the tube dimensions selected (3 - 5 cm) and at a distance of 50 cm they are practically flat. There are no wall effects.

It is planned to finish off these investigations by testing individual shock waves (which are set up by a power crowbar system and in the wake of which noothers follow) as to their homologous behaviour. Initial measurements of reflections promise interesting results as well.

4.2.2 Microwave Investigations (W. Makios)

Series measurements were carried out on shock waves in hydrogen with the 4-mm microwave reflectometer (annual report for 1963) and the results were compared with those of Brinkschulte and Makios.

Doppler effect measurements of the velocity showed that at initial pressures of 1 to 5 torr with low Mach numbers ($5 < M < 8$) the luminous front reflects, while at higher velocities ($12 < M < 20$) the 4-mm waves are reflected by the shock front itself. In the intermediate region ($8 < M < 12$) the shock front is partially permeable, and so the two velocities can be determined from beats.

For this medium range the electron density in the shock front could be determined exactly to a factor of 2. The results confirm entirely the other investigations and complete the picture.

These investigations are to be continued in the form of transmission measurements. Developed for this purpose were both rectangular discharge tubes of glass and plexiglass (plates $n \cdot (\lambda/2)$ thick) and a special coupler which enables the power distribution in the branches of the transmission interferometer to be set to full advantage. Moreover, new antennae and slits for "bunching" the waves were designed and tested, and the technique for producing them was considerably improved.

4.2.3 Measurement of Currents and Magnetic Fields (H. Kolig)

Quite a number of measuring methods (Langmuir probes, $\underline{v} \times \underline{B}$ probes etc.) can be substantially impaired by currents in a shock wave plasma or discharge plasma. The distribution in space and time of the currents in the T tube was therefore determined with magnetic probes by measuring the magnetic fields interlinked. These measurements, too, were carried out in H_2 . Use of a power crowbar system (and simultaneous streak photographs) greatly facilitated interpretation of the signals.

Although the measurements show that practically the entire discharge current remains between the electrodes those parts drifting with the discharge plasma (max. approx. 10 %) are still in the order of up to 20 kA. Their strength decreases approximately linearly as the distance from the electrodes becomes greater and is highly pressure-dependent. At a distance of 20 cm currents could no longer be measured. The results indicate, moreover, that existing motion theories are invariably one-sided in their treatment of these phenomena.

4.3 Diaphragm Tube Device for Investigating the Interaction between Shock Wave and Magnetic Field

Investigations of interaction first require an initial plasma of known properties. In order to produce such a plasma a start was made in 1963 to planning and constructing a diaphragm tube device (annual report for 1963). All aspects of this experiment were set up and elaborated in 1964:

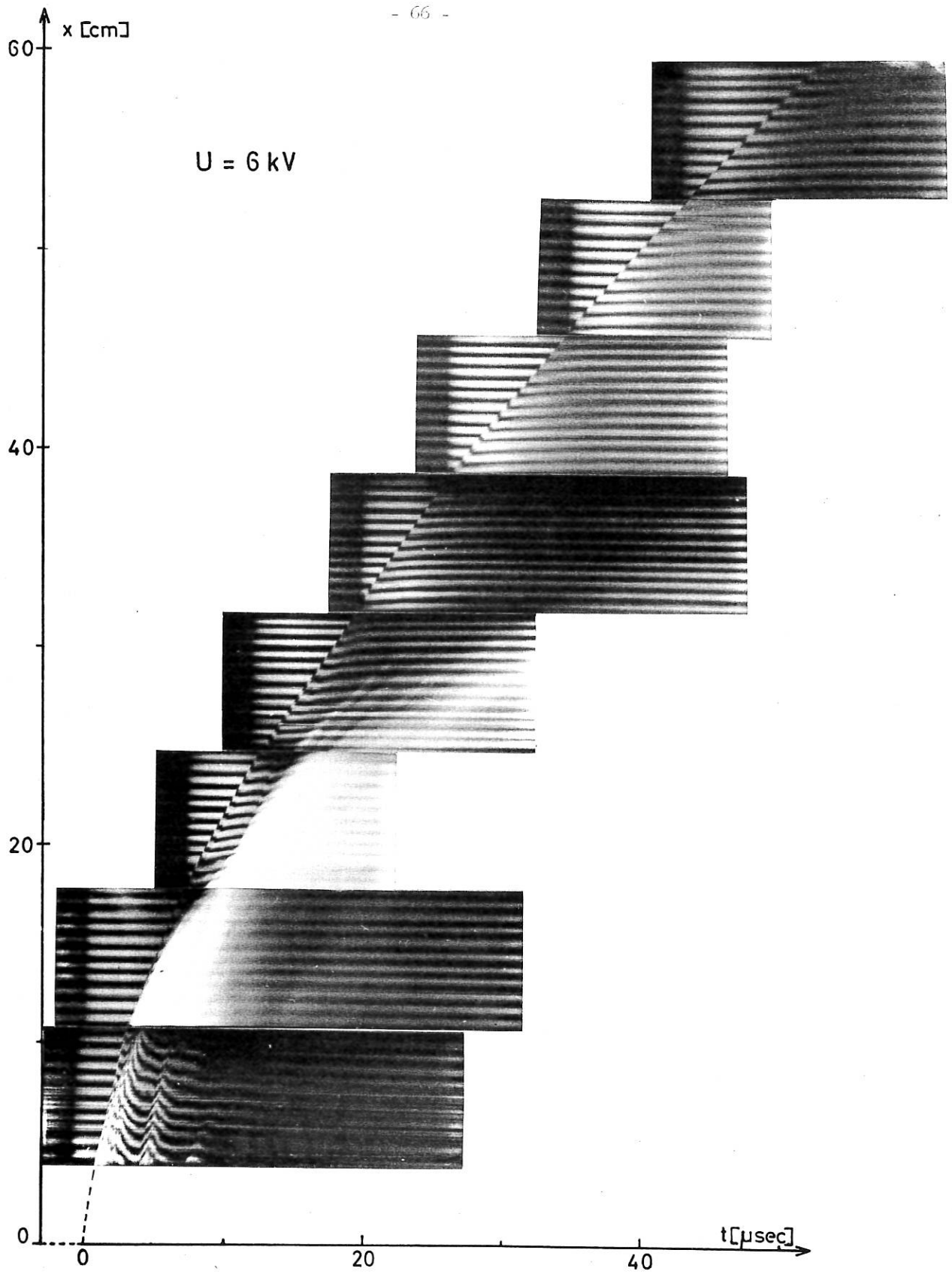


Fig. 8 Interference figure of the path-time distribution of a T tube shock wave in hydrogen ($p_0 = 5$ torr).

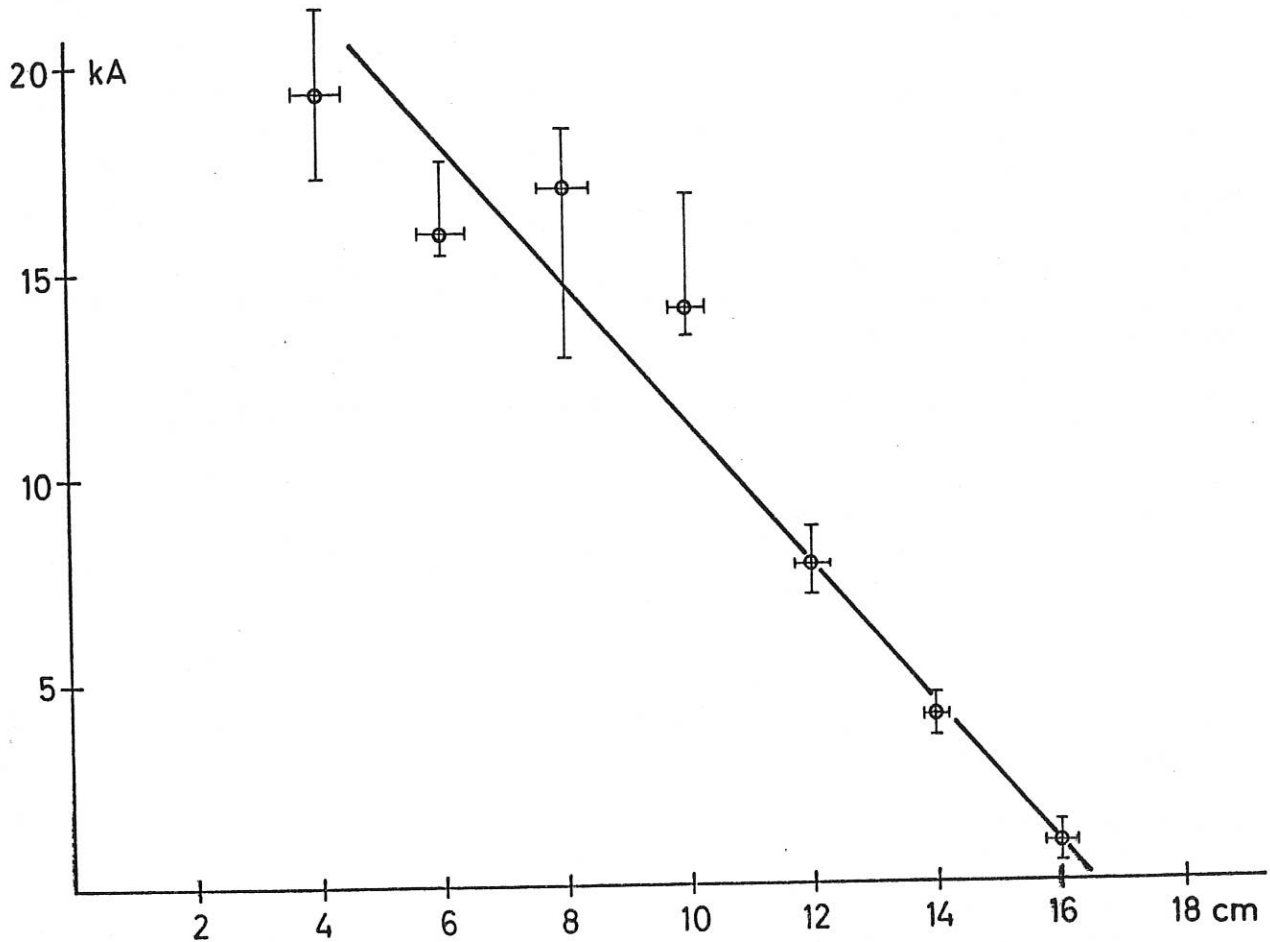


Fig. 9 Ring current in the discharge plasma as a function of the distance from the electrodes ($p_0 = 0.3$ torr, max. main discharge current 152 kA).

4.3.1 Theoretical Consideration of the "Reflection" of Shock Waves in Magnetic Fields
(E. Rebhan)

In collaboration with the Theory Department it was possible to extend and improve on the rough estimates (minimum magnetic field, required shock Mach number). A method was developed for determining individually the gas-dynamic phenomena occurring (shock waves, rarefaction waves, energy and momentum input).

With the entry of the shock front into the magnetic field an interaction is initiated which is at first essentially in an unsteady state, but which then gradually assumes a stationary character once the front has left the field at the other end. Investigation is made of the asymptotic final state in which the strengths of the shock and rarefaction waves involved have assumed values constant in time and the flow in the field region is stationary.

The method consists in linking together in a suitable manner the gas-dynamic conservation laws for the transitions at field and waves so as to determine thereby the nature and strength of the reflected waves. - Energy input leads to acceleration, momentum input alternatively to slowing down or acceleration of the primary shock wave.

4.3.2 Preliminary Experimental Investigations (H. Brinkschulte)

By way of clarifying a few problems that are particularly difficult to follow theoretically, especially in connection with electron emission and electrode falls, shock waves were produced in a T tube with electrodes in the side walls perpendicular to a magnetic field, these waves leading in hydrogen, $p_0 = 5$ torr, $M = 10$, B approx. 5 kG , electrode surface area $3 \times 10 \text{ cm}^2$, to short-circuit currents of approx. 5000 A and 20 μsec duration. Traces indicate that an arc discharge is involved which (as expected) appears to be inclined between the electrodes. This yielded important information for the design of measuring chambers in the diaphragm tube.

4.3.3 Calculation of the Optimum Dimensions for the Device (P. Javel, H. Nett)

The device is designed in such a way that the measuring time in the chamber is determined by the reflected shock wave, in no case by the reflected rarefaction wave. The ideal dimensions were calculated; the measuring time covers as well the passage of the contact discontinuity through the measuring chamber.

For a whole number of gas combinations that might be suitable for the investigations the jump values and shock Mach numbers were calculated as a function of the initial pressure condition and represented in graph form. Calculations were made with and without allowance for dissociation and ionization.

4.3.4 Technical Problems of the Diaphragm Tube (P. Javel, H. Nett)

When the diaphragm bursts the high-pressure end of the tube is subjected to a thrust of 5 to 10 t, which is transmitted along the tube to the sensitive measuring chamber. The inrushing gas causes considerable forces at the dump tank as well. These are uncoupled (from the measuring chamber) by telescopic sections at either end of the tube.

In close collaboration with the Engineering Department two measuring chambers were developed, a few control points being provided in the form of intermediate sections for connecting various kinds of diagnostic equipment. The Engineering Department developed a coil system for producing magnetic fields and a capacitor bank (20 kJ) as power supply.

For triggering the measuring devices a unit was developed to deliver pulses the time delay of which is determined by the velocity of the shock wave.

Gas warning signals act as a safety precaution in work with hydrogen at high pressure.

4.3.5 Initial Experiments (H. Nett)

In some of the intermediate sections piezoelectric probes were incorporated which, once some experience had been gained in their production, gave signals with a rise time of approx. 1 μsec . They indicate pressure jumps of as little as a few torr. - Investigations of the shock waves with these probes showed that the measured velocities agree with those calculated within the measuring accuracy (better than 1 %). This also makes it possible to calibrate the pressure probes, which till now could not be performed in any other way.

Density measurements with a differential interferometer and also shadow and schlieren investigations can be started before long.

5. Construction of Laboratory Block L 5 and Rectifier Centre L 5 E

(H. Dickopp, H. Muntenbruch, R. Wienecke, S. Witkowski)

Planning was completed in 1963 and by December the shell was ready so that in the report year work could proceed on the interior of the two buildings. In collaboration with the construction department of the Institute, the architect and the construction department of the TH it was possible in planning and implementing detailed work to make use of a great deal of experience gained in the erection of previous Institute buildings. Furthermore, allowance could be made for requirements which had meanwhile arisen in the course of experiments.

Although completion was scheduled for March 1965 moving in began as early as December 1964.

THEORY (PROF. DR. A. SCHLÜTER)

1. Summary

In 1964 work on the interaction of radiation and plasma became particularly wide in scope. This was in large part due to the application of powerful lasers for plasma diagnostics and to their possible use for heating and ionization. As it is not always feasible to divide this kind of work between "microscopic" and "macroscopic" treatment an appropriate report will be given in a separate section. Investigations of those aspects emphasized hitherto were continued: numerical plasma dynamics and microscopic derivation of stability criteria and kinetic equations. Contact with the experimental groups was further enhanced by the collaboration of other theorists in the work of these groups.

Dr. Hertweck took charge of the computing system as successor to Dr. Hain. Dr. Gorenflo accepted responsibility for supervising the programmers, O. Eder for training them.

2. Macroscopic Theory

2.1 Two-Dimensional Theta Pinch Calculations (F. Hertweck)

With the theta pinch programme already described in the annual report for 1963 axial contraction in antiparallel magnetic fields was treated. It was found to be practical to study the motion of the plasma by integrating the macroscopic velocity field, whereby particle trajectories $\mathcal{W}(\mathcal{W}_0, t)$ are obtained. If the snapshots of the particle distribution are transferred in succession to a cine film the dynamics of the phenomenon can be made visible by running off the film strip. Figs. 1 and 2 show two snapshots taken at the moments of successive maximum compression ($t = 0.58$ and $1.08 \mu\text{sec}$).

Furthermore, the theta pinch programme was used to study the occurrence of resistive instabilities in the presence of antiparallel magnetic fields. The initial condition was a current sheath i.e. a B_z magnetic field passing through zero, with the secondary condition.

$$\int_0^{r_{\text{coil}}} B_z r dr = 0$$

and an equilibrium distribution

$$p + \frac{B_z^2}{8\pi} = \text{const}$$

of a plasma of constant temperature. Perturbation was caused by superimposing a statistical equilibrium field (mean velocity approx. $0.2 \times$ thermal velocity). Figs. 3 and 4 show the level chart for $t = 0.04 \mu\text{sec}$ and $t = 0.27 \mu\text{sec}$. It is seen that in agreement with the theory the wavelength with the highest rate of increase is of the order of the sheath thickness. This programme is to be used to help in studying the influence of dynamics on the resistive instabilities.

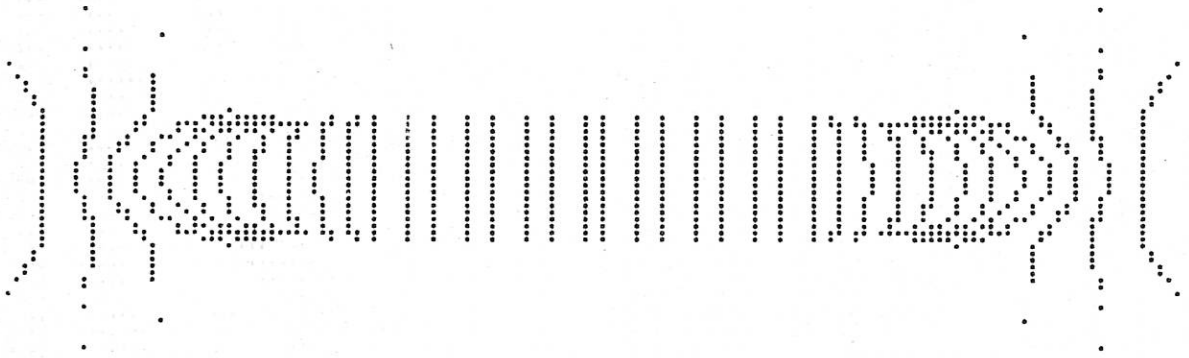


Fig. 1 $t = 0.58 \mu\text{sec.}$

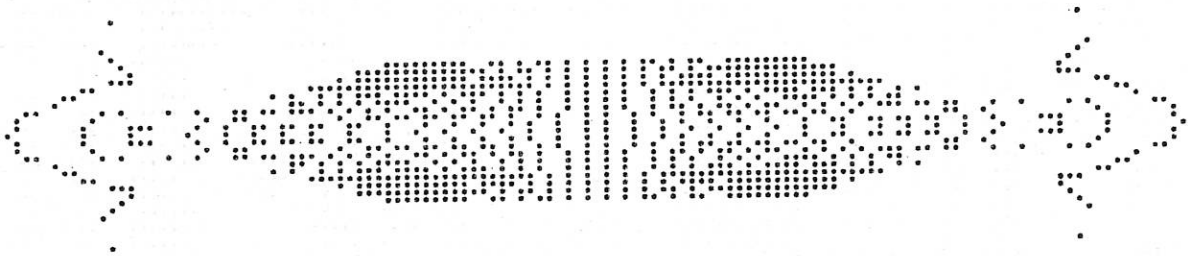


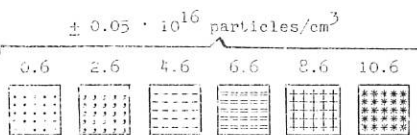
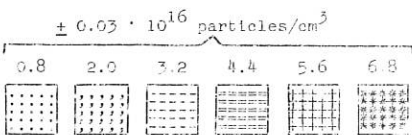
Fig. 2 $t = 1.08 \mu\text{sec.}$

The figures show two snapshots of the locations which at the outset are in a meridian plane of evenly distributed points ($t = 0.58 \mu\text{sec}$ and $t = 1.08 \mu\text{sec}$ are moments of successive maximum compression).



Fig. 3 0.07 μsec

Fig. 4 0.42 μsec



The figures show the density distribution in the current sheath. The signs represent various density levels.

2.2 One-Dimensional Pinch Calculations (H. Fisser)

Pinch calculations were again initiated in order to determine the parameters of the theta pinch discharge at fixed energy content of the capacitor bank in such a way that the thermal energy content of the plasma is maximum. Since at fairly low initial densities the compression oscillations can bring about gyro relaxation heating, calculations should be made with anisotropic ion pressure.

2.3 Transport Coefficients (W. Feneberg, H. Fisser)

Investigations of the transport phenomena in the plasma with a magnetic field present were continued in order to derive for the electric and thermal conductivity analytical and sufficiently exact expressions. As early as 1963 it was shown that with the 13-moment approximation without magnetic field the result is an electron thermal conductivity which is smaller by a factor of 1.6 than that given by Spitzer and Härm. From the supplementary note¹⁾ by R. Landshoff to his paper²⁾ on transport coefficients in the plasma it is seen that the electron thermal conductivity approximates within a few % to the Spitzer-Härm value, if the distribution function is developed according to Hermitian polynomials to and including the fifth order. In the case of the Lorentz gas, unfortunately, it was found that in the presence of a magnetic field this approximation yields values for the thermal conductivity which exceed the exact value by a factor of up to 3. At present a check is therefore being made to find what number of Hermitian polynomials is necessary for reproducing the correct distribution of transport coefficients also when a magnetic field is present.

2.4 Equilibrium with Plane Magnetic Fields (R. Gorenflo, P. Merkel)

The investigation of plane magnetohydrostatic equilibria with complete separation of magnetic field and plasma was continued by R. Gorenflo [IPP 6/14; 26]. In his dissertation P. Merkel devised a new method (v. Dept. 1, sect. 5 of this report).

2.5 Stability of M+S Surfaces (D. Pfirsch, H. Wobig, MPI)

The stability behaviour of a M+S surface was investigated, the starting point being a general differential equation for the M+S equilibrium and the energy principle. Only those perturbations were considered which leave the energy of the magnetic field unchanged, so that outside walls have no stabilizing influence on these perturbations. It was found that with closed lines of magnetic force such perturbations are always possible on the surface. Moreover, the area calculated by F. Meyer and H.U. Schmidt proved to be unstable when subjected to these perturbations, the plasma splitting up along a line of force. In order to achieve stability in the presence of these perturbations there have to be areas of favourable curvature along each line of magnetic force. It was possible to give an adequate criterion of stability. The method used is valid also for other equilibria with $\beta = 1$. Preparations are being made to extend the method to asymmetrical M+S surfaces and to perturbations with variation of the magnetic-field energy.

1) Phys. Rev. 82,442 (1951)

2) Phys. Rev. 76,904 (1949)

2.6 Diffusion of a Plasma in a Magnetic Field (G. Knorr, D. Pfirsch)

The Frieman time scale method was used to solve the time-dependent diffusion problem for a plasma. Serving as a basis is the two-fluid model. The case of the linear cylindrical plasma was discussed. Work is being done toward applying the theory to a toroidal plasma.

2.7 Equilibrium between Surface Currents (Magnetic Laval Valve) (W. Lünow)

In connection with the problem of determining the external coil configuration of a slim magnetic LAVAL valve the equilibrium between a current distribution flowing on the plasma surface about the axis and a surface current distribution coaxial to it and representing the external coil was described in terms of an integral equation which was solved numerically in approximation.

3. Microscopic Theory

3.1 Microinstabilities in Homogeneous Plasma (D. Pfirsch MPI)

For a plasma without magnetic field a necessary and sufficient stability criterion for purely transversal waves was derived and general statements made on certain simple anisotropic distributions. For wave propagation parallel to an external homogeneous magnetic field a necessary and sufficient stability criterion was also given and for wave propagation perpendicular to a magnetic field it was possible to give a sufficient criterion of instability. In these cases as well the examples investigated were simple anisotropic distributions.

3.2 Kinetic Equations

3.2.1 Derivation of Kinetic Equations by Time Scale Formalism (S. Priess)

The investigations begun in the preceding year by D. Frank, D. Pfirsch and S. Priess on the derivation of kinetic equations by means of the time scale formalism from the Liouville equation were continued.

a) Derivation of kinetic equations from the Liouville equation

On the basis of several examples the mathematic formalism of the Frieman-Sandri¹⁾ method and the Su²⁾ method was discussed as a way of solving the BBGKY equations [MPI-PA-7/64]. It was shown that there is justification for the scepticism as regards the automatic satisfaction of the integrability condition with this method. This shortcoming can in many cases be eliminated by a less restricted initial condition.

1) E.A. Frieman, Princeton University, Rep. Matt-106 (1962)
E.A. Frieman, J. Math. Phys. 4, 410 (1963)
G. Sandri, "The Foundations of Nonequilibrium Statistical Mechanics",
Lecture Notes, Rutgers University (1961 - 1962)

2) C.H. Su, "Kinetic Theory of Weakly Coupled Gases",
Thesis in the Department of Aeronautical Engineering, Princeton University 1964

b) Irreversibility with reference to the Liouville equation

A method of expanding a function depending on N particles into certain correlation terms was devised. With this method and the appropriately applied time scale formalism of Frieman and Sandri kinetic equations, such as the Landau and Master equations, can be derived directly from the Liouville equation, that is, without resort to the hierarchy equations. This approach includes the Frieman-Sandri and also the Balescu-Prigogine¹⁾ methods. For the case of poor interaction and spatially homogeneous systems the Liouville equation was solved to the second order in the interaction parameter ($=$ ratio of the mean potential energy to the mean kinetic energy of the random particle motion). The solutions allow simultaneous discussion of the H functions which are obtained by the N particle function or by the single-particle function formed by integration from the N particle function and by the Master function. The result provides an interpretation of irreversibility within the framework of the Liouville equation as phase mixing between the individual systems of the virtual whole described by a Liouville function.

3.2.2 Kinetic Equations and Correlations (P.P.J.M. Schram)

Investigations on the kinetic equation for a plasma in a homogeneous magnetic field were concluded [IPP 6/15, 68]. A report summarizing the theory of kinetic equations and correlations was compiled [68].

3.3 Spatial Correlations (M. Feix, K. von Hagenow, W. Kegel, P.P.J.M. Schram)

3.3.1 Classical Treatment of the Spatial Correlation Function of a Single-Component

Plasma (K. von Hagenow)

The investigation mentioned on page 192 of the annual report for 1963 was continued. With regard to long-range potentials a correction of the first order could generally be determined in the plasma parameter for the Debye potential.

Application to a classical electron plasma gives a positive two-particle function finite for all distances. The interaction energy thus calculated agrees with that obtained by Salpeter, Abe et al. by means of cluster expansion. The correction factor for the Debye value includes the logarithm of the plasma parameter.

3.3.2 Quantum Theoretical Treatment of Thermal Equilibrium (K. von Hagenow)

The method mentioned in section 3.3.1 can be applied to the quantum mechanical effective potential according to v. Hagenow-Koppe [30]. The expression thus obtained for the interaction energy includes in the logarithmic correction factor the ratio of the thermal de Broglie wavelength to the Debye length instead of the plasma parameter, the other terms being the same as in the case of the classical plasma (section 3.3.1). This investigation formed the subject of a paper read in summer 1964 at the Physics Colloquium of the University of Kiel. It is possible here to apply this method to a two-component plasma, and such plans are afoot.

1) I. Prigogine, R. Balescu, "Irreversible Processes in Gases" I, II, III, Physica 25, 281, 302 (1959); 26, 145 (1960)

3.3.3 Correlation in Non-equilibrium (M. Feix, K. von Hagenow)

The generalized Nyquist theorem (Kubo et al.) makes it possible to calculate the spectrum of the density fluctuations in time and space in thermal equilibrium from the expected density value in the presence of an external perturbation in the linearized approximation, i.e. for approximate determination of the correlation all that is necessary is to solve the linearized Vlasov equation. This relationship was extended to spatially homogeneous non-equilibria: It was possible to give a simply determined function whose expectation value in the presence of an external perturbation provides the correlation in this case as well, in agreement with a result arrived at previously by Rostoker.

A report on this subject was given by M. Feix at the Conference of the Plasma Division of the A.P.S. in New York, Nov. 1964.

3.3.4 Correlations and Scattering Cross Section (W.H. Kegel, P.P.J.M. Schram)

The scattering cross section for light scattering in a plasma is determined by the spatial correlations. With this in mind P.P.J.M. Schram and W.H. Kegel determined the spatial correlations in a two-component plasma in non-equilibrium, once with the aid of the hierarchy equations and once with the aid of the test particle method. In the special case where the ions and electrons have a Maxwellian distribution it was shown that for $T_e < T_i$ "anti-screening" occurs. This means that the spatial electron-electron correlation function reverses the sign at a certain distance [IPP 6/28, 69].

3.4 Electrostatic Instability (H. Völk)

Within the framework of the investigations on (electrostatic) microinstabilities an extremum principle put forward by Dawson and Oberman was extended to the general case of a spatially one-dimensional plasma. It was shown that this variational method generally seems to represent only an extremum principle and not a genuine minimum principle. It is equivalent to determining marginally unstable solutions of the linearized Vlasov equation. In this connection the Penrose criterion was again derived and given an informative interpretation. An analogous, likewise necessary and sufficient criterion is obtained for the case of a plasma in a homogeneous magnetic field. Treatment of the trapping instabilities involved essentially the same results as those of Rosenbluth and Krall. In conclusion, the stability behaviour of one-dimensional electrostatic waves (Bernstein, Greene, Kruskal) was investigated. According to this method a large class of these solutions should also be unstable. A paper was published [70].

3.5 Thermalization by Coulomb Collisions (B. Lamborn)

A study was made of the momentum and energy changes which a particle undergoes as a result of multiple Coulomb collisions. If the spatial integration is not extended to a maximum impact parameter, but to a fixed maximum value of the shortest distance achieved, the integration can be effected analytically using the velocity in a Maxwell plasma.

As the resulting equations preserve the symmetry between field and test particles they are suitable for describing energy transport and thermalization in a multi-component system [IPP 6/17].

3.6 Theory of the Resonance Probe (H.K. Wimmel)

Work on the theory of the resonance probe (annual report for 1963, laboratory report [IPP 6/11]) was concluded. The results were announced in the form of a conference paper [IPP 6/16, 75] and a publication [76].

3.7 The Adiabatic Approximation to the Motion of a Charged Particle

3.7.1 Motion in a Time-Constant Inhomogeneous Magnetic Field (P.P.J.M. Schram, H. Völk)

The motion of a particle, e.g. in a mirror field, is distinguished by several characteristic times, namely the gyration time, the travel time between the mirrors and the period of precession on the surfaces of constant $|B|$. The method of Frieman and Sandri seems to be best suited to the problem. The aptness of this method for the present problem is due to the fact that the expansion parameter chosen has to be time-dependent, namely in accordance with the solution of the order zero. Among other things, the results give the Alfvén approximation. Higher orders involve the characteristic difficulty of meeting the consistency condition for equality of the cross derivatives after various times and at the same time avoiding secularities which would violate the constancy of the longitudinal invariant. Similar problems in the kinetic theory are not so harmful in their context because they do not destroy the relaxation into equilibrium. This obstacle is to be overcome by extending the method.

3.7.2 The Adiabatic Invariant for the Time-Dependent Harmonic Oscillator (G. Knorr, D. Pfirsch)

The differential equation for the harmonic oscillator with time-dependent ω , which at the same time also describes the motion of a charged particle in a homogeneous magnetic field variable with time, was converted into a Volterra-type integral equation. The solution can then be represented in the form of a Neumann-type series which converges absolutely. This means that the variation of the adiabatic invariant μ for various asymptotic limiting cases can be discussed:

- a) very small and very rapid variations in ω ;
- b) very slow variation in ω .

3.8 Thermal Deviations from the Holtsmark Line Profile (H.K. Wimmel)

The revised formula for the thermal deviation from the Holtsmark line profile (annual report for 1963) was numerically evaluated, agreement being obtained with the results of V.I. Kogan. This was followed by a short publication [75].

4. Radiation and Waves

4.1 Non-linear Plasma Optics

4.1.1 Coherent Scattered Light (W.H. Kegel)

The investigations on light mixing (non-linear coherent scattered light) in a plasma with external magnetic field were concluded and outlined in a report together with the theory of linear scattering [IPP 6/21, 40].

4.1.2 Incoherent Scattered Light (A. Salat)

On the basis of a system of equations including the single-particle character of the plasma investigation of incoherent non-linear scattered light of the second order was terminated. Because of too low intensity the combination frequencies involved do not seem to be experimentally accessible.

4.1.3 Light Mixing in Finite Plasma Volumes (A. Salat)

Under the influence of two monochromatic laser beams there occur in the plasma as a result of non-linear effects density fluctuations with sum and difference frequencies. If the latter is set equal to the plasma frequency the amplitude increases as a result of resonance to such an extent that the plasma oscillations can be verified on the basis of the scattered light which arises on illumination by a third beam. The advantages and disadvantages of two or three-laser systems in relation to intensity, angle sharpness and the requirements for experimental realization were investigated [66 c, 66 d].

4.1.4 Emission of the Second Harmonic (A. Salat, A. Schlüter)

Under the influence of an external light source scattered light of double the frequency occurs in the plasma as a result of non-linear effects. When a coherent light source (laser) is used partial waves from various points of the scattered volume are in phase only for a certain angle of emission. Since this angle depends solely on the ratio of plasma frequency to light frequency the electron density can be determined by measuring the angle. Intensity and angle sharpness were investigated [IPP 6/30, 66 a 66 b].

4.1.5 Direct Numerical Treatment (W. Lünow, A. Schlüter)

The system of non-linear partial differential equations which describes exactly a collisionless electron gas of temperature zero in interaction with an electromagnetic field was solved numerically for various initial and periodic boundary conditions.

4.2 Interaction with Laser Radiation

4.2.1 Heating Plasmas with Laser Radiation (H. Hora)

Earlier estimates by Basov and Krokhin, Engelhard, and Dawson as to whether plasmas can be heated with giant laser pulses to temperatures of interest for thermonuclear conditions were continued from the standpoint that the high radiation field strengths bring about a resonanceless ionization [IPP 6/32].

4.2.2 Ionization of Gases by Laser Radiation (H. Hora, D. Pfirsch MPI)

Further to the experimental results of Meyerand and Haught and also other authors showing that in helium, neon and other gases with pressures of 1 to more than 10^2 atm. laser radiation with field strengths of between 10^6 and 10^7 V/cm causes ionization, a consistency study was conducted on the basis of a model. In the cases mentioned, electrons, which primarily are spontaneously present, absorb the light and lose energy to the gas as a result of collisions.

4.2.3 Absorption Constants of Dense Plasmas (H. Hora)

In order to clarify the optical properties of plasmas with densities of between 10^{17} and 10^{23} cm^{-3} and temperatures of between 10 and a few 10^4 eV when subjected to ruby laser light, the absorption constants and refractive indices for the light elements up to neon were calculated from the macroscopic linearized equations of the two-fluid model with collisions. These were compared with the absorption constants of a microscopic plasma theory and those of the inverse bremsstrahlung processes, with due allowance for the induced emission [IPP 6/27].

4.3 The Harmonics of the Electron Cyclotron Frequency in Plasmas (E. Canobbio, R. Croci)

Suggested in 1963, the model of the emission of intensive radiation from a plasma at the harmonics of the electron cyclotron frequency, first reported in 1961 by G. Landauer, was further developed. Investigations were concerned in particular with

1. the microscopic dispersion relation of the plasma and
2. the radiation emitted by an electron moving in a spiral path in a medium with a certain refractive index.

a) The dispersion relation for the system of the Vlasov and Maxwell equations was solved within certain density, temperature and frequency ranges for directions of propagation which are virtually perpendicular to the direction of the magnetic field [IPP 6/26]. The unperturbed distribution function is generally regarded as a Maxwell distribution. The longitudinal waves, however, are considered as well in plasmas with beams and anisotropic temperature. In the immediate vicinity of the harmonics quasi-longitudinal waves were found with wavelengths shorter than the gyration radius of the thermal electrons. These very waves are of interest in explaining the measured radiation.

b) The mean value in time of the output of the gyrating electrons was calculated as the sum of the quantities originating from the various waves which may be propagated in a plasma. It was shown that the radiation derives essentially from the above-mentioned longitudinal waves. Calculations are being continued.

4.4 Dispersion at the Harmonics of the Cyclotron Frequency (B. Lamborn)

At high electron temperatures measurements of the phase shifts of microwaves apparently give too low values for the density of the hot electrons. Using the non relativistic and the relativistic forms of the Vlasov equation, numerical calculations are made to ascertain whether this discrepancy can be attributed to the influence of the finite widths of the resonances at the harmonics of the cyclotron frequency.

4.5 Electron Cyclotron Resonance Heating in a Plasma (H.K. Wimmel, K.H. Wöhler - Experimental Plasma Physics 2)

The cyclotron frequency heating of the plasma electrons in a magnetic mirror field was roughly estimated. Individual electrons in a magnetic mirror field with combined electromagnetic vacuum wave field are investigated. It is thereby assumed that heating is effective only in relatively narrow regions ("resonant zones").

a) Resonance condition (maximum energy)

At the suggestion of G. von Gierke and colleagues an investigation was conducted in collaboration with K.H. Wöhler to find for what electron energies W there are resonances in a given mirror field. In this connection the relativistic mass variation and the Doppler effect in the B direction are taken into account. Moreover, constancy of the magnetic moment μ is required beyond the resonances. Only pairs of values (W, μ) corresponding to trapped particles are admissible. When applied to an experiment by Dandl and colleagues, Oak Ridge, with $\lambda = 3$ cm and the mirror ratio $R = 3$, it follows that

$$\begin{aligned} \text{for } \underline{k} \perp \underline{B} & : W < 290 \text{ keV} \\ \text{for } \underline{k} \parallel \underline{B} & : W < 580 \text{ keV.} \end{aligned}$$

The figures are compatible with the abundance maximum found experimentally when $W \approx 100$ keV, but they do not account for the occurrence of 1-MeV electrons.

b) Heating rate

In collaboration with K.H. Wöhler the magnitude of the heating rate of the electrons was estimated for certain parameters ($\lambda = 3$ cm, $P = 40$ kW, $V = 400$ litres, $L = 100$ cm) by means of cyclotron resonance heating. Relativistic effects and Doppler effect were ignored for the time being as were the collisions; the electromagnetic wave was again set up as a vacuum wave. The relative energy variation per gyration is:

$$(1) \quad \frac{\delta_c W_{\perp}}{W_{\perp}} = 2\pi \frac{Ec}{B v_{\perp}}$$

the number of the effective gyrations per resonant zone:

$$(2) \quad N \approx \sqrt{\frac{3\omega_c}{2\pi v_{\parallel}}} \cdot \left(\frac{\partial \ln B}{\partial z} \right)^{-\frac{1}{2}},$$

the effective thickness of a resonant zone:

$$(3) \quad \delta z \approx \sqrt{\frac{6\pi v_{\parallel}}{\omega_c}} \cdot \left(\frac{\partial \ln B}{\partial z} \right)^{-\frac{1}{2}},$$

the energy variation per resonant zone (phase difference 0 or π):

$$(4) \quad W_{\perp} + \delta W_{\perp} \approx \left[\sqrt{W_{\perp}} \mp \frac{2E}{c} \cdot \sqrt{\frac{3\pi ec}{m B v_{\parallel}}} \cdot \left(\frac{\partial \ln B}{\partial z} \right)^{-\frac{1}{2}} \right]^2.$$

W_{\perp} and δW_{\perp} are thereby measured in units of mc^2 . In the energy range $25 \text{ eV} \leq W_{\perp, \parallel} \leq 75 \text{ keV}$, assuming $E = 25$ V/cm, it follows that

$$1.4 \cdot 10^{-2} \geq \delta_c W_{\perp} / W_{\perp} \geq 2.7 \cdot 10^{-4}; \quad 53 \gg N \gg 8; \quad 1.6 \text{ cm} \leq \delta z \leq 11 \text{ cm}.$$

It is here a condition that $(\partial \ln B / \partial z) = 3.5/L$. In the case of electrons which cross resonant zones many times the heating rate can be estimated. Equation (4) shows that the variation in W_{\perp} can be considered as the superposition of a time-constant energy increase (quadratic term) with a random-walk process on the W_{\perp} axis (compound term), if the phase correlation between various resonant-zone crossings is made equal to zero. If only the quadratic term is taken into account heating occurs to $W_{\perp} = 100$ eV in 10^{-6} sec and to $W_{\perp} = 30$ keV in $3 \cdot 10^{-4}$ sec. Evaluation of the random-walk process has yet to be undertaken; a rough estimate gives for it times of similar magnitude. These heating times are shorter than the particle loss times of 10^{-4} to 10^{-1} sec measured in similar experiments (Dandl et al.,

Oak Ridge). The principal uncertainties of estimation are due to the uncertainty as to E and as to whether the electrons cross the resonant zones often enough ($> 10^4$).

c) Numerical calculation of electron trajectories

In order to investigate the heating rate more accurately numerical calculation of electron trajectories was undertaken in collaboration with K.H. Wöhler. Equations of motion are used which are averaged over a gyration period. Collisions are ignored for the time being. The crossing of one or more resonant zones in the non-relativistic case is to be investigated first of all.

4.6 Microwave Passage through a Cylindrical Plasma (W. Lünow, together with M. Tutter)

The case of non-absorbing plasmas was treated with the aid of a wave-optical multi-sheath model. The calculation is being extended to absorbing plasmas.

5. Other Theoretical Work

5.1 Gas Discharge Diode with Laser Anode (H. Hora)

While it is possible in p semiconductors for laser excitation to effect a population inversion conductively by means of a p-n junction or by absorption of light or by multiple pair formation with 100-keV electrons, estimates were made to establish whether the electrons of a discharge which recombine in a p semiconductor anode can produce a laser mechanism. The minimum current density for I-V semiconductors and GaAs was determined on the basis of the Schawlow-Townes condition, allowance being made for the possible excitation and absorption mechanism in the semiconductors, for the natural width of the spontaneous recombination and also for the diffraction and absorption losses. Because very thin semiconductor plates can be chosen surprisingly low values of the current density of approx. 10 amp/cm² are sufficient [IPP 6/31, 35, 36].

5.2 Light Distribution in a Ruby Laser (H. Hora, B. Kronast (Dept.1), H.J. Kunze (Dept. 1))

As a continuation of the investigations mentioned under the same heading in the last annual report (page 207) the results were presented in the form of a publication [37].

5.3 Scattering Coefficient in Stars (W.H. Kegel)

Investigation was made as to how far the reduction of the scattering coefficient as a result of collective effects is important in connection with radiation transfer in stars. Numerical calculations showed that any appreciable influencing of the scattering coefficient by collective effects occurs only in those temperature and pressure ranges where as regards the radiation transfer the scattering in relation to the absorption is to be ignored.

5.4 Knudsen Flow (R. Gorenflo, M. Pacco)

In collaboration with Dr. Blauth and Mr. Scherzer of the Ultra-high Vacuum Group the flow of a Knudsen gas through a long, thin tube is investigated. Of special interest here is the initial flow at the tube outlet. The appropriate integral equations were formed. Since it appears difficult, however, to solve them numerically or analytically the physical phenomenon

is simulated on the IBM 7090. The SHARE random generator RDM used for the purpose was tested as to its statistical properties.

6. Numerical Mathematics and Data Processing

6.1 Evaluation of Spectroscopic Measurements (R. Gorenflo, H. Hora, Y. Kovetz, W. Lünow)

Evaluation of measurements on cylindrically symmetric plasmas, which had to be undertaken on a large scale, was largely automated in several parts with the collaboration of Dr. Eberhagen (Exp. Dept. 1). H. Hora devised a programme by means of which the measurement curves, after being sorted point by point, can be rotated, rectified and calibrated and which under specially selectable, individual spectroscopic conditions provides the light intensities.

R. Gorenflo and Mrs. Y. Kovetz were responsible for the numerical solution of the Abel-type integral equation that was then necessary

$$i(r) = \frac{1}{\pi} \int_{x=r}^1 \frac{dI(x)}{\sqrt{x^2 - r^2}}, \quad 0 \leq r \leq 1, \quad -1 \leq x \leq 1,$$

This integral transform causes perturbations which are superimposed on the measured function $I(x)$ to become amplified in the calculated function $i(r)$, which is often very rough and at intervals even negative although it has to be positive.

Both effects can be avoided by approximating $I(x)$ by means of a not too long sum of suitable orthogonal functions whose transform is known and which uses the extra information $i(r) \geq 0$ as a secondary condition.

Discretization gives rise to a quadratic programming problem for the expansion coefficients. A modification of the method is in order when $I(x)$ is not measured constantly, but is present only in the form of a small number (e.g. 7 or 8) of perturbed mean values in adjacent intervals. IBM 7090 programmes were compiled and used for both cases. It should be possible to devise purely discrete smoothing methods as well in which only the monotony and curvature properties of the perturbed function $I(x)$ in the form of as few parameters as possible are included in the calculation [IPP 6/19, IPP 6/29].

Finally, line and continuum intensities for optically thin hydrogen plasmas were calculated by W. Lünow as a function of temperature and density. A numerical method was devised by means of which temperatures and density can be determined from intensity measurements.

6.2 Investigations on Numerical Stability (O. Eder)

In the investigation of the stability of a homogeneous linear but, with regard to the integration interval, singular integral equation an infinite determinant in which the individual elements themselves were again transcendental functions in the eigenvalues was produced on substituting the occurring integral by summation. An adequate criterion for determining the stability in this general case could not be found. A method was devised, however, which makes possible here an explanation of the question that is satisfactory for practical purposes.

In connection with this work the behaviour of the eigenvalues when finite expressions are substituted for the integral was investigated. While the number of eigenvalues is fixed by the integral equations, their number increases on approximation with the degree of the determinant, which is the larger, the more accurate the integral of the nucleus is approximated by summation.

6.3 Interpolation (O. Eder)

For interpolation between given points it is customary to use curves that in certain coordinate systems correspond to simple functional relationships. In several practical cases there was no point in specifying definite coordinates. For the case where all that is known is that the curvature is an obvious function of the arc length, interpolation was now carried out for a number of given points by purely differential geometrical means. Generalization toward spherical curves by addition of the winding and also toward plane surfaces can be effected without difficulty.

6.4 Calculation of Plasma Density Profiles (O. Eder)

With due allowance for "Bohm" diffusion, recombination and also for classical diffusion and like-particle diffusion the radial profile of the plasma density is sufficient for a non-linear differential equation of the fourth order which is dependent on four parameters and for which there is present a secondary condition in the form of an integral equation (formulated by G. Grieger MPI). The solution was made after linearization by the difference method.

Ignoring classical diffusion and like-particle diffusion, the behaviour of the plasma density was described by a differential equation of the second order (D. Eckhardt MPI) which could be solved analytically for special parameter values.

6.5 Numerical Solution of Differential Equations (O. Eder)

Further progress was made on a project begun in 1962 for the mechanical solution of differential equations by power series formulation or Taylor expansion or by the method of the repeated quadrature and also by error adjustment methods in accordance with given approximation functions. As comprehensive a class of differential equations as possible depending on the largest possible number of parameters had to be considered. With the present mechanical facilities this is generally possible even as a function of two parameters.

6.6 Training of Programmers (O. Eder)

From 1st October till the end of the year a daily two-hour course with practicals was held which was also attended by other interested persons from our Institute, the MPI and the Institute for Inorganic Chemistry of the University of Munich.

6.7 Formulation of a Script (O. Eder)

A start was made to formulating a script on the courses on mathematical methods and Fortran programming conducted by O. Eder in 1963 and 1964.

6.8 Computer IBM 7090

In the course of 1964 the mean computing time consumption rose to about 270 hours/month. The table gives a classification according to institutes:

C o m p u t i n g t i m e c o n s u m p t i o n i n 1 9 6 4		
	h. min.	h. min.
Institut für Plasmaphysik	1 108.18	
Experimental Plasma Physics 1		331.20
Experimental Plasma Physics 2		15.05
Experimental Plasma Physics 3		129.04
Theory		374.19
Theory Computer ^{x)}		128.48
Administration		112.27
Engineering		17.15
Other institutes	1 934.39	
CERN, Geneva		9.42
MPI f. Arbeitspsychologie		1.13
MPI f. Eiweiss- und Lederforschung		352.55
MPI f. Astrophysik		242.43
MPI f. Biochemie		0.25
MPI f. Extraterrestrische Forschung		50.28
MPI f. Kernphysik, Heidelberg		7.59
MPI f. Physik		569.41
Fritz Haber Institut, Berlin		0.26
Technische Hochschule, Munich		196.02
University of Hamburg		4.41
University of Munich		490.08
Bavarian Academy of Sciences		8.16
Total	3 042.57	

x) Work is here performed on the Fortran system.

6.9 Increasing the Input/Output Capacity

Since past experience has shown that in 3-tier operation the input/output capacity of a 1401 system is not sufficient on its own to handle the volume of work possible with a 7090, an IBM 360 model is to be hired for 1st January 1966. The printer of the 360 is almost twice as fast as the previous system. Plans are also afoot to link up the 360 to a channel of the 7090 via a direct data connection. The 360 will then contain the operating system, while the 7090 is to serve as a "satellite". Because of the greater flexibility for input and output and the possibility of multi-programming with the 360 this arrangement has the advantage of obtaining a more rapid passage time of test programmes (an estimated reduction of a few hours to less than 1/4 hour). All programmes required for the purpose are to be compiled in the Institute.

7. Scientific Documentation of Plasma Physics

(D. Hilsenbeck)

The Institute is planning to establish a system of scientific documentation of plasma physics for the purpose of:

1. Ensuring the quickest possible dissemination of the latest scientific results in the field of plasma physics by compiling records to be issued regularly;
2. Reducing to a minimum the amount of time and effort spent on literature research on particular subjects;
3. Establishing an information centre in which, if possible, all works in the field of plasma physics are kept and can be made available to interested persons at the earliest.

Re 1.

It is intended to provide quarterly registers arranged according to authors, institutes and subjects and also a monthly bibliography section. Description of the subject is to be done by means of key words contained in a key word list. It is planned to store the bibliography information and the key words on recording tape and to use electronic data processing units for further processing up to the issuing of the register.

Re 2.

For literature research the question is expressed in terms of a combination of key words which is compared with the stored key words. This covers all those works which contain the stated combination of key words.

Re 3.

In order to ensure that the information provided in the registers is topical and complete, all works should be available in the Institute as soon as possible.

For this purpose steps were taken to arrange for an exchange of laboratory reports, annual reports and title lists with almost every relevant institute in Europe and overseas. The possibility of receiving literature directly from countries of the Eastern bloc is at present being investigated.

The work started in the Institute on 1st September was devoted mainly to:

- a) Settling objectives 1 - 3;
- b) Establishing contact and discussing the programme with the Institut für Dokumentationswesen, the Zentralstelle für maschinelle Dokumentation, the Gmelin-Institut in Frankfurt, the Deutsches Rechenzentrum in Darmstadt and the Documentation Department of the Deutsches Elektronen-Synchrotron in Hamburg;
- c) Determining which documentation works in the Federal Republic can be enlisted for documenting plasma physics (nuclear energy documentation of the Gmelin-Institut and documentation of elementary-particle physics of the Deutsches Elektronen-Synchrotron);
- d) Compiling a list of key words for plasma physics.

ENGINEERING DEPARTMENT (DIPL.-ING. K.H. SCHMITTER)

1. Summary

Moving the Engineering Department to block II took till February 1964. The group engaged on high-voltage technique, however, could not begin full-scale operations till November when construction work on the high-voltage hall was finished. The resulting wait had its affects on the development and testing of components. More serious failure to meet deadlines, particularly in the construction of the 2.6-MJ capacitor bank, could be avoided by erecting makeshift laboratories.

Present requirements were satisfied by extending the scope of the Department to include the field of installation technique and chemistry, while the hitherto separate fields of vacuum technique and general technology were merged to form a single group. As the service for electronic equipment introduced in 1963 had been so successful, a service for vacuum equipment as well was put into operation in the middle of the year.

The wide scope of experimental work at the Institute resulted in 1964, too, in a correspondingly wide diversity of technical operations. From devices and equipment for fast discharges to those for stationary operation, assignments had to be handled on behalf of nearly all the experimental branches in plasma physics. In keeping with the requirements of the individual experiments due emphasis was placed on various specialized groups. Again in the forefront, for instance, were development and production assignments for theta pinch experiments, particularly in the fields of planning, high-voltage technique and design. In the electronics field the caesium experiments accounted for the biggest share of the assignments handled, while the developments in magnetic-field technique were of use for, besides the caesium experiments, mainly the arc experiments and the "Hourglass".

The work of the Department was appreciably facilitated by using the standard equipment developed in past years. About ten other standard units and components were developed to supplement those already in service. Laboratories abroad showed keen interest in one of those units in particular, namely the universal image converter.

Development work left relatively little room for the very necessary technical groundwork. In the field of hard superconductors headway was made in accounting for the degradation effect. The principles determining the dimensions of fast banks were expanded.

The central workshops, including the electronics and electrical-engineering workshop, were transferred before the end of the year to the new facilities in the ZW block. In 1964 a total of 429 assignments were handled in the mechanical workshops and 138 orders prepared for passing on to outside workshops. The total of 46 936 man hours represented an increase of 27.5 % on the previous year. This performance was spread over the various departments roughly in accordance with the agreed schedule.

The capacity of the carpentry shop was increased in the same proportion. A total of 6 642 man hours was recorded.

By the end of the year the electronics and electrical-engineering workshops produced 164 series devices and farmed out the production of another 115 devices of its own design to outside firms.

The balance shows that the amount of work required of these workshops by Departments 1 and 2 deviates more sharply from the agreed schedule.

2. Planning Group

(A. Knobloch)

2.1 Project Supervision and Technical Clarification for the 1.5 (2.6)-MJ Capacitor Bank

(A. Knobloch, H. Schlageter, in collaboration with Dept. 1)

Installation work by the AEG/SSW industrial association on the bank racks and on the auxiliary equipment was concluded at the end of January 1964. A sixth of the collector system designed in the IPP and constructed by Krauss-Maffei was then installed by IPP staff (v. report on Design Group), the appropriate pulse cables being laid at the same time by SSW. At the end of May 1964 a start could be made (together with Dept. 1 and ARGE) on attempts to put the bank into operation without matching capacitors. In the course of these experiments the spark gaps were converted from 3-electrode to 4-electrode operation (with insulated trigger pin). Because of magnetic influence caused by the iron racks of the bank the Simatic chokes were removed from the bank and arranged together shielded in a cabinet. Discharges were effected, mainly at a charging voltage of 30 kV and finally with the entire sixth of the bank (250 kJ at 30 kV) on a 30-cm section of the original coil. In a total of 66 experiments with the sixth at 30 kV the result each time was 3150 kA at 30 kc/s, which is equivalent to a maximum field in the coil of approx. 130 kG. In order to adhere to deadlines it was decided not to pursue experiments with the sixth up to 40 kV, and at the beginning of August 1964 work was resumed on installing the collector and laying the appropriate cables. It was possible to finish installation of the cables and precollector by the end of September 1964, while installation of the main collector, including fitting of the 1.5-m long load coil sub-divided into several single coils, took till the end of November 1964. Since then introductory measurements (conducted by the IPP and ARGE) on the completed device (including matching capacitors) have been in progress. Regulation of the bank control system (Simatic), voltage tests on the entire collector system and also initial discharge experiments with parts of the bank at 30 kV have been carried out.

The need for keeping to a schedule meant that the preliminary experiments with a vacuum switch serving as a crowbar switch originally planned on a precollector could not be conducted. It is intended to test this switch in a separate discharge device.

Under the heading of technical clarification the contact experiments on 1-cm wide samples with a maximum of 200 kA/cm at 25 kc/s were continued. Without impairing the contact properties tests were carried out on: 2 contact combinations equivalent to precollectors (mean load 61 kA/cm) 80 kA/cm: 1500 discharges; a contact combination equivalent to coil contacting (mean load 147 kA/cm) 170 - 200 kA/cm: a few 100 discharges.

The mechanically prestressed precollector insulation was subjected in the actual device to a surge voltage fatigue test (together with the High-Voltage Group) with damped 25-kc/s discharge with superposed radiofrequency (cable reflections) corresponding to a peak voltage of 71 kV. A service life of 22 000 discharges was obtained.

Fig. 1 shows the installed collector system with a 30-cm section of the load coil.

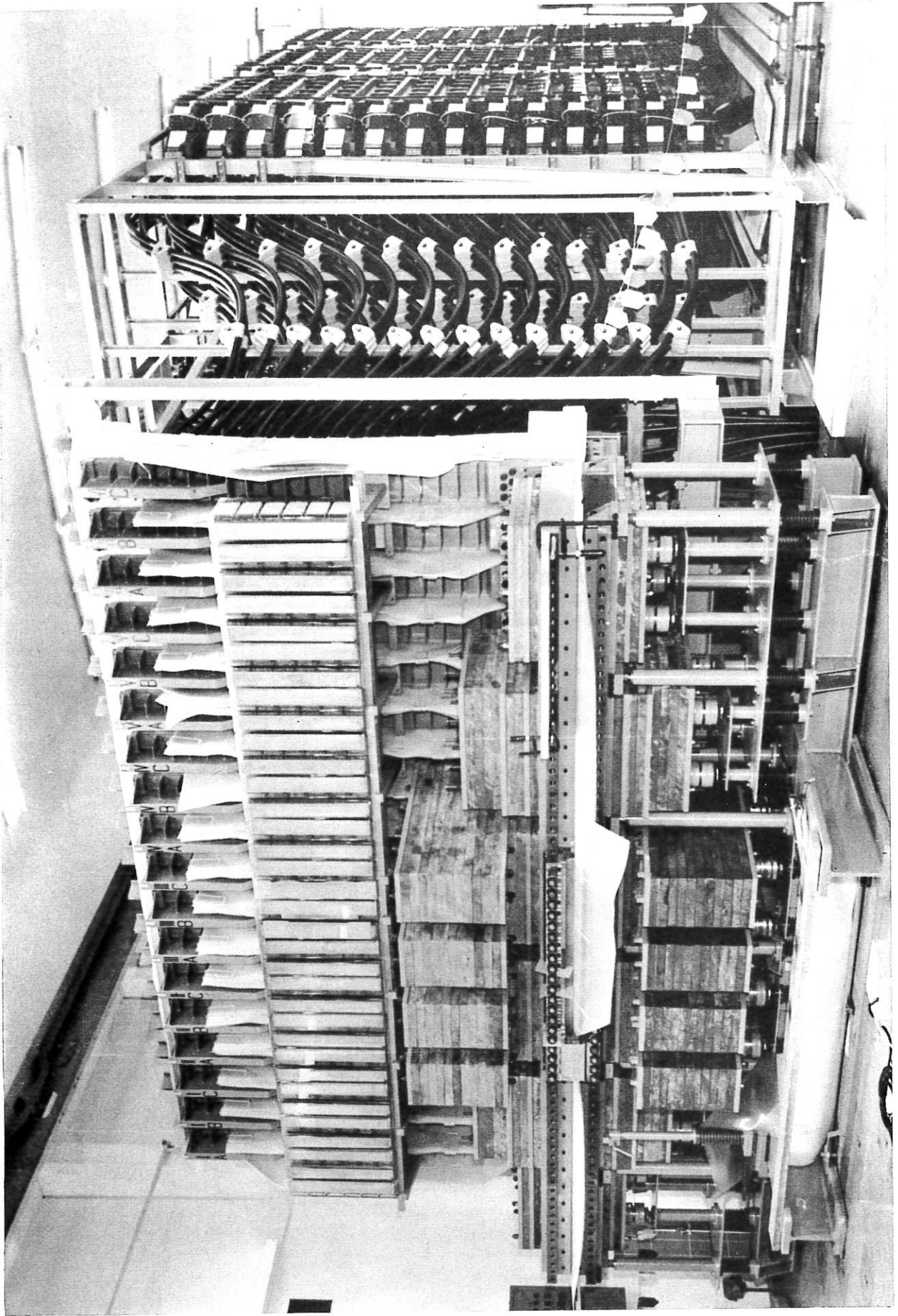


Fig. 1 1.5 (2.6)-MJ capacitor bank, December 1964

2.2 Planning (A. Knobloch)

2.2.1 Preliminary Technical Clarification for the Helios Project

2.2.2 In the course of discussion concerning another fairly large theta pinch experiment (v. annual report for 1963: "500-kJ bank") the Engineering Department suggested as flexible as possible a capacitor bank. For this purpose 2 preliminary projects for 2 x 30 kV and 2 x 40 kV respectively were drawn up. Tenders, particularly for capacitors, were invited.

2.3 Elaboration of the Analogue Method ((J. Deleplanque), G. Herppich, A. Knobloch, H. Schlageter, F. Werner)

The existing analogue methods were elaborated so as to ensure early detection of possible perturbing effects, e.g. in the experiments for putting into service part of the 1.5 (2.6)-MJ bank, for the purpose of detailed technical clarification and as an aid to design work.

2.3.1 The low-voltage model system was expanded; the jitter of the switches used is now ± 300 nsec so that when a maximum time transformation of 1:100 is included the majority of the circuit problems occurring can be treated in the model.

The following are some of the cases for which model measurements were made:

- 1) 1.5 (2.6)-MJ experiment
- 2) 500 or 400-kJ project
- 3) Two-part capacitor bank with double-feed load coil
- 4) Optimum RC matching of pulse cables. These measurements have now been concluded for cable types 20P1 and 40P3, a report on which is now under preparation.

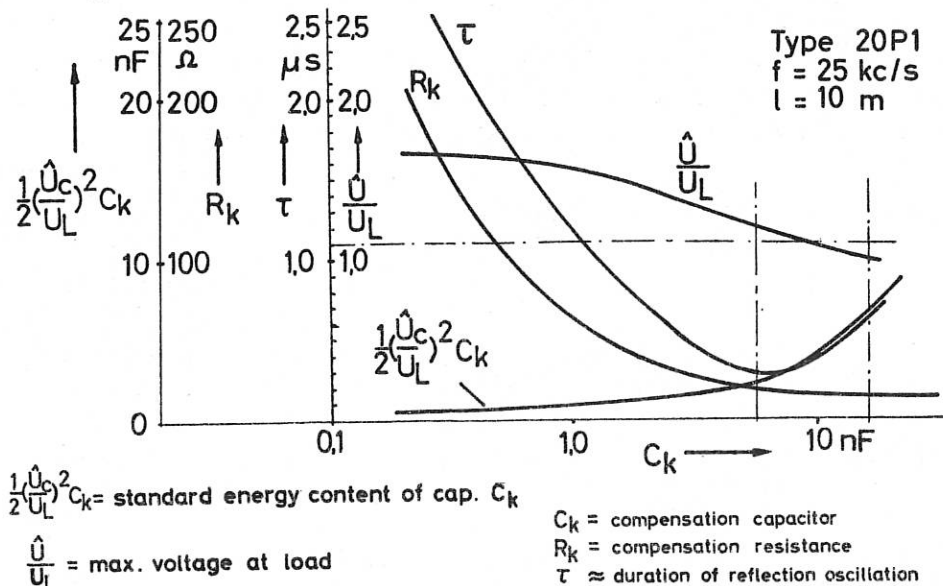


Fig. 2 RC matching at the load end of inductively loaded pulse cables. Characteristic data of the RC matching and the resulting voltage for a 10-m long 20-kV cable (\hat{U}_L = charging voltage).

Fig. 2 shows for one example the characteristic curves for the matching per cable according to which optimization is possible.

5) Systems using circuits with producible pulse forms.

2.3.2 Plane and spatial radio-frequency fields in the region of discharge devices were investigated with appropriately increased frequency by means of models. In order to increase the capacity of this analogue method a broad-band amplifier for 200 VA (100 A_{SS}; 10 kc/s - 500 kc/s) is being constructed by the Electronics Groups. The approximate determination of spatial radio-frequency fields and distributions is accomplished by a newly tested method in an electrolytic tank in which metal components are copied in insulating materials. The scanning system designed for the tank is under construction.

2.4 Plans, Design Principles and Mathematical Data for Dimensioning Discharge Devices

(K.H. Fertl, A. Knobloch, H. Schlageter)

2.4.1 Survey of the data of inductively loaded capacitive energy-storing devices in standard representation (ignoring damping). Standardization according to the quantities E* (stored energy per unit length of the straight cylindrical load coil), f (discharge frequency) and u (energy efficiency) allows a simple survey of possible values of the maximum induction and the field variation with time.

Fig. 3 refers to an example with mean values of the specific stress on the structural elements, the basis being the collector system according to 4.3 (D = load coil diameter; U_{res} = resulting charging voltage with series connection)

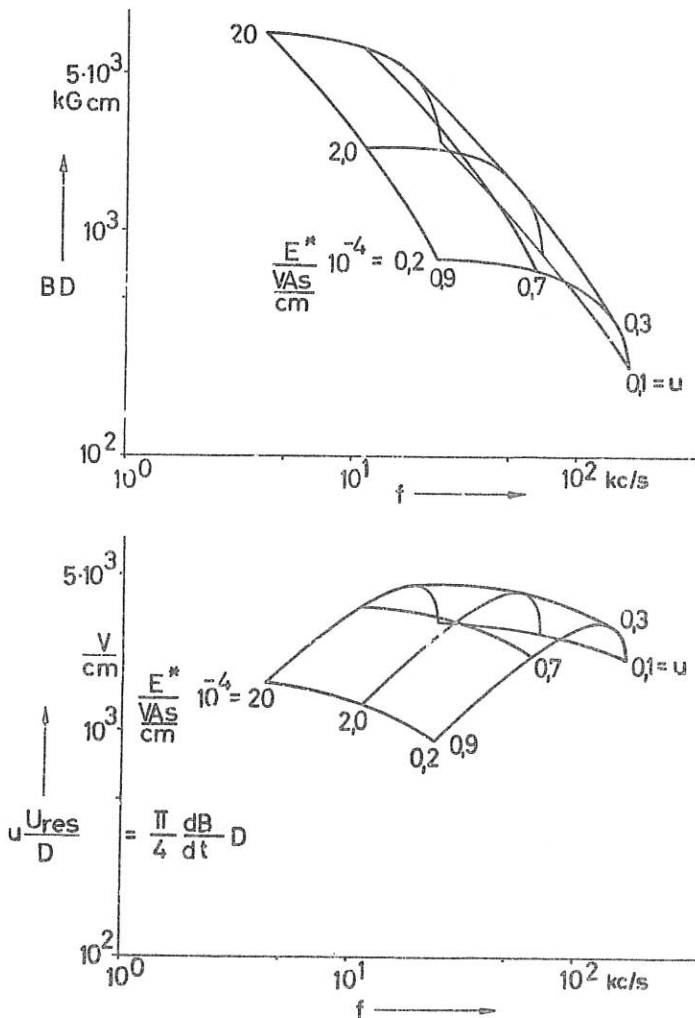


Fig. 3
"Natural" frequency dependence of the maximum value and the time variation velocity of the magnetic flux density in a single-turn coil fed from a capacitive energy-storing device.

2.4.2 Calculation of a pulse-shaped current (space and time dependent) in a metal conductor (assistance with programming from the Theory Department).

2.4.3 Design and model treatment of a collector with particularly low flux density for very high load currents (obtained by means of contacts positioned at a slant to the electric flux) and relatively long loads.

Fig. 4 shows a conductor and insulation diagram of a single collector. Such collectors can be arranged alongside one another for feeding long loads.

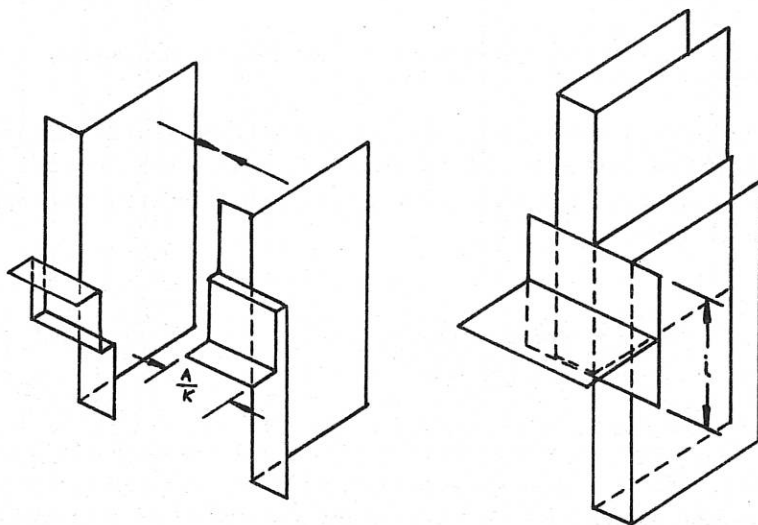


Fig. 4 Low-inductance collector. Conductor and insulation diagram

Fig. 5 presents an inductance comparison between the collector system as set up in the 1.5 (2.6)-MJ bank and the low-inductance collector for $k = 20$. The dependence on the cable connection area in relation to the load length and on the necessary insulation overlapping is shown.

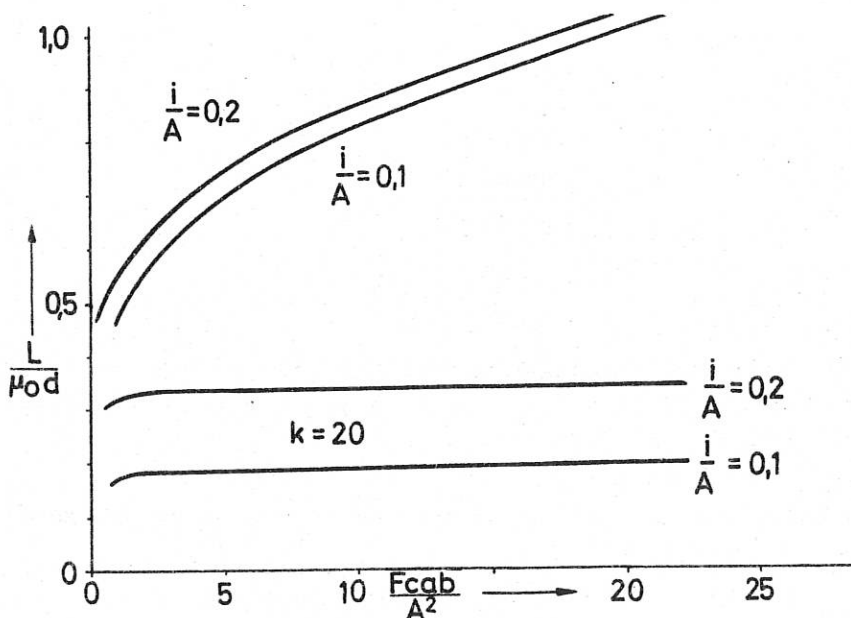


Fig. 5 Low-inductance collector - inductance comparison with the 1.5 (2.6)-MJ collector system

2.5 Experimental Bank (F. Werner)

Preliminary experiments for producing magnetic fields in the 1-MG range are to be conducted by the Engineering Department on an experimental bank. For this purpose a suitable collector was designed and built and also a few experimental coils constructed.

2.6 Special Assignments ((J. Deleplanque), J. Mantel)

Literature studies were initiated to consider technical questions of energy conversion with the aid of MHD and EHD generators.

2.7 General Assignments in the Engineering Department (J. Mantel, H. Schlageter)

The Department was provided with a documentation section and a library with periodicals section. With the exception of the medium-frequency generators the power sets for the general power room of the Department have been approved and will be installed with the relevant switchgear at the beginning of 1965.

3. Design Group

(G. Wulff)

As in the previous year, a major part of the working capacity was earmarked this year for the 2.6-MJ theta pinch experiment. The drawings were completed. After supervising production at the firm of Krauss-Maffei the designers collaborated with the fitters from the mechanical workshops of the Central Workshop in installing the precollector and main collector (E. Breit, M. Eberwein, G. Kaspar, G. Thater, A. Wasner, G. Wulff). In charge of these operations was the Planning Group.

Together with the High-Voltage Group, moreover, a matching capacitor in a plexiglass case with sandwich conductor connection was developed and constructed for this experiment (W. Ertl, G. Wulff). (For dimensions and electrical data see Fig. 6).

Design orders:

	Balance sheet
Carry-over from 1963	29 orders
New	29 orders
Completed	28 orders
Cancelled	<u>9 orders</u>
Carry-over	21 orders

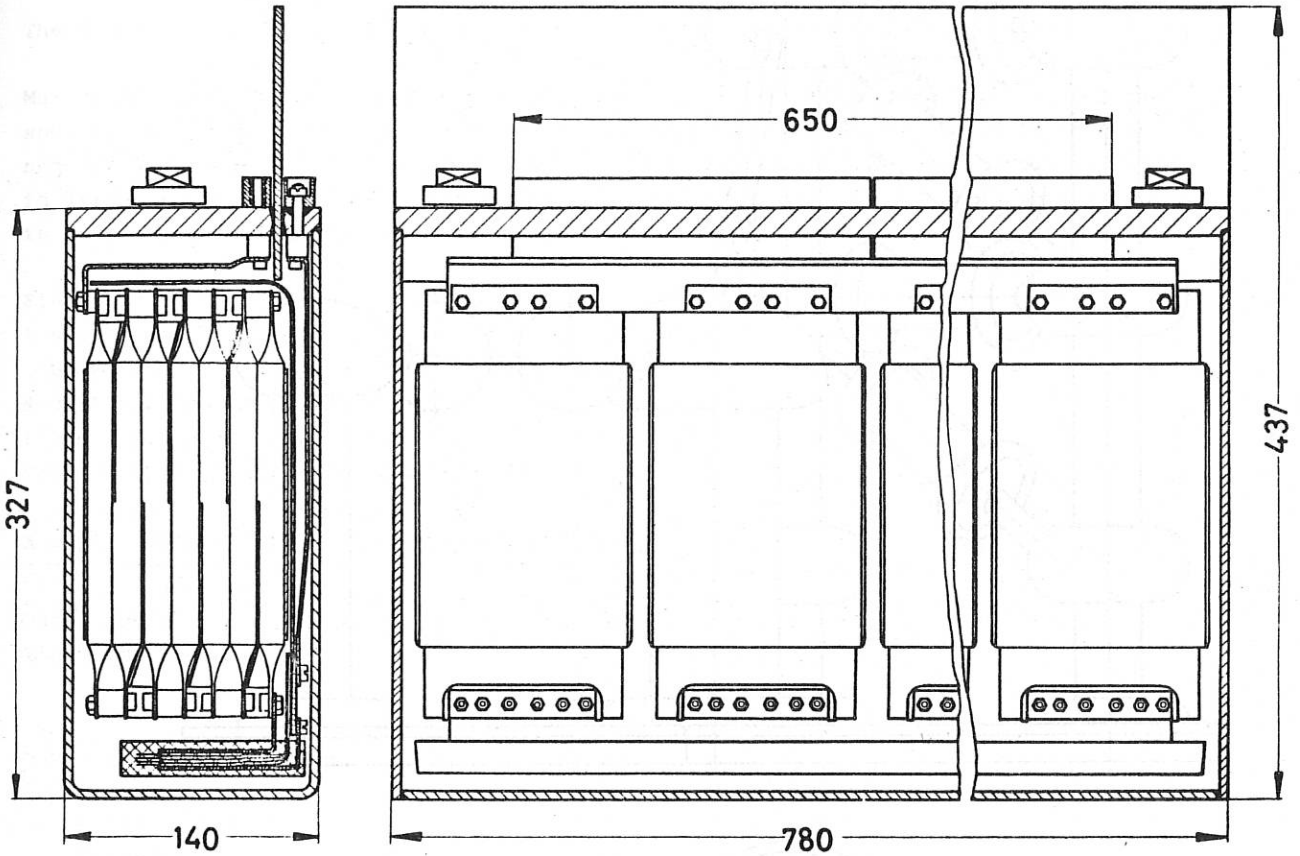
The following orders are worth noting:

1) Unit No. 118 Serial No. 64/231 (Fig. 7)

Design of vessel with magnetic coils for investigating arcs. Jet and electrode can be shifted, possible to measure magnetic field distribution by means of probe in the arc. For this purpose 130 drawings were made (J. Kaufmann, R. Zickert).

2) Unit No. 92 Serial No. 64/16

In collaboration with the High-Voltage Group a high-voltage testing system was designed for 320 kV at 60 mA (Fig. 8) (N. Debudey, A. Wasner)



Circuit: 7 windings in series, 6-W packs in parallel, shock voltage $U = 50$ kV, testing shock voltage $U_p = 70$ kV; capacitance = $0.133 \mu\text{F}$; inductance = 6 to 7 nH; series resistance = 1.05Ω .

Fig. 6

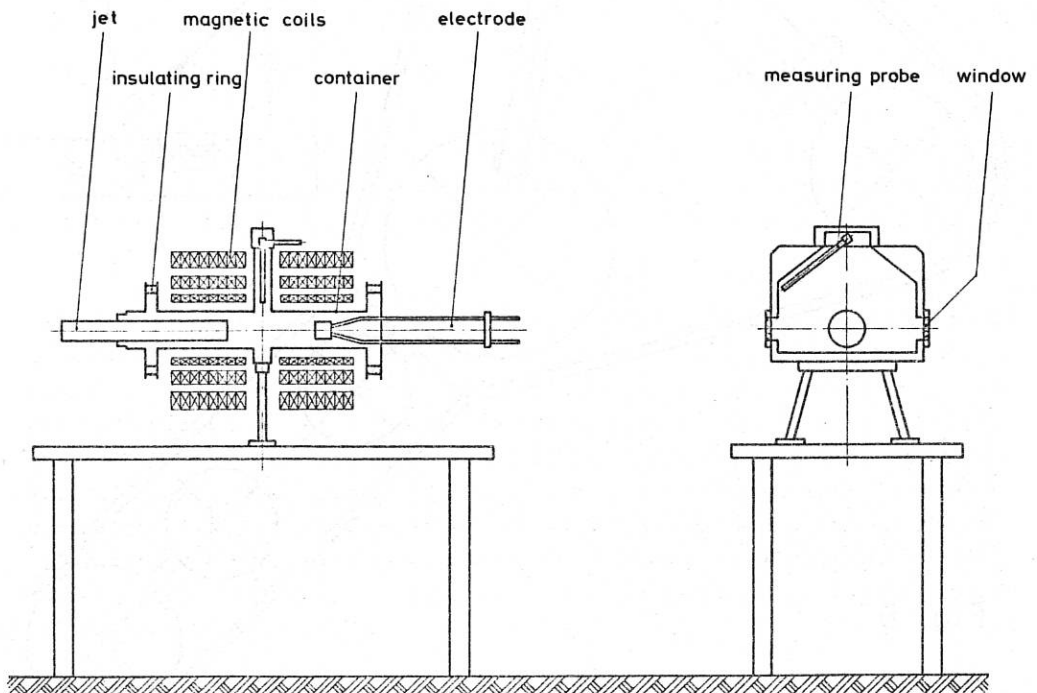


Fig. 7

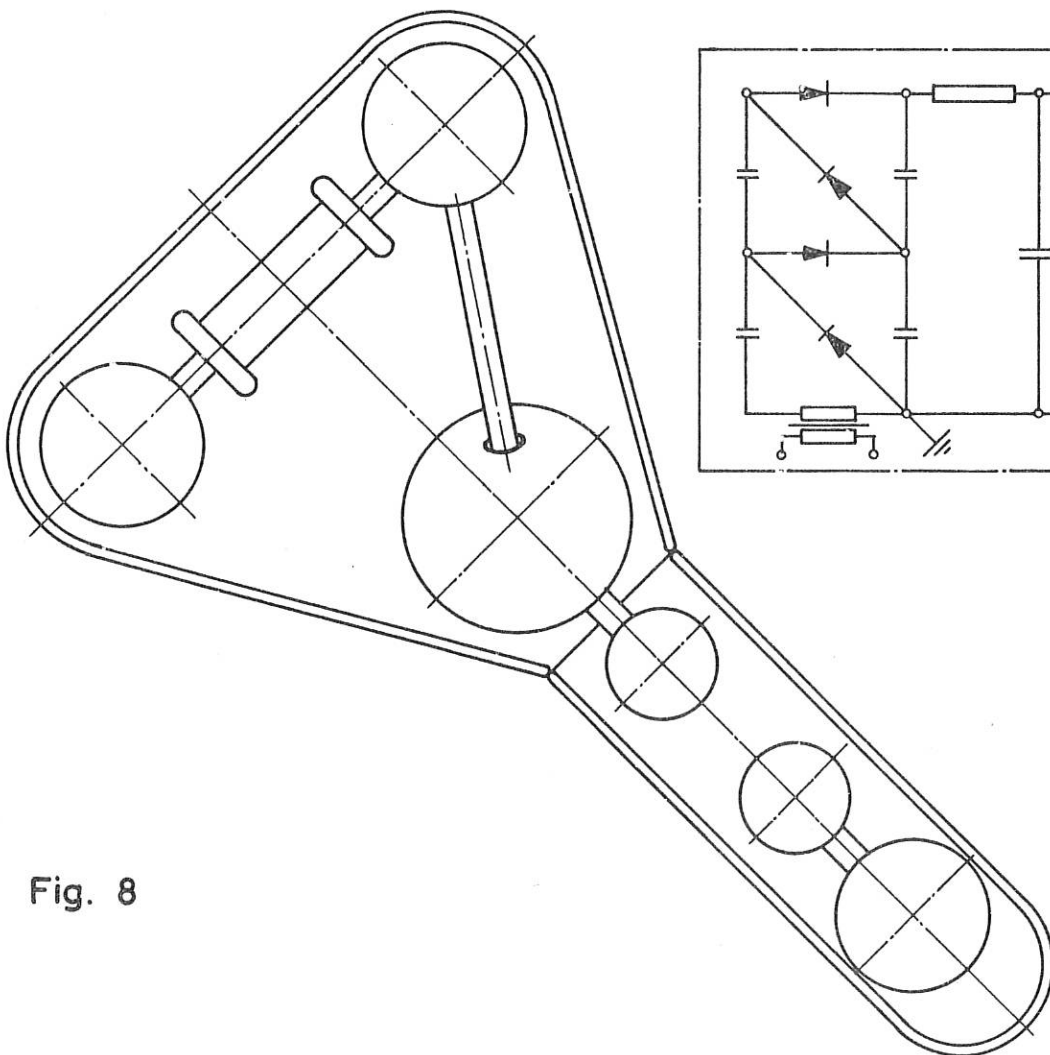
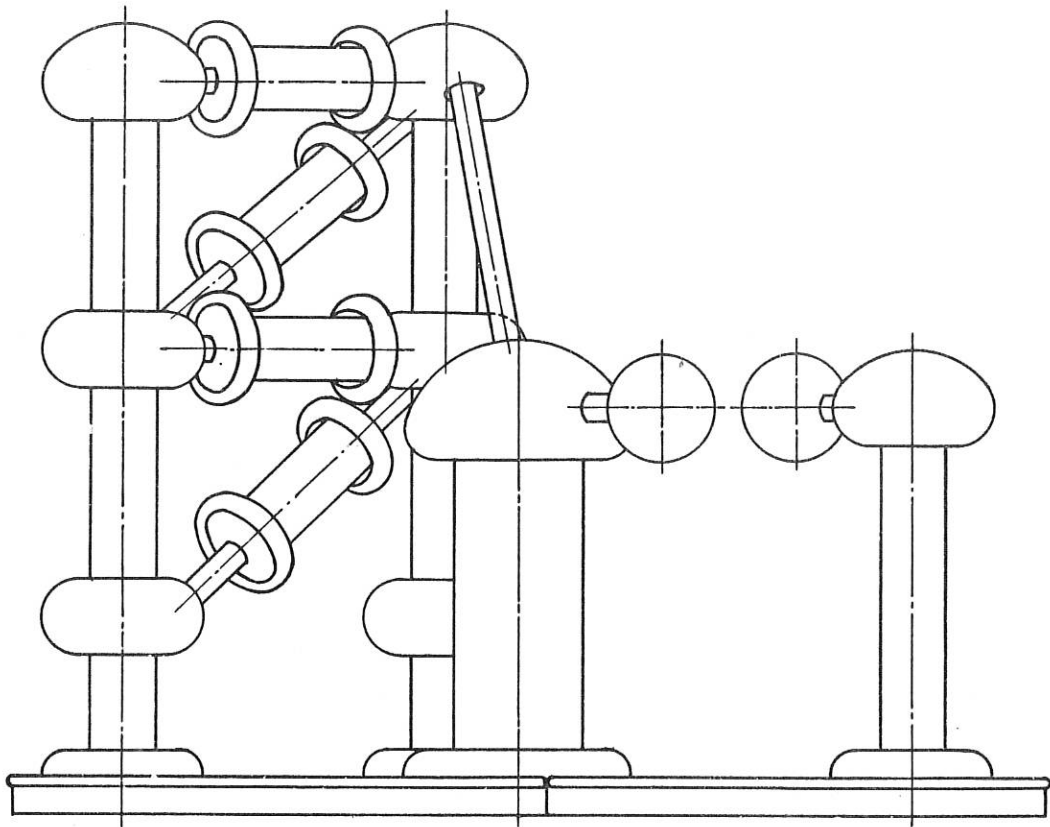


Fig. 8

The dimensions of the installation are as follows:

Max. height 3005 mm; max. length 4750 mm; max. width 2540 mm. The diameter of the two spheres is 400 mm, one of them being so fitted as to be mobile. The distance between the spheres is adjustable from 0 - 500 mm, the travel speed being 0.5 m/min. The carriage is driven via a spindle by a three-phase stop geared motor. The distance between the spheres is selected by a setting device in the control desk.

Electrical data:

4 selenium extra-high-voltage rectifiers
peak inverse voltage 147 kV; current 60 mA
4 doubler capacitors 0.04 μ F; 167 kV
1 shock capacitor 0.16 μ F; 334 kV
Total output of installation: 320 kV; 60 mA.

Annual statement of hours expended on design

Total hours	23 362.5		
Incl. for holidays	1 935.0	=	8.3 %
illness	1 344.0	=	5.8 %
filing	1 127.0	=	4.8 %
Hours expended on design	18 956.5	=	100.0 %
For Department 1	7 316.0	=	38.6 %
Department 2	3 062.5	=	16.2 %
Department 3	5 341.0	=	28.2 %
Department 4	2 672.0	=	14.0 %
Department 6	430.0	=	2.3 %
M P I	135.0	=	0.7 %

4. High-Voltage Group

(R.-C. Kunze)

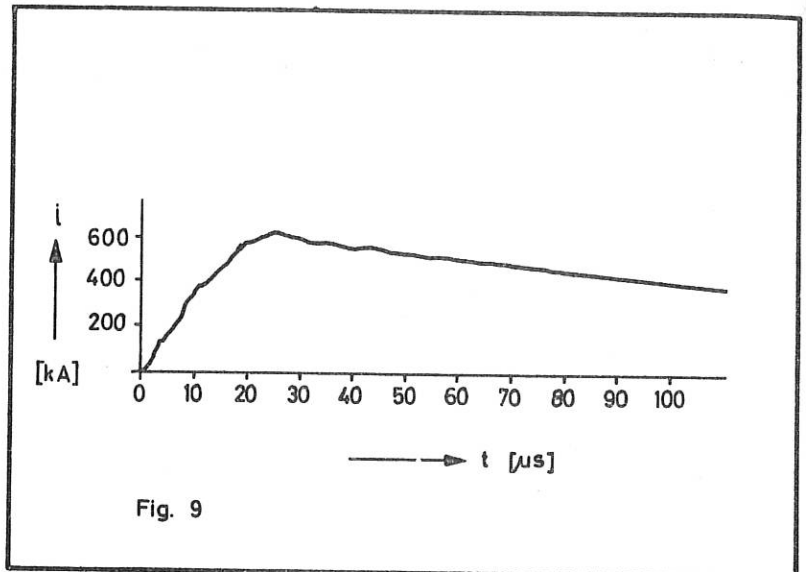
4.1 Work relating to the 2.6-MJ Bank (J. Bäumlner, J. Gruber, R.-C. Kunze, G. Klement)

Outstanding questions of insulation in partial collectors and in the connection for the matching capacitors were clarified in collaboration with the Planning Group. The approval tests on the pulse cables at the firm of SSW were concluded without any objections being raised.

With the assistance of the Design Group the matching capacitors were modified in accordance with their new characteristic data (cf. annual report for 1963). Two experimental capacitors were tested at nominal voltage and withstood 300 000 discharges without breakdown. At the same time a fatigue test was conducted on two capacitor samples of the firm of Tobe Deutschmann which were offered for the same loading example. These capacitors already broke down after 1800 and 6000 discharges respectively. Production of all matching capacitors was then initiated in collaboration with SSW. The cases presented difficulties. As the manufacturers were unable to fulfil definite promises to supply oil-proof cases in polyethylene, the Group developed containers in plexiglass on their own. The production, testing and installation of the capacitor were concluded.

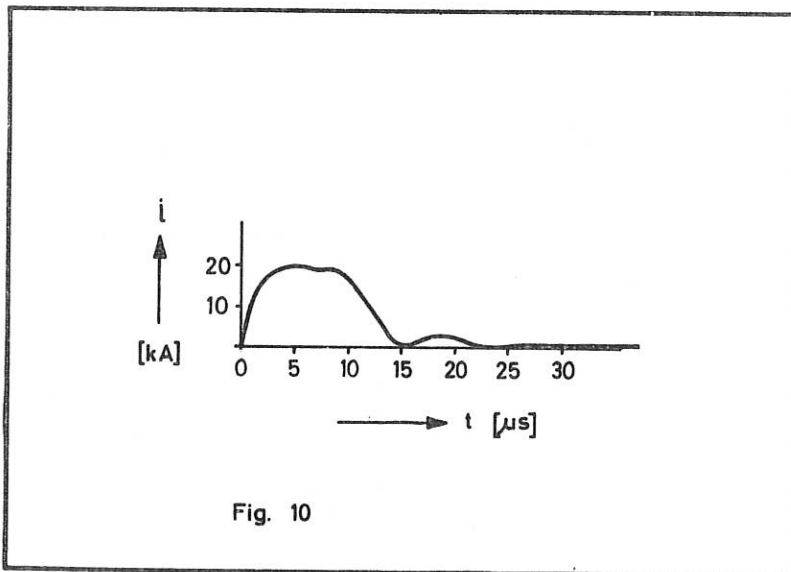
The magnetic field bank including control system and charger was constructed and tested. The final version had the following data:

Total capacitance	900 μ F
Charging voltage	10 kV
Peak current	625 kA
Rise time	15.3 μ sec
Decay time constant	140 μ sec
Frequency in oscillating operation	12.1 kc/s



The harmonics in the current curve are caused by the stray capacitances of the collector and the matching capacitors.

As second supplementary installation the preionization bank was constructed in the form of a transit-time assembly with charging device and control system. The assembly has the following data: 5 x 1.1 μ F; 5 x 1.0 μ H



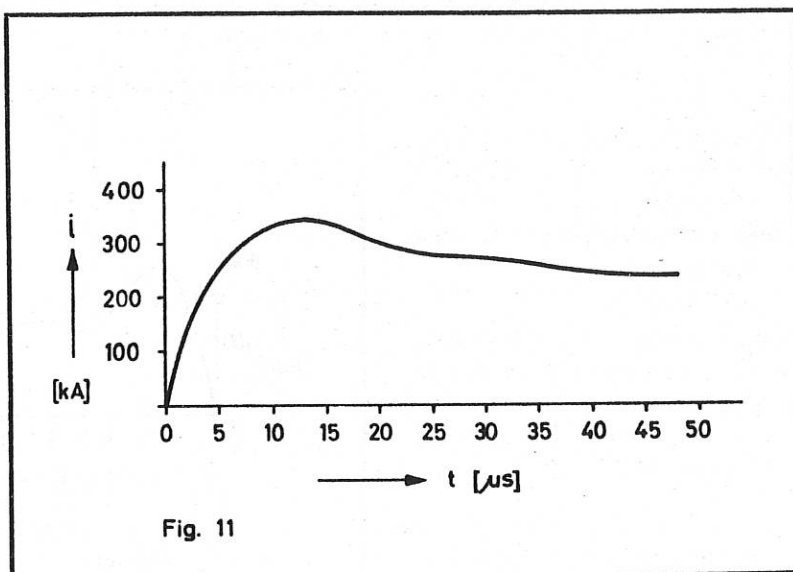
Charging voltage	40 kV
Pulse height	20 kA
Rise time	2 μ sec
Peak duration	7 μ sec
Decay time	5 μ sec

In addition, a measuring device for controlling the capacitors by C and $tg \delta$ measurements was constructed. With it all sections of the installation can be measured.

4.2 Magnetic-Field Bank for Dept. 1 (cf. annual report for 1963) (G. Klement, R.-C. Kunze)

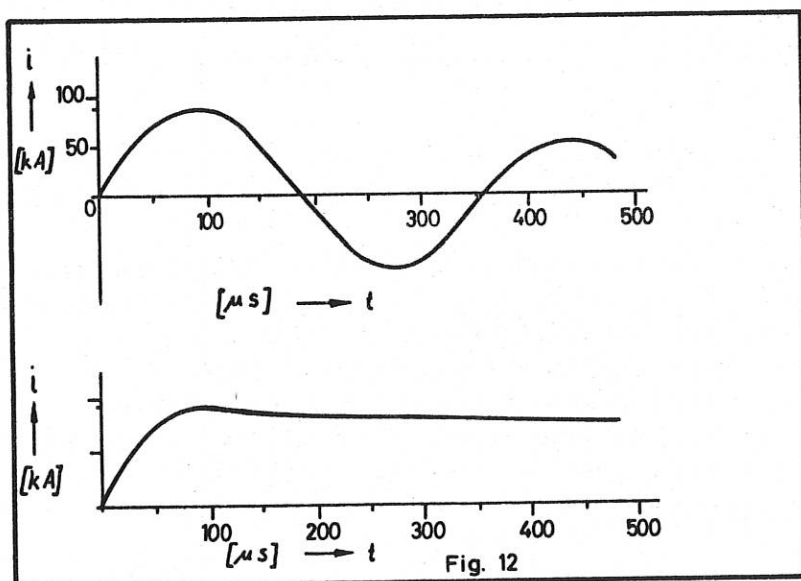
For an existing experiment a magnetic-field bank with a charging energy of 15 kJ which includes a control system and charging device was installed and put into service. The measured values of the bank when short-circuited at the collector are:

Total capacitance	300 μ F
Charging voltage	10 kV
Peak current	360 kA
Rise time	12 μ sec
Decay time constant	150 μ sec
Frequency in oscillating operation	19.2 kc/s



4.3 Crowbar Bank for Dept. 3 (J. Gruber, G. Klement)

Designed and produced as an integral part of the shock tube experiment was a capacitor bank with a charging energy of 30 kJ connected on the crowbar system. The bank was constructed from the same components as the magnetic-field banks for Dept. 1 already mentioned. With the control and charging systems it was put into service. On the bank with load (two-turn coil with $L = 5.5 \mu$ H) the following characteristic data were measured:

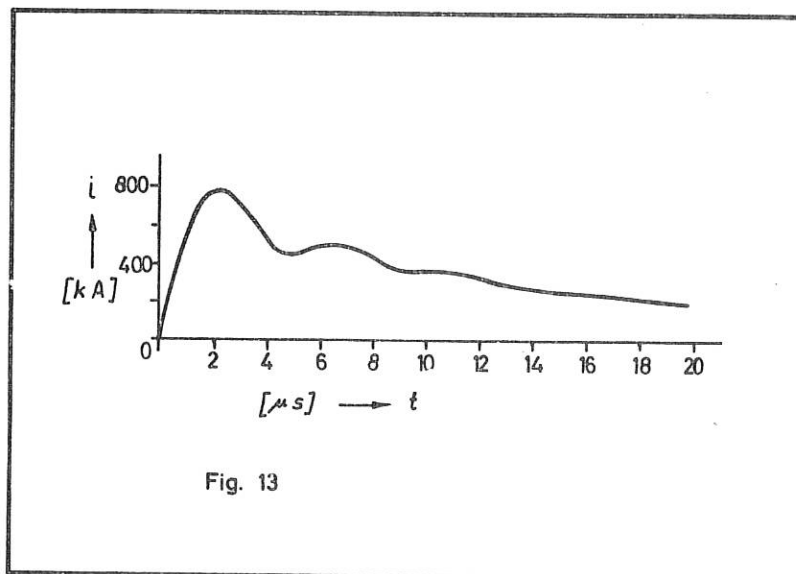


Capacitance	623 μ F
Charging voltage	10 kV
Peak current	90 kA
Rise time	90 μ sec
Decay time constant	1.5 msec

4.4 Crowbar Bank for Dept. 4 (R.-C. Kunze, E. v. Mark)

For various experiments in Dept. 4 a fast capacitor bank with charging device and control system was constructed. The bank is fitted with coaxial spark gaps as starting switches and with ignitrons GL 7703 as crowbar switches. It comprises 10 single capacitors, each provided with a starting and a crowbar switch. With the bank short-circuited at the collector the following results were obtained:

Capacitance	72.5 μ F
Charging voltage	10...18 kV
Self-resonant frequency	135 kc/s
Stray of the starting switches	\pm 10 nsec
Peak current	800 kA
Decay time constant	10.5 μ sec
Ripple	10 %



4.5 Chargers for Capacitor Banks (J. Bäumlner)

The following chargers, all of them in voltage doubler connection, were constructed in collaboration with the El. Eng. Workshop:

1 unit	50 kV/200 mA	for Dept. 1
2 units	10 kV/500 mA	for Dept. 1
1 unit	10 kV/500 mA	for Dept. 3
1 unit	25 kV/300 mA	for Dept. 4
1 unit	10 kV/500 mA	for Dept. 4

4.6 Crowbar Spark Gap (R.-C. Kunze, E. v. Mark)

A spark gap was developed which can be used as a crowbar switch and which is at present being tested. The spark gap is constructed similarly to the coaxial starting spark gap, but the two parts of the cascade are ignited by uncoupled trigger circuits. Investigations hitherto have shown that the spark gap can be triggered in the region of ± 2 kV on either side of the zero crossing of the voltage with stray of less than ± 50 nsec. Ignition of the spark gap is also perfectly possible beyond this range, but the voltage above the spark gap causes a straying structure of the discharge. The setting of the spark gap with regard to its static breakdown voltage is uncritical, and so a high operational life (minor influence of burn-up) can be expected.

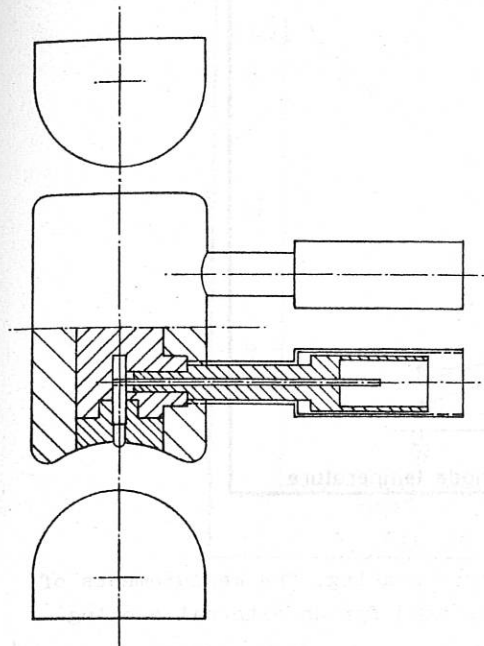


Fig. 14

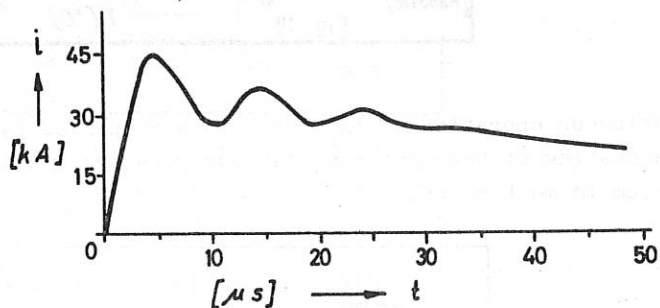
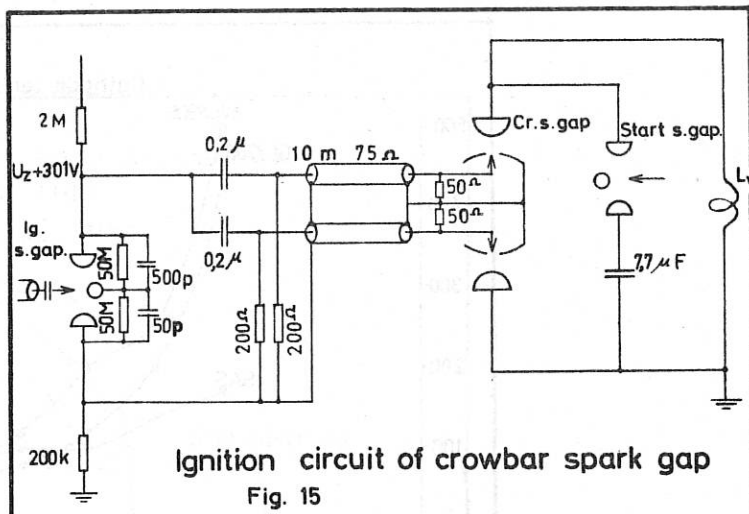


Fig. 16

4.7 Investigations of Pulse Ignitrons (c.f. annual report for 1963) (J. Gruber)

The measurements of the delay and jitter of ignitrons were continued. Newly developed ignitrons with anodes of austenite steel from the firm Schneider-Westinghouse, Paris, show less delay and jitter compared with the ignitrons of type G1 7703 (General Electric) and WL 8306 (Westinghouse) mostly used hitherto.

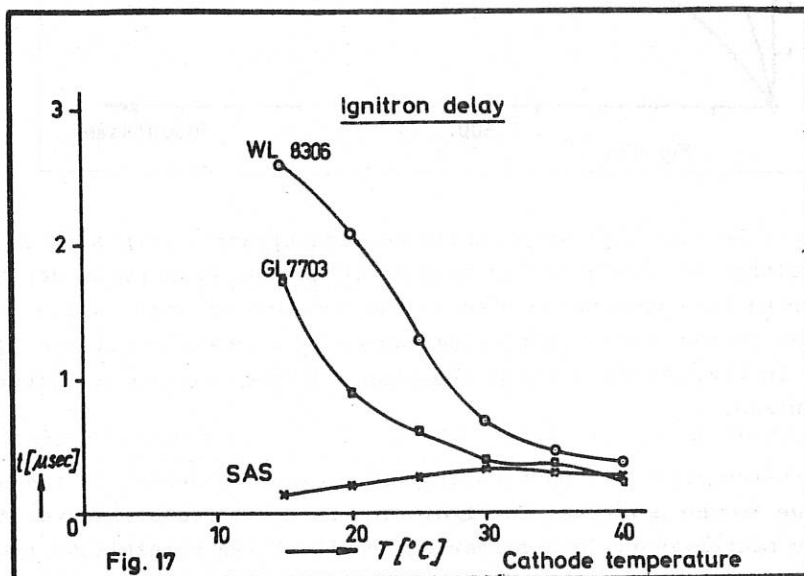
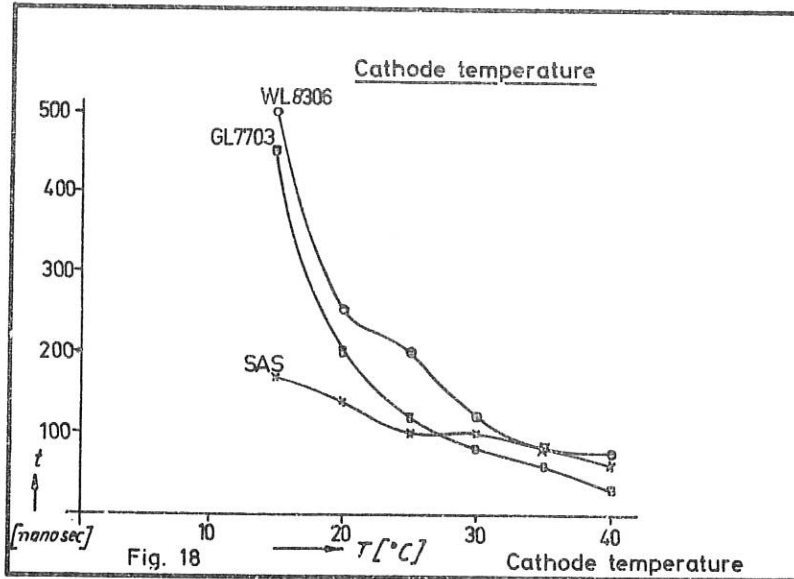
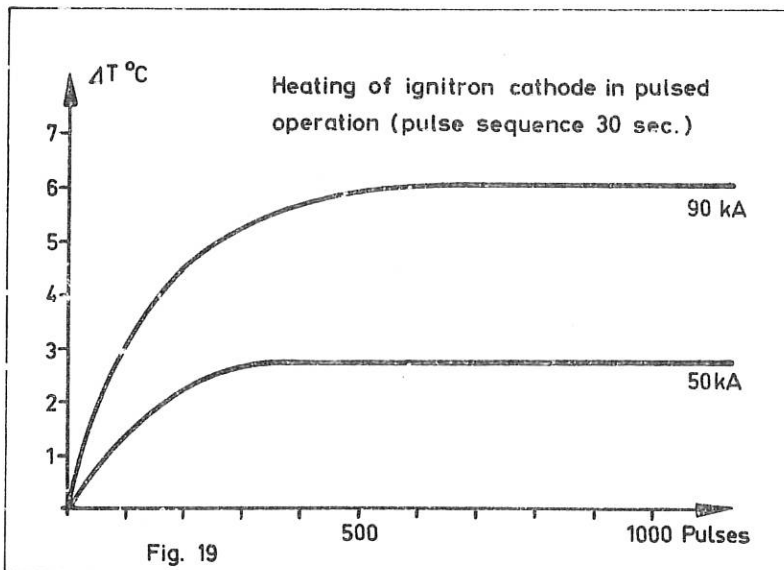


Fig. 17

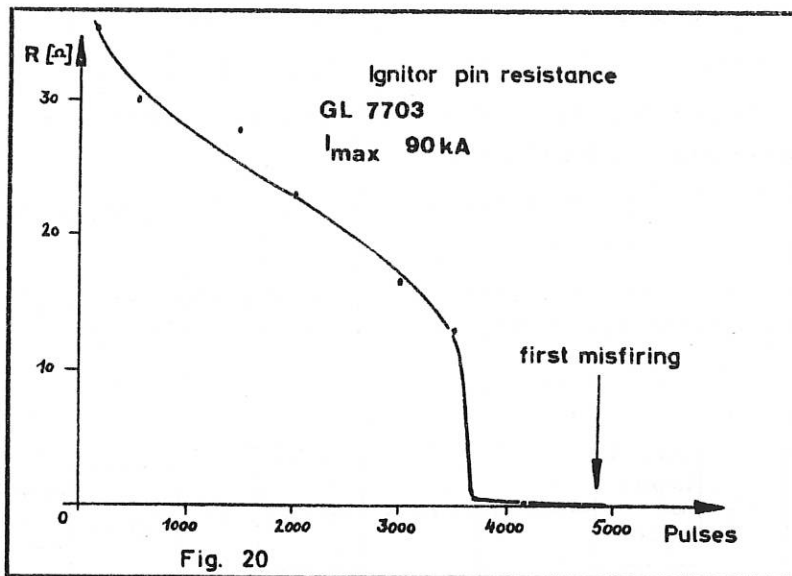


Continuous operation of ignitrons is accompanied by inherent heating. The measurements of the heating of the ignitron cathode show that there is no need for an external cooling system in most cases.



The investigations on service life were continued with higher currents (peak current 90 kA) and an operating voltage of 18 kV: In the case of tubes with graphite anodes the end of the service life is marked by a pronounced rise in the arc-through rate, while in the case of ignitrons with metal anodes mostly misfiring caused by a reduction of the ignitor resistance occurs. In Fig. 20 the ignitor resistance is represented as a function of the number of pulses.

Of interest in discharge circuits, particularly in crowbar circuits, is the additional ohmic resistance due to the switches. The ignitron internal resistance was determined by current and voltage measurement. In a suitable circuit it was possible to measure the ohmic voltage drop of the ignitron directly after the strong inductive voltage component was compensated for.



4.8 Miscellaneous Work

Construction of a capacitor bank of 12.5 kJ/9 kV for lasers (J. Bäumlner)

Development and production of a bakeable 100-kV duct for UHV (J. Bäumlner)

Development and production of a 15-kV capacitor for image converters (J. Gruber)

Determination of the lifetime and measurement of the characteristics of pulse capacitors made bei SSW and BICC (J. Bäumlner, G. Müller)

Construction of a device for magnetic shrink fitting of ends to coaxial cable and use of the same (J. Bäumlner, J. Gruber)

Investigation of insulating materials and parts for electrical strength (G. Klement, G. Müller)

Measurement and construction of a current-limiting resistance for 200-kV accelerators (G. Klement)

Investigation of ionization fire alarms (J. Bäumlner)

5. Electronics Group

(A. Steinhausen)

5.1 Power Sources

5.1.1 Stabilized High-Voltage Sources 0.6 - 5 kV/20 W (W. Melkus, W. Reinhardt)

Development work on this stabilized high-voltage source, which was mentioned in the last annual report, was completed. The source is fully transistorized and has the advantage that the available output voltage can be adapted to prevailing requirements by simple modification of the high-voltage section.

Output voltage: 0.6 - 5 kV set in 3 rough stages and infinitely variable in between.

Output power: 20 W in all ranges, but output current not more than 15 mA.

Variation of output voltage when mains voltage varies by $\pm 10\%$: $\pm 1\%$.

Variation of output voltage by load variation from no load to full load: 1% .

Ripple: 0.2% - 0.8% depending on load.

The polarity of the output voltage can be reversed by changing the wiring in the source.

The principle is shown in the block wiring diagram (Fig. 21).

It comprises a series pack, of which 20 units, 10 of them with modified output voltage, have already been built. Sources for maximum voltages of 10 and 20 kV are being constructed.

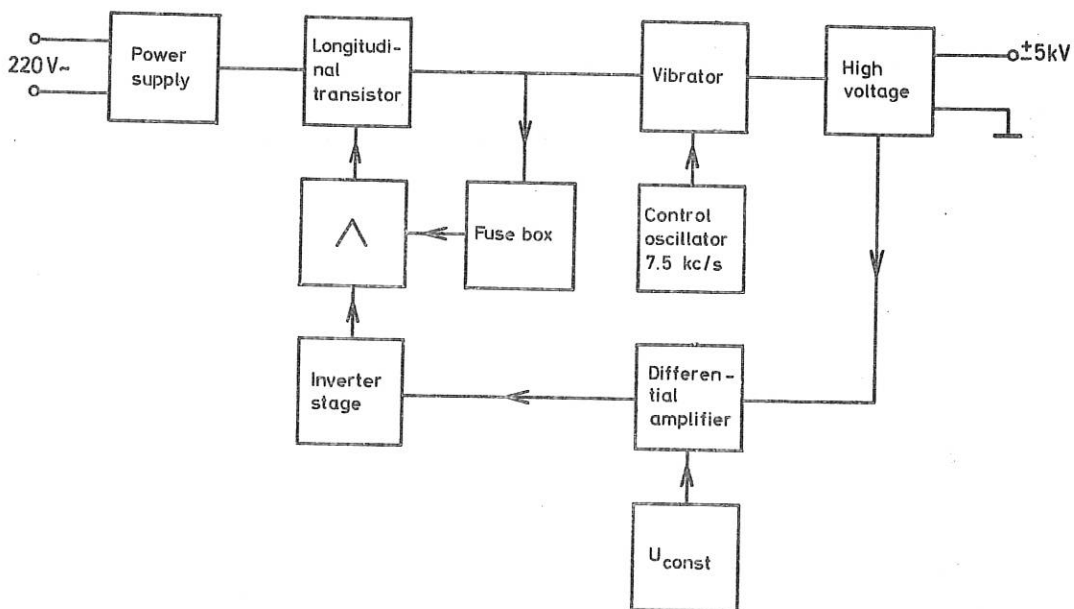


Fig. 21

5.1.2 Coil Current Supply Source 6 - 10 A at 2.2 Ω (F. Skerjanc)

A transistorized current stabilizer was developed for supplying current to a magnetic-field coil ($R = 2.2$ ohms). The current can be adjusted in stages of 6-7 A, 8-9 A, 9-10 A and infinitely to 1% .

Fluctuation of the supply voltage by $\pm 10\%$ varies the output current by $\pm 1\%$. At 9 A and with 2.2-ohm load the amount of ripple is 0.7% .

A built-in electronic microfuse safeguards the source against overloading.

5.1.3 Emission Current Stabilizer (F. Skerjanc)

A regulated emission current stabilizer was developed for a mass spectrometer. The emission current can be selected between 100 μ A and 3.8 mA. The filament voltage hereby is adjusted from 0 - 3 volts. The whole device is insulated up to 5 kV from the grounded outer case.

5.1.4 Constant-Voltage Source 20 to + 200 V; 3 A (W. Melkus)

Development is proceeding on a constant-voltage source which can take power at negative voltages. The equipment consists essentially of two control circuits, one with controlled silicon rectifiers for the rough adjustment and one with transistors ensuring a voltage constancy of $\pm 1\%$. Noteworthy is the high efficiency, hence the low heat generation of this circuit. It is therefore expected that appreciably higher outputs, higher currents in particular, will be attained.

5.2 Measuring Amplifiers

5.2.1 RF Broad-Band Amplifier 50 kc/s - 5 Mc/s / 70 V_{SS} (F. Skerjanc)

For ion resonance measurement an amplifier of this type was constructed and connected to a sine-wave generator. At a load resistance of 50 ohms it supplies 70 V_{SS}. Its output resistance is approx. 5 ohms. The amplification is 10. The output stages work on the cascade principle.

5.2.2. High-Resistance Logarithmic DC Amplifier (F. Skerjanc)

For measuring a probe current a logarithmic amplifier was developed whose input resistance is approx. 500 Gohms. Connected to a power source of 10 mV to 10 V with an internal resistance of $10^9 \Omega$, it attains a band width of 0 to 2 kc/s. Chosen as the input stage was a special cathode follower combination circuit which ensures a very high input resistance and the smallest possible input capacitance. This is followed by a linear amplifier the logarithm of whose output voltage is taken by a silicon diode stage.

5.2.3 Probe Cathode Follower (G. Roos)

For an electrolytic tank a probe amplifier is being developed which at an input impedance of approx. 1 Gohm and with parallel capacitance of a few pF has an output range of 300 V_{SS}. The wide range is attained by a special version of the bootstrap principle. The voltage amplification is about 0.995; the output impedance approx. 100 ohms and the frequency range 0 to a few kc/s.

5.3 Fast Control System (F. Skerjanc)

Developed as an additional feature of the time delay programme was a series unit with which trigger pulses can be delayed up to about 11 msec in the following manner:

10 stages of 1 msec, 10 stages of 0.1 msec and infinitely between 0-0.1 msec.

5.4 Slow Control System (W. Melkus)

The device has four identical time stages, each of which triggers the following stage after a period infinitely variable between 0.1 - 1; 1 - 10; 10 - 100 sec. The time interval is determined by RC circuits which trigger a thyatron, this in turn actuating a relay. The unit affords wide scope for application.

So far 15 of these devices have been produced.

5.5 Image Converters

5.5.1 Image Converter Camera for High-Speed Photography with the RCA Tube 4449A

(F. Hofmeister, W. Urbas)

The development of image converters with the RCA tube 4449A was introduced by the group in 1961 with the reproduction of a type designed earlier by A. Steinhausen. With this as a basis, several progressively improved models materialized in due course, the last of these being type EL 085, completed in October 1964. Construction was started on a series of this type; the first completed unit was supplied by the end of the year to CEA, Fontenay-aux-Roses.

With the advent of image converter EL 085 this development series can be considered on the whole as complete. Improvement of the electronic system means that the image quality is now virtually determined only by the properties of the tubes used. The image converter can be made available for various purposes by means of exchangeable plug-in units. For present requirements the following types were developed:

- a) Plug-in unit for sweep photographs with a sweep speed adjustable between 100 mm/ μ sec and 5 mm/ μ sec;
- b) Plug-in unit for rapid sets of three with time intervals adjustable between 50 nsec and 500 nsec and with exposure times of 10 nsec - 50 nsec;
- c) Plug-in unit for slow sets of three with time intervals adjustable between 5 μ sec and 100 μ sec and exposure times of 0.05 μ sec - 1 μ sec.

Extension of the plug-in unit programme later is possible. It is intended to develop a slower streak photograph plug-in unit and a μ sec plug-in unit for seven very rapid photographs of size 5 x 25 mm for spectrographic use.

5.5.2 Image Converter for Light Amplification and High-Speed Photography with EEV Tube P 829 A

(A. Steinhausen)

In this image converter further technical improvements were carried out on the supply systems, the rapid control system and on the optical equipment. The image converter was used for the arc experiment (C. Mahn, H. Ringler).

5.5.3 Generation of Fast Pulses (A. Steinhausen)

General investigations were conducted with gas tubes to produce small rise and fall times. In particular, pulses with rise times of about 1 nsec were obtained at 4 kV.

5.6 Ruby Lasers

5.6.1 Laser Head (K. Maischberger, G. Roos, (H. Häglsperger))

The type with elliptical high-eccentricity mirror and direct cooling of the ruby rod described in the annual report was adapted for an appreciably higher flash energy. The maximum energy of the lamp used (EGG, Type FX 47) is 10 kJ, but this should be limited to 7.5 kJ to ensure a long service life of the lamp.

5.6.2 Laser Bank (G. Roos)

As power supply for 4 lamps, arranged crosswise, of a purchased laser a bank with a storage capacity of 4 x 10 kJ was developed and partly constructed. Owing to the large dimensions and the weight the unit was divided up into 4 mobile banks of 2100 μ F each at a max. operating voltage of 4 kV. Incorporated in the individual bank carriages are the charger, discharger, a series choke for the lamp and an ignitron. The control system of the unit is located in a separate rack shared by all four banks, and so the laser and the banks can be set up in an experiment room of their own.

A special feature worth mentioning is the preionization device for extending the lifetime of lamps: about 30 μ sec after the high-voltage ignition pulse the discharge currents are switched to the lamps; each by a different ignitron.

5.7 Other Diagnostic Tools

5.7.1 Integrator (K. Maischberger)

This equipment was developed for current integration in an ion accelerator. It has 2 electronic counters and a five-figure counting relay with digital indicator and enables the charge $Q = \int I dt$ to be recorded over time intervals of 1 minute to 28 hours. A changeover switch allows 2 current ranges of 10^{-7} to 10^{-5} A and 10^{-5} to 10^{-2} A to be selected. The unit can be used without being grounded and has an accuracy of 1 %.

5.7.2 RF Pulse Transmitter (G. Roos, F. Skerjanc)

The requirements to be met by the RF pulse transmitter described on page 155 of the annual report for 1963 were rather high. This made it necessary to develop a new version.

In the old model the gate pulse served directly as DC voltage. In its successor the door pulse is compensated and a variable DC voltage connected in series.

The circuit consists of a symmetrical diode gate to which a double push-pull output stage is connected to the output. This is constructed in such a way that it can be changed over to 2 end stages with inphase-opposed output signal. The adjustable DC voltage is connected to the amplifier output via a C-L unit.

5.7.3 Electron Beam Compensation (K. Maischberger)

The deflection which an electron beam undergoes on passing a gas discharge because of the latter's electric field can be compensated by creating an equally large field by means of auxiliary electrodes. This affords a convenient method of measuring electric fields in gas discharges which can be extended to provide electronically controlled compensation. Such an experimental device has been constructed.

5.8 Transmitters

5.8.1 1.5-MW Pulse Transmitter (G. Roos)

A coaxial power line system for fitting a load to the transmitter was calculated and designed in collaboration with the Design Group. The load, the plasma column, is known

only approximately. The line system is therefore provided with several connections of varying impedance.

Parts of the control system for the transmitter, such as control panels for supplying the pulse stage with DC voltage and the appropriate linking circuits for the transmitter and the experiment, are complete.

5.9 Maintenance (B. Heine)

Repair and maintenance work was performed on 469 units. Costs for spare parts came to DM 7 888.63. Another 11 units had to be sent out for repair. These repairs cost DM 1 167.65.

6. Magnetic-Field Group

(B. Oswald)

6.1 Intense Stationary Magnetic Fields (B. Oswald)

In order to create the conditions for developing intense magnetic fields of up to over 100 kG in small field volumes and medium fields in models of fairly large volume and at the same time to enable heavy-duty magnetic coils to be tested, a motor generator set was installed in the Group's facilities and is to be put into service soon. The converter consists of a drive motor and two DC generators which can be connected in series or in parallel as required. The continuous rating is 2 x 700 kW at a current strength of 2 x 2500 A. In short-time operation the set can be loaded up to 2 x 700 kW at 2 x 7000 A. The firm of Schorch in Rheydt was responsible for the construction and installation of this converter.

Available since the beginning of the year for investigations on superconducting materials and for other kinds of measurement work is an iron magnet for homogeneous and time-accurate fields of up to 50 kG.

6.2 Water-Cooled Coils (H. Lohnert)

In collaboration with the Design Group and the Workshop series production of coil type Sp 300/12 was initiated. 60 coils of type Sp 100/13 have been produced and some of them tested. For the purpose of testing the winding insulation it was necessary to develop a RF generator for 200 - 500 kc/s.

Curves and tables relating to the field distribution of individual coils were published in the form of an IPP report. Tables of operating values and design data are being compiled.

6.3 Coils for Hourglass Magnetic Fields (A. Kellerbauer, P. Krüger, B. Oswald)

Several new pancake-type coils with fairly large dimensions (inner diameter 80 mm, axial length 500 mm or 600 mm) were produced. In designing these coils special care had to be taken to preserve the rotational symmetry of the field. In this connection the time dependence of the field was also investigated more closely as the current rose and during transition to the extended current peak.

Allowance was made for the steepest possible field drop at the coil ends by providing one of the coils with 2 moveable counter-field coils.

6.4 Magnetic Field for Shock Tube (A. Kellerbauer, P. Krüger)

In order to produce as homogeneous a magnetic field as possible of about $10 \text{ k}\Gamma$ for the shock tube being constructed for Dept. 3 it was necessary to develop a rectangular coil which had to be adapted to a given capacitor bank.

A pair of two-turn coils were tentatively put into operation. In the magnetic-field measurement of this device the influence of eddy currents in the solid copper electrodes on the field distribution was investigated more closely.

6.5 B-min Field (P. Krüger, B. Oswald, R. Pöhlchen)

In connection with "HELIOS" and "HELIOSIS" the Group contributed to discussions on the technical realization of B-minimum fields. Because of the requirements to be met both by the mirror coils and the Joffe bars it was necessary to consider optimization more exactly in view of the extent of ohmic loss.

A four-pole B-minimum coil model was constructed, the contours $|B| = \text{const}$ being measured for a mirror ratio of 1:3 and compiled in graph form. Such a set of curves is represented in Fig. 22 for the median plane between 2 Joffe bars.

With regard to the current density and the joulean heat in the Joffe bars it was necessary to make a comparison between four-pole and six-pole arrangements.

6.6 Superconducting Coils (H. Lohnert, P. Krüger, B. Oswald)

In a fairly small metal cryostat 2 experimental coils with an inner diameter of 25 mm, an outer diameter of about 70 mm and an axial length of 65 mm were tested first. One of these coils was wound with single-insulated Nb₂S₅Zr wire with a bare diameter of 0.254 mm and attained a maximum magnetic flux density of $30 \text{ k}\Gamma$ on the coil axis. The second consisted of copper-plated Nb₂S₅Zr wire and had the same dimensions. Together with a small insert coil with an inner diameter of 10 mm it was excited to just over $60 \text{ k}\Gamma$.

In the variable field of the large coil the quench characteristic of the insert coil was recorded. It was here found that in the upper field range the limiting values of this coil agreed with the curve given for wire samples, and so only in the lower field range could a slight degradation effect be observed (v. Fig. 23).

At a magnetic flux density of $10 \text{ k}\Gamma$ the maximum current density measured was 10^5 A/cm^2 .

After completion of a larger cryostat with a freely accessible inner diameter of 30 mm a pair of coils with a minor diameter of 50 mm, an outer diameter of 152 mm and 158 mm respectively and an axial length of 50 mm was constructed. Besides producing an effective field of about $40 \text{ k}\Gamma$, this device was intended for investigating the dependence of the quench characteristic on the coil size and investigating the split-pair effect. The design made it possible to modify the distance between the coils and excite different parts of the windings (v. Fig. 24).

B-min field; B = const. lines; mirror ratio 1:3; 4-pole Joffe field
 $J \cdot w_{\text{mirror}} : J \cdot w_{\text{counter}} : J \cdot w_{\text{Joffe}} = 5:1:5$

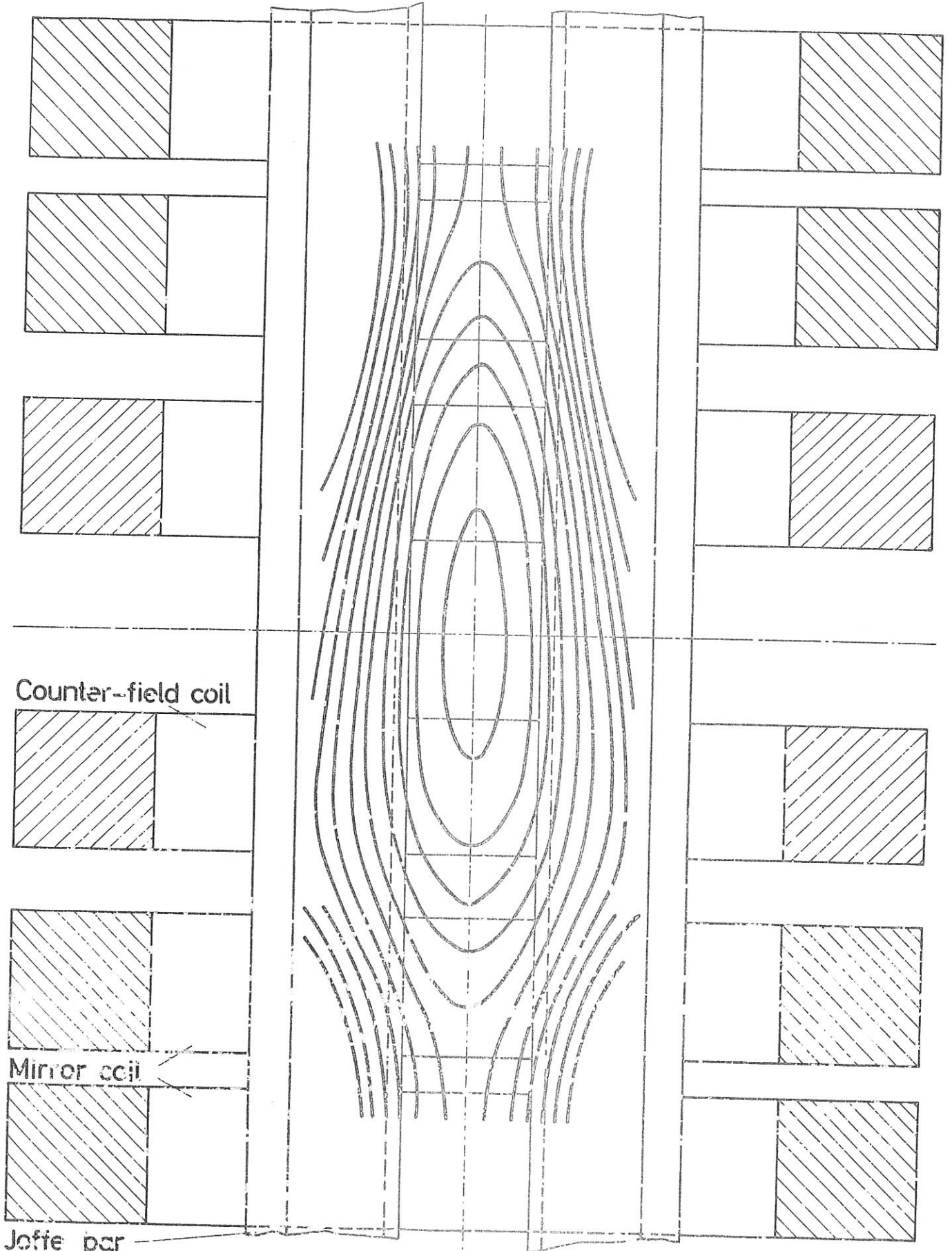


Fig. 22

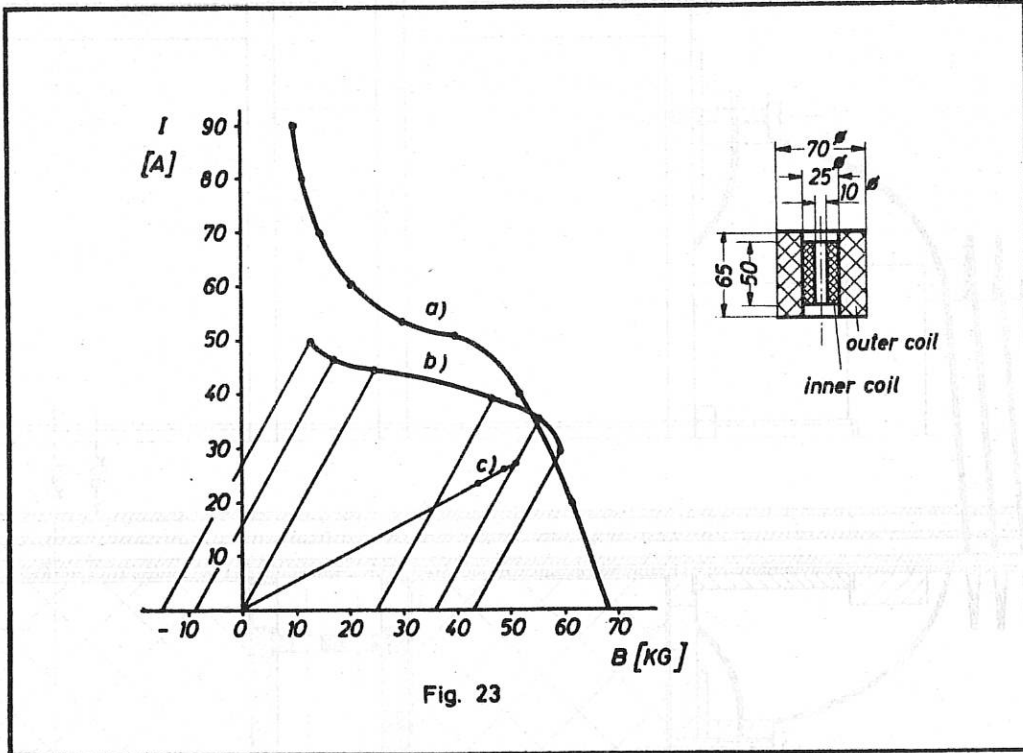


Fig. 23

Fig. 23 Limiting characteristic of superconducting coils
a) Wire sample Nb₂₅Zr, 0.254 mm, copper-plated
b) Inner coil
c) Outer coil

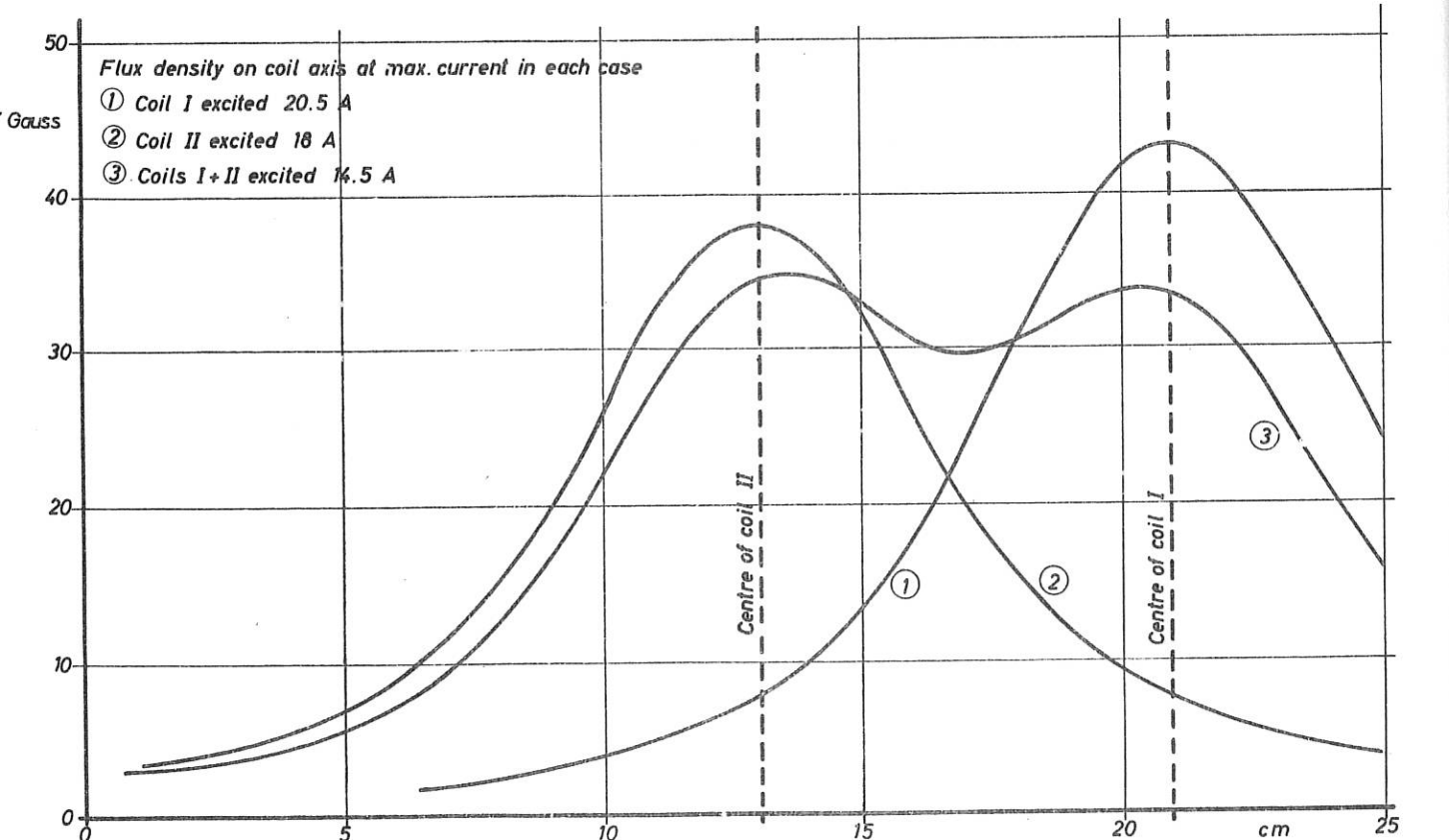
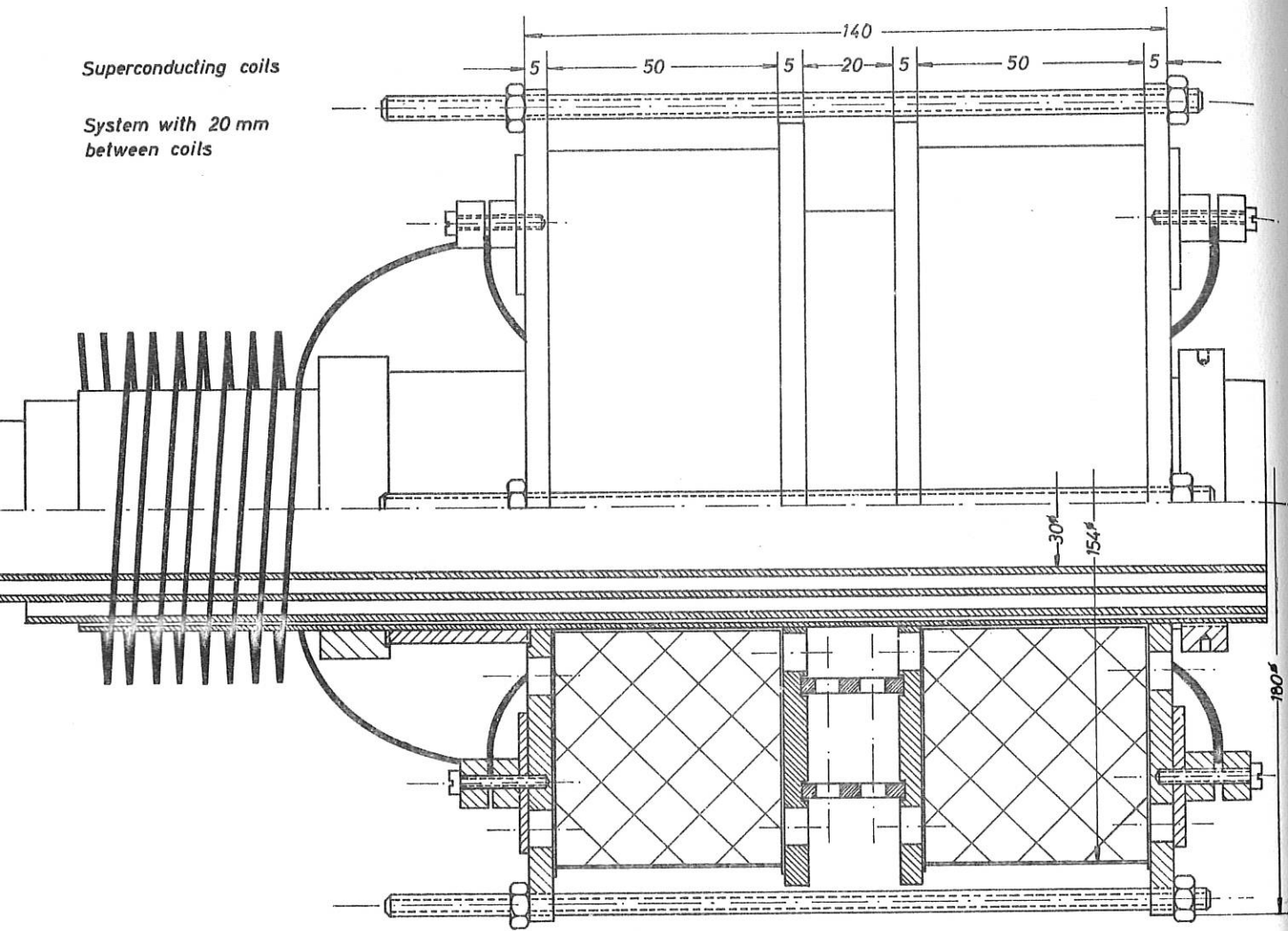
The latest experiments show that it is not difficult to construct superconducting coils of up to 50 kG for diameters up to 50 mm. The size of the field volumes required in plasma physics makes it necessary, however, to develop larger coils. Special importance is here attached to further investigation of the degradation effect. This work is therefore being performed in conjunction with investigations of the Special Physico-technical Group on wire samples since an explanation can be expected from the physical behaviour of the superconductor itself. Together with the Vacuum Group a start was made to constructing an experimental cryostat for large coils.

Superconducting coils with high energy content call for safety precautions in the event of an unintentional normal transition. An appropriate protective circuit was built for the coils described above.

At present there are hardly any wires or strips available for fairly intense magnetic fields. A trial coil of Niostan strip (Nb₃Sn) failed by a wide margin to reach the limiting values given for short samples. A small coil of NbTi wire is being prepared.

6.7 Magnetic Energy Storage (B. Oswald)

Magnetic energy storage devices may be of interest mainly in the case of ohmic loads. At the present level of superconducting technique superconducting storage units for very high discharge voltages would have to be devised first before useful discharge velocities could be attained.



Another difficulty arises from the fact that hard superconductors tend to become normal conductors as a result of rapid variations of field or current.

Further theoretical consideration was given to the discharge characteristic of magnetic energy storage devices and to the usefulness and efficiency of superconducting storage devices (v. IPP 4/13).

6.8 Extreme Magnetic Fields (H. Lohnert)

Preparatory work was done towards producing extreme magnetic fields of up to 1 MF and carrying out the measurements entailed. In small multi-turn coils it was possible to obtain short-time flux densities of up to 600 kG.

6.9 Magnetic-Field Measuring Technique (A. Kellerbauer, P. Krüger)

In order to do justice to the diversity of measurement work, the measuring equipment for both stationary and radio-frequency magnetic fields was improved. A non-magnetic X-Y probe guide of high accuracy is now available for Hall and magnetic probes. A proton resonance probe for calibrating magnetic field probes is being prepared.

7. Vacuum and Technology Group

(H. Häglsperger)

7.1 Vacuum Technique

7.1.1 Laboratory Pump Stand P 121 (H. Häglsperger, H. Münch)

A pump stand was developed for laboratory purposes. The pump system comprises a backing pump RZ 12, a diffusion pump DO 121, a high-vacuum slide valve, three small-flanged valves without stuffing box for the prevacuum, for the by-pass and for ventilating the recipient, and also a safety valve combined with ventilating valve for the backing pump. Besides the high-vacuum pump nozzle there is a prevacuum pump nozzle for work in the fine-vacuum range.

Data:	
Final total pressure without cooling trap	$1 \cdot 10^{-6}$ torr
Final total pressure with colling trap	$5 \cdot 10^{-7}$ torr
Effective suction capacity at pump nozzle	50 l/sec

7.1.2 High-Vacuum Slide Valve (H. Münch)

Two sizes were developed, NW 32 and NW 65. The valves have small dimensions for fitting purposes, allow completely free passage when open and withstand atmospheric pressure in both directions. The connection dimensions correspond with those of the usual standard flange.

7.1.3 Metal Cooling Traps for Liquid Nitrogen (H. Häglsperger, H. Münch)

Two types of cooling trap were developed:

- a) Bakeable UHV cooling traps NW 32 and NW 65, which are designed for both horizontal and vertical installation, maximum coverage of the condensation surfaces with liquid

nitrogen being guaranteed in each case.

Conductance of cooling trap NW 32	5 l/sec
Capacity	4 l
Consumption	≈ 0.3 l/h

The data of cooling trap NW 65 are not yet available.

- b) Angled cooling trap NW 65 for dismantling, suitable for incorporation in vacuum systems instead of a tube turn NW 65, with maximum utilization of the coolant. For cleaning the condensation surface the cooling trap can be taken apart without undoing the connection points to the vacuum apparatus. Data on the cooling trap are not yet available.

7.1.4 Rapid-Opening UHV Valve (H. Häglsperger)

A valve for measuring molecular flow was designed and constructed.

Valve stroke	20 mm
Opening time	< 1/50 sec
Shutting force against which opening is possible	approx. 7 kp
Leak	< 10 ⁻¹⁰ torr l/sec

The valve is opened by means of a lifting magnet and then locked. An attached mechanism allows the valve disc to be returned smoothly to the closed position. This is necessary because the valve seat takes the form of a glass capillary tube.

7.1.5 Effusion Cell (H. Häglsperger, (A. Wasner))

For measuring vapour pressures according to the crystal oscillator method a so-called effusion cell was designed. The nitrogen bath is pumped off via a manostat to keep the temperature constant. A replenishing device for mounting on top in which the temperature of the liquid nitrogen is also set and kept constant by lowering the pressure above the surface of the bath enables the liquid nitrogen to be replenished at reduced pressure.

7.1.6 Pump Stand with Recipient (H. Münch)

For the purpose of investigating the trigger mechanism in plasma switches a pump stand with appropriately designed recipients was developed and constructed.

7.1.7 Service for Vacuum Pumps (H. Münch)

This facility was introduced to make possible the testing, maintenance and repair of vacuum pumps on the spot.

7.1.8 Other Work (H. Häglsperger, H. Münch)

Coating of parts in high vacuums, leak detecting and testing work on vacuum components and apparatus

7.2 Low-Temperature Technique

7.2.1 Standard Transfer Line for Liquid Nitrogen (H. Häglsperger)

Standard transfer lines were developed and made for the "PAGAN" 100-l nitrogen cans of the British Oxygen Company Ltd. in use at the Institute. The transfer line unit comprises

can connection with safety valve, connection for combined pressure build-up and release valve, connection for stand-type gauge, and vacuum-insulated transfer line.

7.2.2 Stand-Type Gauge for 100-l Cans (H. Häglsperger, (K. Maischberger))

A stand-type gauge was developed as a supplement to the standard transfer lines described. On being switched over, the gauge measures each time in a quarter of the can volume. Once a minimum level is reached an acoustic signal is given.

7.2.3 Automatic Cooling-Trap Replenishing Device (H. Häglsperger, R. Scherzer)

A start was made to developing an automatic replenishing device for cooling traps. A vapour pressure thermometer dependent on the filling level of the cooling trap actuates a control piston which in turn clears or shuts openings in the control cylinder. This causes appropriate lines to make the connection of compressed air to can to cooling trap, i.e. replenishment, and also the connection of can to atmosphere, i.e. ventilation of the can.

7.2.4 Storage Tank for Liquid Nitrogen (H. Häglsperger)

A storage tank for liquid nitrogen with a capacity of 200 l of liquid gas was planned and ordered. The storage tank is intended as a container for the liquid gas produced on the premises. The contents can be tapped by the force of gravity, using either a liquid-gas pump or pressure build-up.

7.3 Technology

7.3.1 In the field of General Technology the following lists some of the assignments for which Mr. Berberich was responsible:

- a) Development of bakeable metal-ceramic compounds
- b) Experimental measurements with extending measuring strips
- c) Experiments with models in the field of photoelasticity
- d) Adhesion experiments on plexiglass and Trovidur parts for capacitor casings
- e) Production of sheaths for electrodes of W, Mo, Ti, stainless steel and Inconel for improving the burn-up properties
- f) General galvanization technique
- g) Glass technique

7.3.2 Electrostatic Coaxial Probes (G. Dietz, H. Häglsperger)

For measuring densities and temperatures in plasma, probes made of brazed metal and ceramic compound were developed and produced. Stipulated values were:

Heat resistance	up to 450 °C
Insulation resistance	> 100 MΩ
Leak	< 10 ⁻⁶ torr l/sec

7.3.3 Plexiglass Experiment Chamber (H. Wetzel)

A plexiglass chamber for shock wave experiments was cemented by means of a reliable gluing method, i.e. by restoring all adhesive compounds to surface adhesion.

7.3.4 Investigation of Coil Models (H. Wetzel)

Investigation of discharge coils was conducted on the basis of photoelasticity. The object of these investigations was to find the ideal shape for such coils in relation to the load expected. Hitherto only cases of static load have been investigated.

7.4 Glass Technique (F. Zitzmann, K. Fritsch, W. Landgraf, R. Ehrlich)

Of 158 orders placed 145 were completed. The total number of hours involved is spread over the separate departments as follows:

Department 1	approx. 100 hours
Department 2	approx. 1 900 hours
Department 3	approx. 40 hours
Department 4	approx. 1 000 hours

Production review:

Tempitron with multiplier	1
Electron gun and chamber system for two-chamber ionization gauge	1
Double-grid probe 60 mm in diam.	1
System build-up for 90° spectrometer	2
Ion-electron converter for 90° spectrometer	2
Farvitron systems	4
Multiplier with flange	1
Probes of various types (guard ring, Urax, grid, dipole and RF probes)	188
Sinter parts for tubes, discharge tubes and vacuum ducts	50
Apparatus for growing monocrystals	3
Glass vessel for gas laser	1
Hg glass pump stands	2
Glass tubing of various diameters	240

Other orders involved new production or repair of vacuum installations, glass equipment and apparatus.

8. Installation Group

(M. Kottmair)

8.1 200-kV Accelerator of Dr. v. Gierke's Department (M. Kottmair)

The control system for the power supply to the ion source was put into service. Wiring diagrams were made complete and line and terminal diagrams compiled.

8.2 Chargers for Capacitor Banks 8-70 μ F, 20 kV and 4-3 μ F, 40 kV (M. Kottmair, W. Jakobus)

On the basis of existing data chargers were designed for the capacitor bank which keep its DC voltage constant in the region of $\pm 1.5\%$. Constancy is maintained by recharging the leakage losses when the capacitor voltage has dropped to the lowest value of the range set. Altogether there are 2 chargers under construction. One unit (20 kV) is already available.

3.3 Rectifier 1000 V, 450 A for MPI, Institut für Extraterrestrische Physik (M. Kottmair)

The installation, including the necessary high-voltage connection, was planned in collaboration with the firms of BBC and SSW and the Construction Department. Delivery is to begin in December 1964 and the unit is to be installed in January 1965.

9. Special Physico-technical Group

(E. Berkl)

9.1 Symposium 1964 (E. Berkl)

In June of this year the 3rd Symposium on Engineering Problems in Thermonuclear Research was held in Munich, responsibility for the organization of which was assumed by the Engineering Department of the Institut für Plasmaphysik. The Secretary on this occasion was a member of the Group. At the close of the conference arrangements were made for publishing a report of the proceedings. The necessary editorial work has meanwhile been completed, and so a start can be made to distributing copies once printing and binding are finished.

9.2 Hard Superconductors (W. Amenda, E. Berkl)

As part of the joint programme with the Magnetic-Field Group on problems of superconduction, measurements were made on short samples of various commercially available hard superconductors. Serving as apparatus for these experiments was a glass cryostat for liquid helium which was originally intended for other investigations (v. annual report for 1963). This cryostat proved satisfactory because of its low evaporation rate and the ease with which it can be dismantled. Since, as already shown elsewhere¹⁾, measuring the critical current of a superconductor by current pulses also gives the correct value and experiments with direct current, besides involving considerable expense on apparatus, almost invariably cause damage to the probe at high, critical currents, we settled for measurement by means of pulses. For this purpose controlled silicon rectifiers were used to construct a pulse generator with the following data:

$5 \mu\text{sec} \leq t_{\text{pulse}} \leq 1.1 \text{ msec}$, $2 \text{ A} \leq I_{\text{pulse}} \leq 130 \text{ A}$ at a load resistance $R_a = 0.5 \Omega$. The pulse generator can be triggered. The transition to normal conduction is determined by means of an oscillograph.

It was shown that the critical current measured depends on the previous magnetic history of the superconductor. I_c - H_c curves are usually determined in such a way that with a constant external field the wire sample acts as a normal conductor when subjected to a current $I > I_c$ and, once recooling has taken place, I_c is gradually approached. In this method frozen fluxes arising from the original switching on of the external field are ignored (denoted in the curve examples by I). If the magnetic field is started up anew prior to each measurement, frozen fluxes are obtained in the hard superconductor which are wholly included in the measurement result (denoted by II). This possibly affords an explanation, in part at least, of the degradation effect (coil comprising hard superconductor shows lower, critical values than those obtained from the short sample). Work continues on this problem.

1) E. Berkl and R. Weyl: Z.f.angew. Phys. 16, 415 (1964)

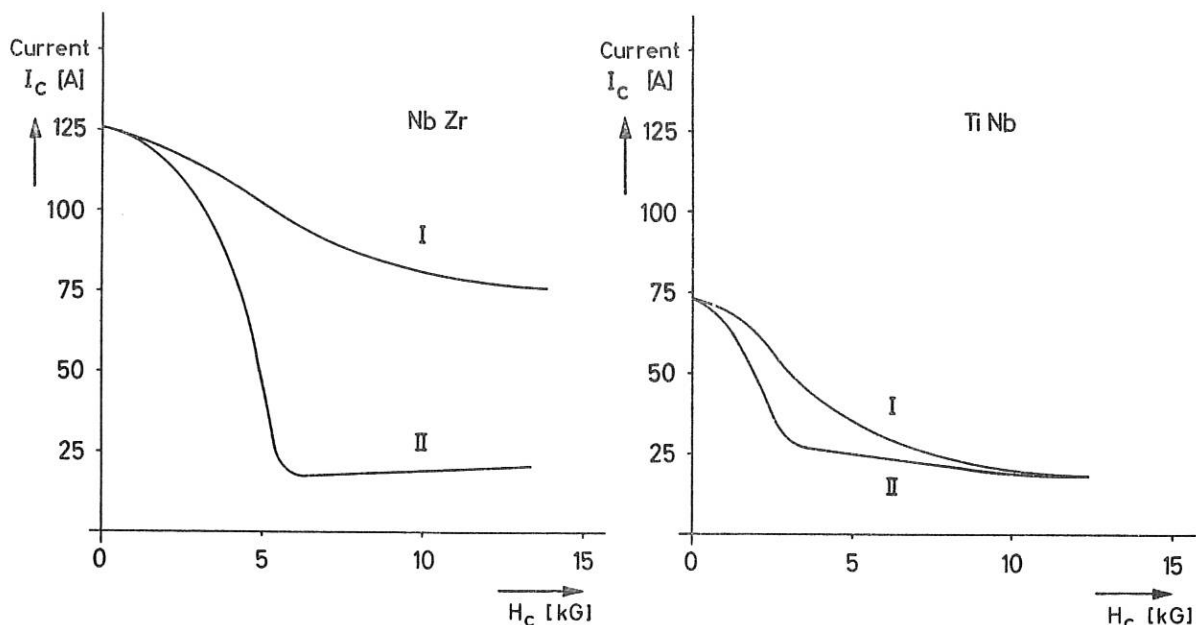


Fig. 25

Preparations for measuring I_C - H_c curves under tensile stress have been concluded and investigations start in December 1964.

9.3 Helium Liquefier (E. Berkl)

One of the responsibilities of the Group is running the Linde helium liquifier He 36. Owing to technical difficulties in the unit, some of which occurred only after incorporation of the new 2-stroke expansion machine according to Doll, regular operation has not been possible so far. After a number of trial runs a few shortcomings were detected, the suppliers being requested to eliminate them.

9.4 Random Sampling (R. Klockenkämper)

When high-voltage capacitors for fast banks are purchased random checks are carried out (High-Voltage Group) in order to assess the truth of guarantee particulars submitted by suppliers. The degree of probability involved was investigated. In random sampling, without replacement the hypergeometrical probability distribution w gives the probability of detecting m defective units among K capacitors tested, if the number of defective units in the total batch of N capacitors is n .

$$w_K(m) = \frac{\binom{n}{m} \cdot \binom{N-n}{K-m}}{\binom{N}{K}}$$

This function was devised to provide a characteristic of the testing method's reliability.

9.5 Frequency Modulation of Laser Light (E. Berkl, R. Klockenkämper)

Work was continued on the problem of frequency modulation of a coherent light beam. From data in literature and personal studies it appears that at the present level of VHF technique it is possible to separate the side bands by approx. 10 Mc/s, using crystals of

the tetragonal space group $\bar{4} 2 m$ as modulators. A KH_2PO_4 monocrystal has already been grown by Mr. Weichselgartner for such experiments.

As compared with the crystals of space group $\bar{4} 2 m$ more favourable values (smaller loss angle, higher limiting frequency) are obtained with many perovskites. These, however, are sometimes difficult to grow since a great many of them are insoluble in water and can therefore only be cultivated as monocrystals from the fused mass.

A He-Ne gas laser for modulation experiments is almost complete.

10. Chemistry Group

(H. Weichselgartner)

10.1 General and Routine Work (H. Weichselgartner, H.-J. Wittich)

The Chemistry Group was entrusted with a great deal of cleaning, degreasing, derusting, descaling and staining work. Some of these processes represented stages preparatory to further surface treatment. For protecting the surface of metal working materials it was generally sufficient to electroplate them with copper, nickel, cadmium or silver.

10.2 Special Electroplating Processes (H. Weichselgartner, H.-J. Wittich)

Included here are those processes which could only be realized after series of detailed experiments. The following can be singled out:

- True-to-size chrome-plating of tungsten wire
- Cadmium-plating of stainless steel with intervening Ni layer
- Consistently strong copper-plating (200μ) of K Monel
- Platinum-plating of brass ball probes with intervening gold layer
- Rhodium-plating of conductor plates.

10.3 General Material Testing (H. Weichselgartner)

Besides a variety of metal analyses prolonged series of experiments were conducted to investigate plastics also as to their resistance to oxidizing agents and other special properties.

10.4 Growing of Large Monocrystals (H. Weichselgartner)

For E. Berkl (Dept. 4) a start was made to growing large monocrystals of potassium dihydrogen phosphate KH_2PO_4 . The latter belongs to the ferroelectric crystals and crystallizes on the orthorhombic system. It has a curie point of 123°C . Good initial results could be obtained by a growing method based on the principle of the temperature difference between a storage vessel and the growing vessel. The largest monocrystal produced in this way measures $22 \times 17 \times 9$ mm (suitable for use) and weighs (with seed surface) a total of 15.25 g. The period of growth was approx. 4 weeks. The temperature in the growing vessel was in the region of $29.5 \pm 0.05^\circ\text{C}$. During the entire growing process the crystal rotated about its longitudinal axis at the rate of 24 r.p.m. Under the polarization microscope it was established that the KH_2PO_4 crystals grow along the crystallographic C axis. The cross section of the completed monocrystals is not dependent here on the growth period, but merely on the seed surface. A larger unit using the three-tank method is at present under construction. This is to allow four monocrystals to be grown simultaneously.

11. Central Workshop Group

(H. Stoll)

11.1 Mechanical Workshops (H. Stoll)

In February of this year work on the new building for the Central Workshop was sufficiently far advanced to allow the machine tools delivered for the new machine shop to be stored for the time being in Hall 3. In July the machines were then set up by the Central Workshop on the appointed sites and made operational but for the electrical connections. In October - November the workshops were moved to their new quarters.

A total of 19 skilled workers were engaged, while 4 left.

Staff strength of the individual workshops as of 31st December 1964

Mechanics	20
Precision Mechanics	10
Fitting and Welding	8
Plastic Workshop	1
Overhauling	1
Tool Stores and General Services	2
Job Preparation	2
Order Registration	1
Total	<u>45</u>

Processing of Production Orders

Order log

Carry-over from 1963	80 orders
Received	625 orders
Completed	<u>567 orders</u>
In hand	138 orders

Of the 567 orders completed 138 (i.e. 25 %) were handled by outside firms. The cost involved amounted to DM 521 904.--. At an hourly rate of DM 15.-- this sum would correspond to a production time of 34 793 hours. The number of hours expended on outside orders thus represents 57.5 % of the total hours expended.

One of the biggest assignments of the Central Workshop was installing the precollector and main collector and also producing individual parts for the 2.6-MJ theta pinch experiment of Dept. 1. This alone accounted for 5 911 hours.

Despite the larger staff and the corresponding increase in working capacity the carry-over of orders at the close of the year rose by approx. 50 % compared with the previous year. The planned production capacity of the new Central Workshop will probably not be attained till 1966.

Annual balance sheet of hours worked

Total hours: 46 936

Department	1	2	3	4	6	7	MPI für extrater. Physik	MPI für Physik	Store
Nominal %	35	23	20	12	1	1	3	-	5
Nominal hours	16 429	10 795	9 388	5 632	469	469	1 408	-	2 346
Actual hours	17 234	11 978	9 609	6 029	499	269	46	174	1 098
%	36.8	25.5	20.5	12.7	1.1	0.6	0.1	0.3	2.4

In the course of the year a new key for distributing the working capacity of the Central Workshop was decided on by the departments of the IPP, the MPI für Physik and the MPI für extraterrestrische Physik. This key forms the basis of the Workshop balance sheet.

11.2 Carpentry Shop (W. Kaehs)

The carpentry shop moved into its new quarters in the Central Workshop block at the beginning of November. The staff was increased from 5 to 6 members.

Production Orders

Order log

Carry-over from 1963	19 orders
Received	195 orders
Completed	176 orders
Cancelled	1 order
Carry-over	<u>37 orders</u>

With this carry-over of orders the carpentry shop has work in hand for approx. 3 - 4 months.

Annual balance sheet of hours worked

Total working time in 1964	6 642 hours
Number of hours for:	
Dept. 1	2 331 = 35.1 %
Dept. 2	1 204 = 18.1 %
Dept. 3	897 = 13.6 %
Dept. 4	1 618 = 24.4 %
Dept. 6	139 = 2.0 %
Dept. 7	452 = 6.8 %

12. Central Electrical and Electronics Workshops

(J. Asenkerschbaumer, E. Hecht, A. Simon)

Staff: 10 - 13 mechanics

<u>Series equipment:</u>	Produced in workshop:	Total:
Trigger unit 3.2 kV	20	31
Trigger unit 1 x 20 channel	3	8
Pulse transformer 3.2 kV	104	239
Power unit 3.2 kV	10	15
Time lag unit 10 msec	1	1
Mains distributor, small	10	31
Mains distributor, 220 V	3	11
Mains distributor, 110 V	12	13
Image converter with RCA tube 4449 A	1	7

<u>Series equipment:</u>	From outside firms:	
Time lag unit 100 μ sec	25	86
Time lag unit 1000 μ sec	25	25
Timer 0.5 - 60 sec	15	15
Socket panel	50	200

Orders to the value of DM 309 262.-- were placed with outside firms.

Hours worked: 8 931

For Department	1	2	3	4
actual %	30	36	21	13
nominal %	39	26	22	13

MANAGEMENT AND ADMINISTRATION

1. Personnel Development

The number of persons employed increased in the course of 1964 from 473 to reach a total of 575.

This figures comprised	Number	%
Scientific and techno-scientific personnel	106	18
Technical personnel in departments and workshops	303	53
General services	118	20
Management and administration	38	7
Scholarship holders	10	2

These figures include 12 staff members sponsored by Euratom. In addition, there were 5 guest research scientists from abroad.

Personnel development since the Institute was founded is given in Fig. 1. The figures quoted for 1965 represent the already approved employment level allowed for in the budget, while the figures for 1966 represent the estimates in the draft budget. Also taken into account are cleaning staff as well as scholarship holders, apprentices and canteen staff for 1965 and 1966. While the absolute number of employees rose at a fairly steady rate, there was a slight, but consistent rise in the number of general members of staff per scientist.

2. Construction Work

At the beginning of the report year 1964 facilities comprised 4 laboratory halls (L1 to L4), 2 workshop laboratory blocks (W1 and W2), a building for general services (T1), a building with rooms for scientists (D1), theory block (D2) with lecture room, library and air-conditioned rooms for the large IBM 7090 computer, the laboratory block for the Engineering Department (I1) with high-tension hall, the central power plant (EZ), the central heating plant (HZ) and also 3 huts with a total effective area of about 28 000 m².

The location and size of the individual buildings can be seen from the layout plan (Fig.2) and the aerial photograph (Fig. 3). In autumn 1964 the building for the Central Workshop and the Central Store (LW) was finished and occupied, the total effective area provided being 5000 m². This represented a substantial improvement in technical working facilities.

A few rooms of the laboratory block (L5) begun in autumn 1963 for Experimental Department 3 could be occupied by the end of 1964; by Easter 1965 the entire building should be ready (effective area 2200 m²).

In conjunction with laboratory block L5 a larger rectifier centre (L5E) was built and should be ready in the course of 1965. This centre is intended for experiments with high requirements in direct current, particularly for producing intense quasi-stationary

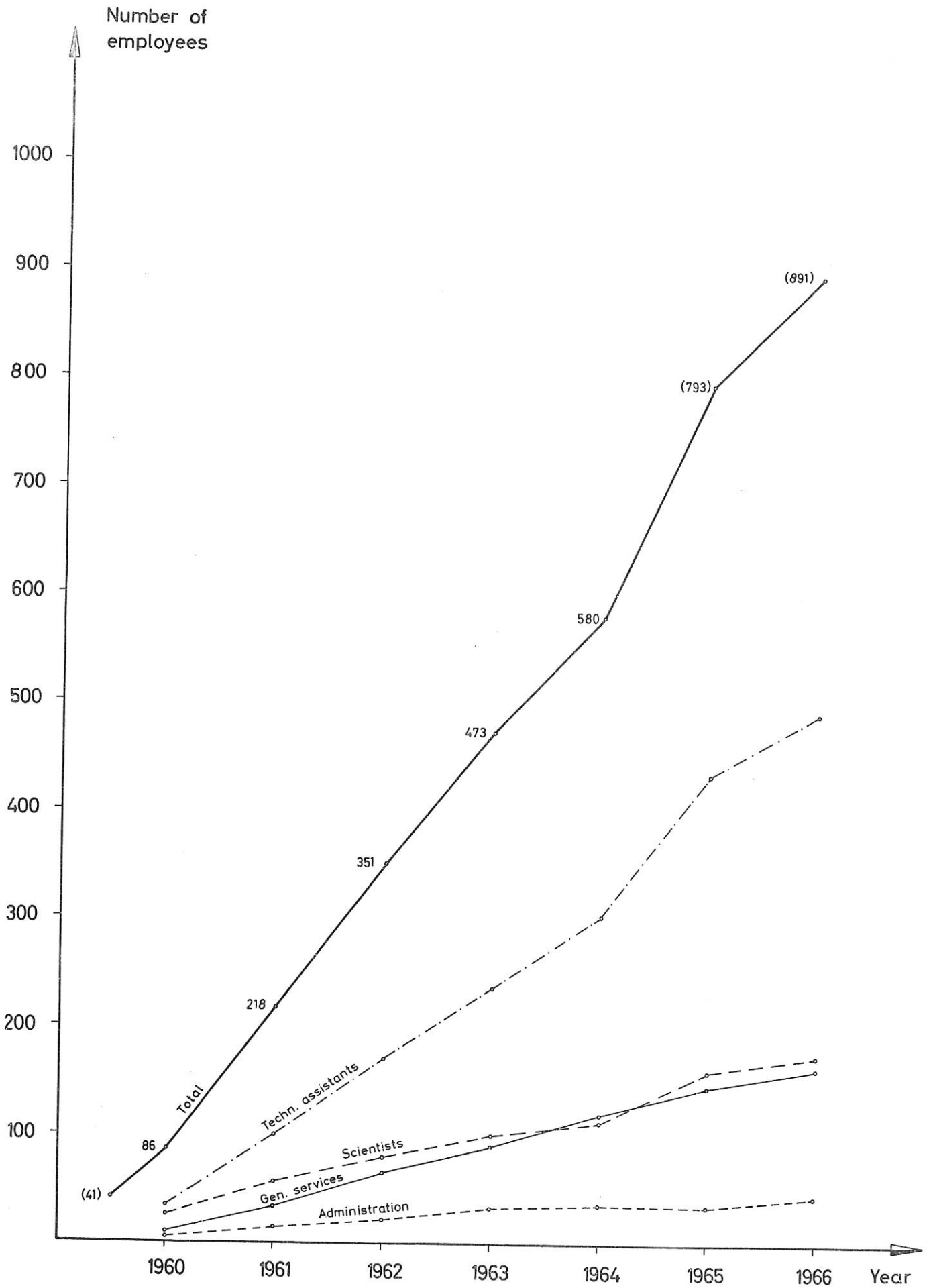
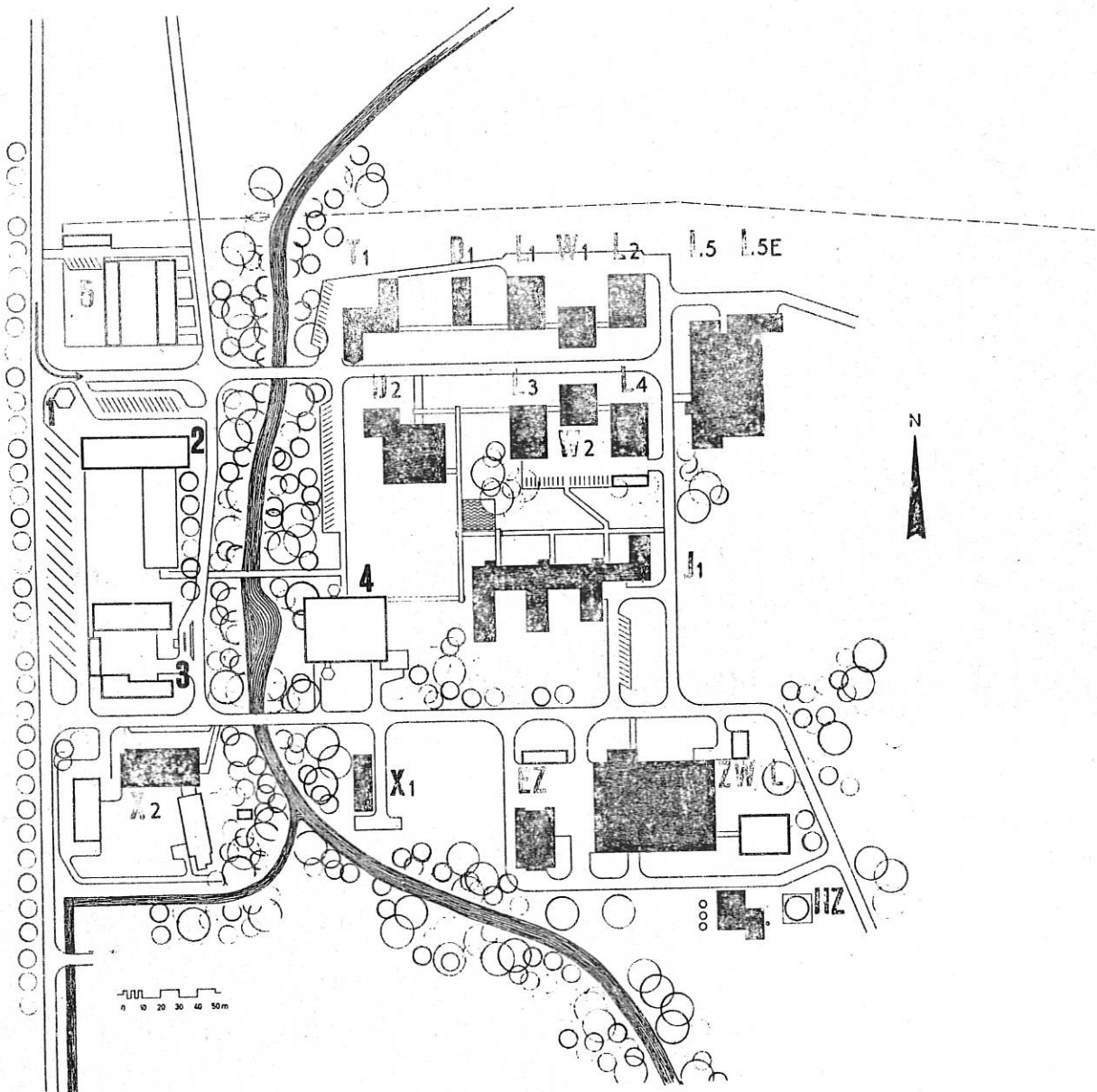


Fig. 1: Personnel Development

(As of 31st Dec.)



Layout Plan of the Institut für Plasmaphysik

1	Entrance and bus park	L5, L5E	Complex of the Department for Experimental Plasma Physics 3
T1, 2	Administration old and new (planned)	I1	Engineering Department Building
3	Transport stand-by service	EZ	Central Power Plant
4	Canteen (planned)	ZW/L	Central Store and Central Workshop with outbuildings
D2	Theory Department Building	HZ	Central heating and cooling plant
D1, L1	Complex of the Department for Experimental Plasma Physics 1	5	Apartments for guests and employees of the Institute
W1, L2			
L3, W2	Complex of the Department for Experimental Plasma Physics 2		
L4			

Max-Planck-Institut für Extraterrestrische Physik

X2	Complex of the Max-Planck-Institut für extraterrestrische Physik	X1	Hut of the Max-Planck-Institut für extraterrestrische Physik
----	--	----	--

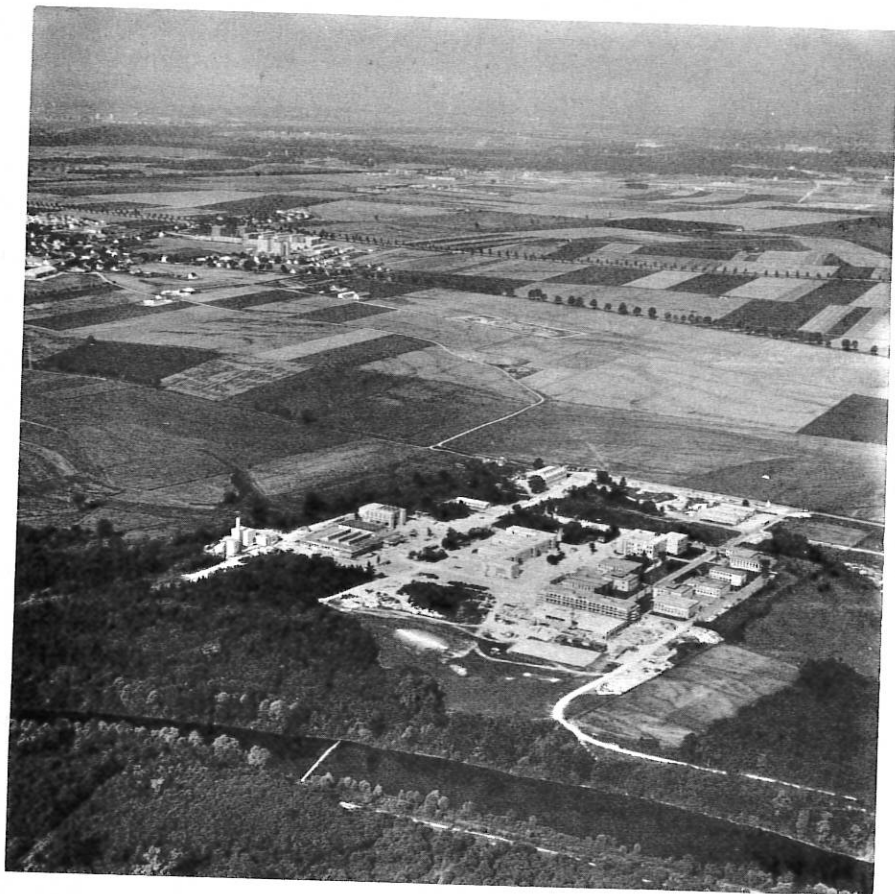


Fig. 3
Aerial photograph of the Institut für Plasmaphysik from the east. In the foreground the River Isar, in the background Garching. (Aerial photograph: Bayerischer Flugdienst Hans Bertram, Riem Airport, Munich; publication of photo No. GA 17/129 authorized by BStfWuV G 4/6003).

Fig. 4
Aerial photograph of the Max Planck Housing Estate on the north side of Garching. In the foreground the Schleissheim approach to the Munich-Nuremberg motorway. In the centre the two multi-storey apartment blocks for employees of the Institut für Plasmaphysik. In the background to the left the Reactor Station of the Munich Technische Hochschule ("Atomic Egg"), and adjoining this site on the right the buildings and installations of the Institut für Plasmaphysik. (Aerial photograph: Bayerischer Flugdienst Hans Bertram, Riem Airport, Munich; publication of photo No. GA 17/122 authorized by BStfWuV G 4/5996)



magnetic fields. The completion of this building marks the realization of the most important constructional conditions for the work of the scientific and technical departments of the Institute, as far as the first development stage is concerned.

In an attempt to concentrate work in one spot the Plasma Physics Department of the Max-Planck-Institut für Physik und Astrophysik in Munich has now been transferred to the site of the Institut für Plasmaphysik at Garching. Since sufficient space is not available in the existing facilities for the present volume of work, an additional hall will have to be built.

The remaining construction work of the first development stage includes the canteen, the transport stand-by service, the administration building and also apartments in the grounds for guests and employees. This will be accompanied by other development schemes.

Planning for the canteen has been completed. Because of the extremely cramped conditions in the present temporary canteen construction will have to be started in the first half of 1965, if possible. The new canteen is intended not only for serving lunches and refreshments, but also as a central meeting place for members of the Institute.

The transport stand-by service will accommodate the vehicles for both the day-to-day business of the Institute and the fire and first-aid services.

At the present main entrance of the Institute, where 3 huts are now located, an office building is to be erected. For the time being the individual sections of the administration are spread over the various buildings comprising the Institute. The new office building is also intended for general purposes. Also to be provided is an information centre, a facility made necessary particularly by the steadily increasing number of visitors. Alongside will be conference rooms with technical facilities for conferences of international study groups conducted in several languages.

The completion and financial settlement of all construction work forming part of the first development stage will take till the end of 1966. A start will then be made on a second development stage mainly involving schemes for extending and supplementing existing facilities. So far no definite decisions have been made in this respect.

On the northern outskirts of Munich, in the immediate vicinity of the Max-Planck-Institut für Physik und Astrophysik, 16 rental apartments for Institute employees were completed in the report year. Together with the 108 apartments in the two multi-storey blocks in Garching (cf. Fig. 4) that were already occupied at the beginning of 1963 these were essential for recruiting and keeping highly qualified personnel.

In the interests of work at the Institute it is imperative that efforts to provide accommodation be stepped up.

3. Organizational and Financial Development

In the report year there were no changes in the organizational structure of the Institute (cf. Fig. 5). The same applies to the persons constituting the business partnership on which the Institute is based and the Scientific Supervisory Board.

The joint research programme with Euratom instituted back in 1961 was successfully continued in 1964 as well. All scientific and technical investigations form an integral part of this programme.

For financing its work the Institute had at its disposal in the business year 1964:

Grants from the Federal Ministry for Scientific Research	DM 18,268,000
Grants from Euratom	DM 5,226,700
Grants from provincial governments via the Max-Planck-Gesellschaft	DM 3,194,000
Personal income	DM 1,037,000
Personnel costs	DM 6,474,800
Costs for materials	DM 1,431,600
General expenses	DM 3,130,300
Non-recurring expenses	DM 16,689,000

Of the non-recurring costs DM 11,161,300 was required for building projects.

The overall financial development since the Institute was founded is shown in Fig. 6. The figures quoted for 1965 represent the approved budget, while the figures for 1966 represent the estimates in the draft budget. These make it clear that recurring expenses, personnel costs forming an integral part, show a steady rate of increase. Building costs and non-recurring expenses, on the other hand, are subject to more marked fluctuations; nevertheless, the actual demand in this respect may be regarded as fairly constant.

Subsequent organizational and financial development will be determined primarily by the progress achieved in the scientific programmes.

<u>Exp. Plasma Physics 1</u> (Blocks D1, L1, W1, L2)	Head: Prof. Dr. Fünfer	<u>Exp. Plasma Physics 2</u> (Blocks L3, W2, L4)	Head: Dr. von Gierke	<u>Exp. Plasma Physics 3</u> (Block L 5)	Head: Prof. Dr. Wienecke	<u>Engineering</u> (Block I1)	Head: Dipl.-Ing. Schmitter	<u>Central Workshop</u> (Block ZW)	<u>Theory</u> (Block D2)
Rapidly variable high-temperature plasmas: theta pinch, tubular pinch, antipinch.	Interaction of ion-electron beam with a plasma, interaction of a radio-frequency field with a plasma, investigation of stationary plasmas, caesium plasma, diffusion in magnetic fields, electric probes, sheath and wall problems, sputtering of solids, ultra-high-vacuum technique, cryopump.	Stationary high-pressure plasmas, shock waves, plasma acceleration and MHD generators.	Technical problems in experimental plasma physics (development, design, production) in the fields of: electronics, high-tension technique, vacuum technique, mechanical technology, general machine construction.	Job preparation, mechanical workshop, precision mechanics, fitting shop, welding shop, plastics workshop, carpentry shop.	Microinstabilities, probe theory, magnetohydrodynamics, solitary waves in plasma, lasers, magnetic-field calculations, evaluation of measurement results, IBM 7090 computer, library, documentation.				
Development and improvement of measuring methods.									
<u>Joint facilities:</u>	<u>Administration</u> (Block I1 and elsewhere)		<u>General Services</u> Building administration internal administration goods delivery and dispatch, stores supervision, transport stand-by, messenger and telephone service, security, accommodation service, canteen supervision						
Budget and finances, personnel department, purchasing department.									

Fig. 5: Organizational structure of the Institut für Plasmaphysik

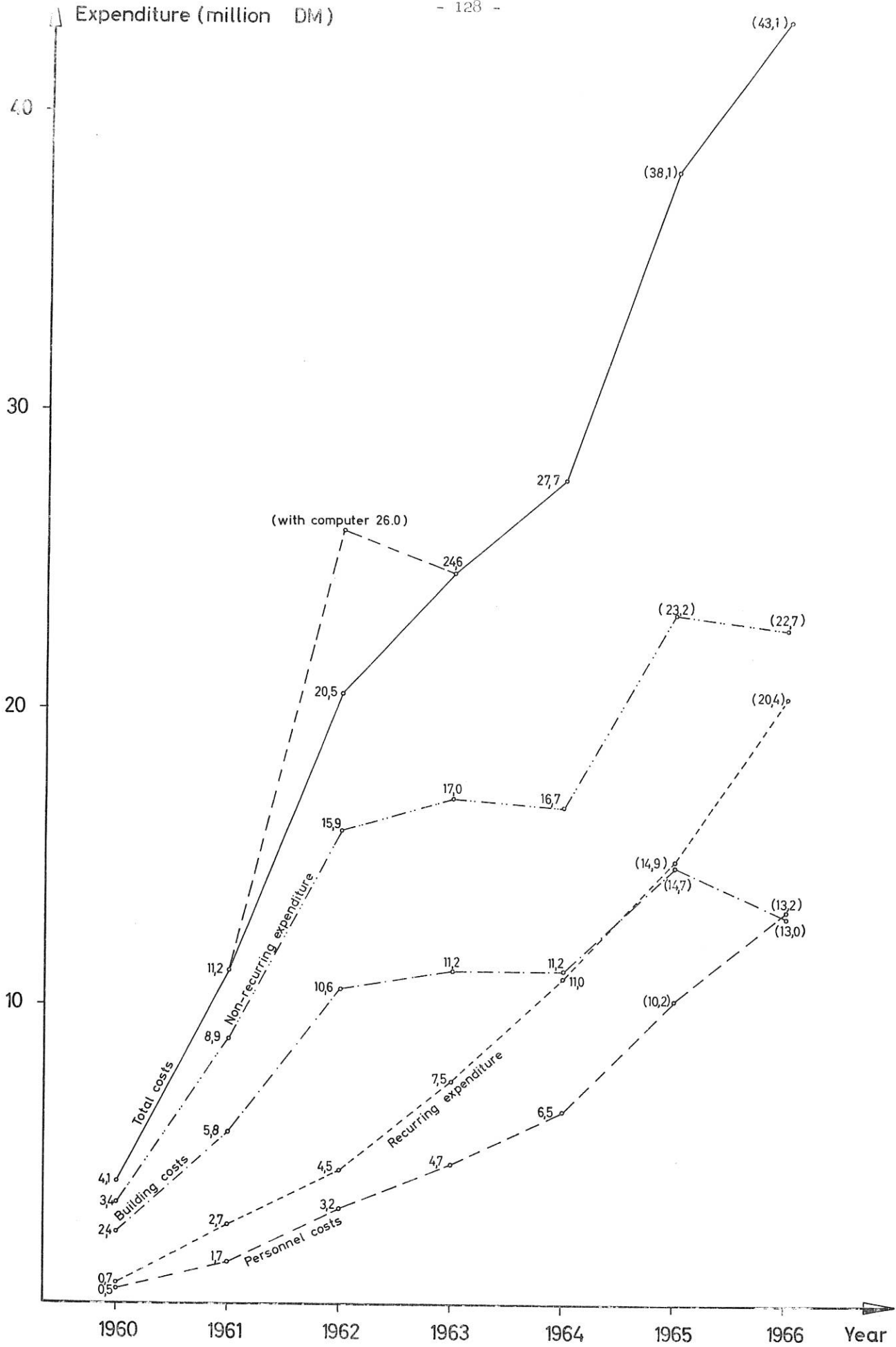


Fig. 6: Development of expenditure

Laboratory Reports

- IPP 1/16 H. Hemmerich, "Spektroskopische Messung der Elektronendichte und Temperatur beim Hohlpinch"
- IPP 1/18 W. Sassin, "Untersuchung einer schnellen koaxialen Blitzlampe als Pumplichtquelle für einen Rubinlaser"
- IPP 1/19 K. Hübner, "Magnetfeldmessungen mit Hilfe des Zeeman-Effekts"
- IPP 1/20 E. Barbian, "Untersuchung der harten Röntgenstrahlung am Theta-Pinch"
- IPP 1/21 R. Chodura, "Zum Zündmechanismus einer Theta-Pinch-Entladung"
- IPP 1/22 P.M. Asam, "Spektroskopische Messung der Elektronendichte und Temperatur bei Vorentladungsplasmen für Theta-Pinche"
- IPP 1/23 A. Eberhagen, W. Lünow, "Tabellen zur Auswertung von Intensitätsmessungen an Wasserstoffplasmen"
6/20
- IPP 1/24 A. Hirt, "Untersuchung der bei heissen Plasmen auftretenden Precursor-Ionisierung mit einem Mikrowellen-Interferometer"
- IPP 1/25 A. Heiss, "Ein Differential-Interferometer und seine Anwendung zur Bestimmung von Elektronendichtegradienten"
- IPP 1/26 G. Weiser, "Äußere und innere Modulation an Rubinlasern"
- IPP 1/27 A. Eberhagen, H. Glaser, "Beobachtungen über Makroinstabilitäten in einem Theta-Pinch mit antiparallel eingefangenen Magnetfeld"
- IPP 1/28 W. Köppendörfer, "Dimensionierung und Vergleich von z-Pinch, Antipinch und Theta-Pinch als Anordnungen zur Erzeugung starker Stoßwellen"
- IPP 1/29 W. Nässl, "Registrierung schnell veränderlicher optischer Linienprofile mit Bildwandler und Multiplier"
- IPP 1/30 H.-J. Kunze, "Messung der lokalen Elektronentemperatur und Elektronendichte in einem Theta-Pinch mittels der Streuung eines Laserstrahls"
- IPP 1/31 F. Pohl, H. Herold, "Numerische Berechnung des Vakuum-Magnetfeldes in Theta-Pinch-Spulen und verwandten Anordnungen"
- IPP 2/34 W. Ott, "Studien zur statischen Schicht"
- IPP 2/35 F. Boeschoten, K. Geißler, G. Siller, "Comparison of a Few Methods for Measuring the Diffusion Rate of Plasma Across a Magnetic Field"
- IPP 2/36 Proceedings of the "International Symposium on Diffusion of Plasma Across a Magnetic Field", Feldafing
- IPP 3/18 R. Wienecke, "Theoretische Grundlagen der magnetoplasmadynamischen Generatoren"
- IPP 3/19 Z. Celinski, "Analyse der Wirkungsweise von MHD-Generatoren der Typen A, B und C mit Hilfe von Vektordiagrammen"
- IPP 3/20 Z. Celinski, "Elektrische Theorie der Gleichstrom-MHD-Generatoren mit stationärer, linearer Gasströmung"

- IPP 3/21 Z. Celinski, "Analyse der Arbeit von Gleichstrom-MHD-Generatoren mit stationärer, linearer Gasströmung mit Hilfe von Vektordiagrammen"
- IPP 3/22 G. Hahn, M. Salvat, "Betrachtungen über die Beschleunigung eines Plasmas mit Hilfe der Lorentzkraft"
- IPP 3/23 S. Witkowski, "Druckerhöhung in der zylindersymmetrischen Lichtbogensäule bei überlagertem axialem Magnetfeld"
- IPP 3/24 H. Brinkschulte, "Interferometrische Untersuchungen an elektro-magnetisch beschleunigten Stoßwellen"
- IPP 4/11 A. Steinhausen, "Diagnostic Methods in the Field of Plasma Physics"
- IPP 4/12 A. Knobloch, "The 2.6-MJ Capacitor Bank at Garching - Arrangement and Collector System"
- IPP 4/13 B. Oswald, "Some Aspects of Superconducting Magnetic Energy Storage"
- IPP 4/14 J. Gruber, "Messung von Induktivität und Widerstand an BICC-Stoßkondensatoren"
- IPP 4/15 B. Berberich, "Kurzbericht Keramik-Metall-Verbindungen"
- IPP 4/16 H. Häglsperger, "Überwachungs- und Steuergeräte für Vakuumpumpstände" (under preparation)
- IPP 4/17 J. Mantel, "Der gegenwärtige Stand der EHD-Forschung", "The State of EHD-Conversion Research Today" (under preparation)
- IPP 4/18 J. Mantel, "Elektronische Röhren als thermionische Konverter", "Electron Tubes as Thermionic Converters" (under preparation)
- IPP 4/19 J. Deleplanque, "Elektrische Festigkeit von Kunststoff-Folien" (under preparation)
- IPP 6/14 R. Gorenflo, "Zweidimensionale innenfeldfreie Plasmakonfigurationen im Gleichgewicht mit einem äußeren Magnetfeld"
- IPP 6/15 P. P. J. M. Schram, "Kinetic Equations for Plasmas", Part II
- IPP 6/16 H. K. Wimmel, "Theorie der Plasma-Resonanzsonde"
- IPP 6/17 B. N. A. Lamborn, "On the Influence of a Tensor Friction upon Diffusion in a Magnetic Field"
- IPP 6/18 M. Feix, "Excitation Level of Plasma Oscillations"
- IPP 6/19 R. Gorenflo, "Numerische Methoden zur Lösung einer ABEL'schen Integralgleichung"
- IPP 6/20
1/23 A. Eberhagen, W. Lünow, "Tabellen zur Auswertung von Intensitätsmessungen an Wasserstoffplasmen"

- IPP 6/21 W. H. Kegel, "Lichtstreuung und Mischung in einem Plasma (Linearisierte Theorie)"
- IPP 6/22 H. Bergold, "Über stoßwellenartige Lösungen der Momentengleichungen für ein Plasma mit anisotropem Druck"
- IPP 6/23 H. Hora, "Abschätzungen zur Aufheizung eines Plasmas mittels Lasern"
- IPP 6/24 W. Lünow, "Magnetische LAVAL-Düse"
- IPP 6/25 W. Lünow, "Umrechnung von Strahlungsintensitäten in Temperatur und Elektronendichte bei Wasserstoffplasmen"
- IPP 6/26 E. Canobbio, R. Croci, "The Harmonics of the Electron Cyclotron Frequency in Plasmas"
- IPP 6/27 H. Hora, "Absorption Coefficient of Ruby-Laser Radiation in Fully Ionized Light Elements"
- IPP 6/28 P. P. J. M. Schram, W. H. Kegel, "Radial Distribution Functions in a Two Component Plasma"
- IPP 6/29 R. Gorenflo, Y. Kovetz, "Solution of an ABEL-Type Integral Equation in the Presence of Noise"
- IPP 6/30 A. Salat, A. Schlüter, "Plasmadiagnostik durch nichtlineare Resonanzwinkelstreuung"
- IPP 6/31 H. Hora, "Laser Excitation in a GaAs-Anode by Slow Electrons"
- MPI-PA-6/64 B. Boldt, W. S. Cooper, "Messung des Linienflügelprofils der Wasserstofflinie Lyman α "
- MPI-PA-7/64 D. Pfirsch, S. Prieß, "Kinetische Gleichungen und Integrabilitätsbedingung im Vielzeitformalismus"
- MPI-PA-10/64 W. Lotz, F. Rau, E. Remy, G. H. Wolf, "Beschleunigung des Plasmas im toroidalen Magnetfeld während der Startphase der Drift"
- MPI-PA-12/64 G. Grieger, "On the Equilibrium of a Plasma in a Curved Magnetic Field in the Presence of Electron Emitting Endplates"
- MPI-PA-13/64 G. Grieger, "Density Profiles determined by Resistive Diffusion, 'Bohm-Diffusion', Like-Particle Diffusion and Recombination" Part I. Special Cases
- MPI-PA-14/64 G. Grieger, "The Recombination-Coefficient in a Plasma Confined Radially by a Strong Magnetic Field and Axially by Electron Emitting Endplates"
- MPI-PA-15/64 G. Grieger, "A Remark on the Diffusion-Coefficient of a Plasma Confined Radially by a Strong Magnetic Field and Axially by Electron Emitting Endplates"

- MPI-PA-16/64 G. Grieger, "Particle Losses of an Alkali Plasma Confined Radially by Strong Magnetic Field and Axially by Electron Emitting Endplates"
- MPI-PA-18/64 D. Dimock, "On Secondary Current in Toroidal Plasmas"
- MPI-PA-19/64 M. Tutter, "Zur Auswertung von Whistlermessungen an Theta-Pinch-Maschinen"
- MPI-PA-20/64 D. Eckhartt, G. Grieger, E. Guillino, M. Hashmi, "Particle Loss Rates of a Cs-Plasma in a Curved Magnetic Field Geometry"
- MPI-PA-21/64 D. Eckhartt, G. Grieger, E. Guillino, M. Hashmi, "Particle Loss Rates of a Cs-Plasma in a Homogeneous Magnetic Field"
- MPI-PA-24/64 H. M. Mayer, "The Pressure Balance of a Plasma Sheath, Part A: The Electrostatic Sheath"
- MPI-PA-25/64 H. M. Mayer, "The Pressure Balance of a Plasma Sheath, Part B: The Sheath in a Quasistationary HF-Perturbation"
- MPI-PA-29/64 D. Eckhartt, G. Grieger, M. Hashmi, "On the Particle Losses of a Cs-Plasma in a Stellarator"
- MPI-PA-19/63 G. Boldt, K. H. Stephan, "Untersuchung des Schwarzschild-Exponenten und des Intermittenzeffekts einiger Photoemulsionen" (under preparation)

Publications

- 1 C. Andelfinger, A. Heiss, "Elektronendichtebestimmung in Plasmen mit einem Differential-Interferometer", talk, Düsseldorf 1964; abstr. in Phys. Verh. DPG 4, 290 (1964).
- 2 C. Andelfinger, A. Hirt, "Untersuchung von Precursorionisierung an stromstarken Pinch-entladungen mit einem Mikrowellen-Interferometer", talk, Düsseldorf 1964; abstr. in Phys. Verh. DPG 4, 289 (1964).
- 3 R. Behrisch, "Festkörperzerstäubung durch Ionenbeschuss", Erg. der Exakt. Naturwiss. XXXV, 295 (1964).
- 4 F. Boeschoten, "Review of Experiments on the Diffusion of Plasma across a Magnetic Field", Plasma Phys. (J. Nucl. Energy Part C) 6, 339 (1964).
- 5 F. Boeschoten, G. Cattanei, G. Siller, "Proposal for the Production of High-Temperature Plasmas (HELIOS and HELIOSIS)", talk, Varenna 1964; Varenna-Report under prep.
- 6 F. Boeschoten, K. Geißler, G. Siller, "Comparison of a Few Methods for Measuring the Diffusion Rate of Plasma Across a Magnetic Field" [IPP 2/35]; EURATOM Bulletin 1964 under the terms of the joint research programme 003-61-1 FUAD.
- 7 G. Boldt, "Measurement of Absorption Oscillator Strengths and Line Broadening in the Wave Length Region from 1000 to 2000 Å", Opacity-Conference in Albuquerque/New Mexico, USA, 1964; Proc. Opacity-Conf.
- 8 G. Boldt, "Messung von Übergangswahrscheinlichkeiten im Vakuum-UV-Spektralbereich", DPG Colloquium in Berlin 1964; abstr. in Phys. Verh. DPG 4, 389 (1964).
- 9 G. Boldt, W. S. Cooper, "Messung des Linienflügelprofiles der Wasserstofflinie Lyman α ", Z. Naturforsch. 19a, 968 (1964).
- 10 G. Brederlow, "The Problem of non-equilibrium Ionization in MHD-Generators", talk, Varenna 1964; Varenna Report under preparation.
- 11 G. Brederlow, R. H. Eustis, W. Riedmüller, "Measurements of Stagnation Gas Temperatures in a MHD-Generator", Intern. Symp. on Magnetohydr. Electr. Power Generation, Paris 1964, Session 2 b, Paper 21.
- 12 H. Brinkschulte, H. Muntenbruch, "Untersuchung von T-Rohr-Stosswellen mit einem Mach-Zehnder-Interferometer", talk, Karlsruhe 1964; abstr. in Phys. Verh. DPG 4, 243 (1964).
- 13 K. Büchl, "Druckmessungen mit piezoelektrischen Sonden an einem linearen z-Pinch", Z. Naturforsch. 19a, 691 (1964).
- 14 Z. Celinski, "Elektrische Theorie der Gleichstrom-MHD-Generatoren mit stationärer, linearer Gasströmung", talk, Karlsruhe 1964; abstr. in Phys. Verh. DPG 4, 242 (1964).

- 15 Z. Celinski, "Analysis of DC MHD Generators with Stationary Linear Gas Flow by means of Vector Diagrams", Intern. Symp. on Magnetohydr. Electr. Power Generation, Paris 1964; Session 3 b, Paper 39.
- 16 R. Chodura, "Zum Zündmechanismus einer Theta-Pinch-Entladung", Z. Naturforsch. 19a, 679 (1964),
talk, Karlsruhe 1964; abstr. in Phys. Verh. DPG 4, 234 (1964).
- 17 G. D. Cormack, "Spektroskopische, zeitaufgelöste Bestimmung der Elektronendichte und Temperatur in extrem irreproduzierbaren lichtschwachen Entladungsplasmen", talk, Düsseldorf 1964; abstr. in Phys. Verh. DPG 4, 290 (1964).
- 18 G. D. Cormack, "The Contact Surface in an Electromagnetic Shock Tube", Z. Naturforsch. 19a, 934 (1964).
- 19 D. Düchs, "Fluid Models for the Plasma in Pinch Experiments", talk, Varenna 1964; Varenna Report under preparation.
- 20 A. Eberhagen, H. Glaser, "Studies on Macroinstabilities in a Theta-Pinch with Antiparallel Magnetic Field", Nuclear Fusion 4, in press.
- 21 D. Eckhardt, G. Grieger, M. Hashmi, "Particle Losses of a Cs Plasma in Toroidal Devices", talk, Varenna 1964; Varenna Report under preparation.
- 22 E. Fünfer, "Plasmaphysik in Gasen", Physikertagung - Düsseldorf 1964, Plenarvorträge 346 (1964).
- 23 G. von Gierke, G. Müller, G. Peter, H. H. Rabben, "On the Influence upon the Resonance Behaviour of a RF-Plasma-Probe", Z. Naturforsch. 19a, 1107 (1964).
- 24 R. W. Gould, "Excitation of Ion-Acoustic Waves", Phys. Rev. 136, A991 (1964).
- 25 R. W. Gould, "Radio Frequency Characteristics of the Plasma Sheath", Phys. Lett. 11, 236 (1964).
- 26 R. Gorenflo, "Eine Anwendung der Funktionentheorie in der Magnetohydrostatik", ZAMM, in press.
- 27 R. Gorenflo, "Über Pseudozufallsgeneratoren und ihre statistischen Eigenschaften", Biometrische Zeitschrift, in press.
- 28 G. Grieger, "Cs Plasma Experiments in Munich", talk at the APS-Meeting on Plasma Physics, New York 1964; abstr. in Bull. Am. Phys. Soc. in press.
- 29 U. Grossmann-Doerth, W. Lotz, F. Rau, E. Remy, G. H. Wolf, "Untersuchung eines Plasmas im toroidalen Theta-Pinch", talk, Karlsruhe 1964; abstr. in Phys. Verh. DPG 4, 252 (1964).
- 30 K. von Hagenow, H. Koppe (Univ. Kiel), "The Partition Function of a Fully Ionized Plasma", Proc. VI. Conf. Ion. Phen. in Gases, Paris 1963, Vol. I. 221.
- 31 U. Heidrich, "Die Energiebilanz einer Wasserstoffbogensäule in einem axialen Magnetfeld", talk, Karlsruhe 1964; abstr. in Phys. Verh. DPG 4, 236 (1964).

- 32 H. Herold, "The MJ Theta-Pinch Experiment at Garching", talk, Varenna 1964; Varenna-Report under preparation.
- 33 W. Herrmann, "Über die Instabilität eines Elektronenstrahlplasmas (Erste Messungen an einem Strahl-Plasma)", EURATOM Microfilm Report No. SP/1/1079 (1964) under the terms of the joint research programme 003-61-1 FUAD.
talk, Karlsruhe 1964; abstr. in Phys. Verh. DPG 4, 256 (1964).
- 34 G. Hofmann, H. Hermansdorfer, "Doppelsondenmessungen mit einem Mikrowellenübertrager", Z. Naturforsch. 18a, 1361 (1963),
talk, Karlsruhe 1964; abstr. in Phys. Verh. DPG 4, 254 (1964).
- 35 H. Hora, "Concerning Stimulated Recombination in a Semiconductor Anode of a Discharge-Diode", ZAMP 16, 98 (1965)
- 36 H. Hora, "Über stimulierte Rekombination in der Halbleiteranode einer Entladungsdiode", Physica Status Solidi 8, 197 (1965).
- 37 H. Hora, B. Kronast, H.-J. Kunze, "Distribution of the Emission from a Rectangular Laser Rod (Ruby)", Proc. IEEE 52, 611 (1964).
- 38 K. Hübner, F. L. Ribe, "Magnetfeldmessungen mit dem Zeeman-Effekt an Theta-Pinchen", talk, Karlsruhe 1964; abstr. in Phys. Verh. DPG 4, 253 (1964).
- 39 F. Karger, "Entladungssperre für Glasrohre mit Neutralgasdurchströmung und für Pirani-Manometerröhren", Vakuumtechnik 13, 152 (1964).
- 40 W. H. Kegel, "Light Mixing and the Generation of the Second Harmonic in a Plasma in an External Magnetic Field", submitted to the Z. Naturforsch.
- 41 H. Kolig, H. Muntenbruch, "Messung der Ströme in Plasmen hinter elektromagnetisch erzeugten Stosswellen mit Magnetfeldsonden", talk, Düsseldorf 1964; abstr. in Phys. Verh. DPG 4, 290 (1964).
- 42 F. P. Küpper, G. Weiser, "Herstellung von Spannungsanstiegen an Kerr-Zellen im Nanosekundenbereich zur Erzeugung von Riesenlaserpulsen sowie Frequenzverschiebungen im sichtbaren Spektralbereich", talk, Düsseldorf 1964; abstr. in Phys. Verh. DPG 4, 284 (1964).
- 43 H.-J. Kunze, "Light Scattering a new Diagnostic Tool in Plasma Physics", talk, Varenna 1964; Varenna Report under preparation.
- 44 H.-J. Kunze, A. Eberhagen, E. Fünfer, "Electron Density and Temperature Measurements in a 26 kJ θ -Pinch by Light Scattering", Phys. Lett. 13, 38 (1964).
- 45 H.-J. Kunze, E. Fünfer, B. Kronast, W. H. Kegel, "Measurement of the Spectral Distribution of Light Scattered by a θ -Pinch Plasma", Phys. Lett. 11, 42 (1964).
- 46 F. Labuhn, "Messung der Absorptionsoszillatorenstärken von NI-Multipletts am Kaskadenlichtbogen im Wellenlängenbereich zwischen 1000 und 1800 Å", Doctorate Thesis, T.H. Munich.

- 47 B. N. A. Lamborn, D. L. Lafferty, "Electrostatic Waves in Bean-Plasma Systems", *Phys. Fluids* 7, 292 (1964).
- 48 G. Lisitano, "Ein Messverfahren zur direkten Anzeige des Übertragungs- und Reflexionsfaktors im mm-Wellenbereich", Doctorate Thesis, T.H. Munich (1964).
- 49 G. Lisitano, "Automatic Phase-Measuring System for an 8-mm Carrier Wave and its 4-mm Harmonic", *Rev. Sci. Instr.*, probably March 1965.
- 50 W. Lotz, F. Rau, E. Remy, G. H. Wolf, "Beschleunigung des Plasmas im toroidalen Magnetfeld während der Startphase der Drift", talk, Karlsruhe 1964; abstr. in *Phys. Verh. DPG* 4, 252 (1964).
- 51 W. Lotz, E. Remy, G. H. Wolf, "The Toroidal Theta-Pinch in M+S-like Configurations", *Nuclear Fusion* 4, 335 (1964).
- 52 W. Lotz, E. Remy, G. H. Wolf, "Der toroidale Theta-Pinch in M+S-artigen Konfigurationen", talk, Karlsruhe 1964; abstr. in *Phys. Verh. DPG* 4, 252 (1964).
- 53 W. Lotz, E. Remy, G. H. Wolf, "The Toroidal Theta-Pinch in M+S-Configuration", talk, Varenna 1964; Varenna Report under preparation.
- 54 C. Mahn, H. Ringler, R. Wienecke, S. Witkowski, G. Zankl, "Experimente zur Erhöhung der Lichtbogentemperatur durch Reduktion der Wärmeleitfähigkeit in einem Magnetfeld", *Z. Naturforsch.* 19a, 1202 (1964).
- 55 C. Mahn, S. Witkowski, "Heliumbogen im Magnetfeld", talk, Karlsruhe 1964; abstr. in *Phys. Verh. DPG* 4, 236 (1964).
- 56 K. Maischberger, A. Steinhausen, "Elektrische Leistungsstabilisierung", *Elektronik*, probably March 1965.
- 57 W. Makios, H. Muntenbruch, "Untersuchung eines Stosswellenplasmas mit Hilfe eines 4 mm-Mikrowellen-Reflektometers", talk, Karlsruhe 1964; abstr. in *Phys. Verh. DPG* 4, 243 (1964).
- 58 G. Müller, G. Peter, "Neuere Untersuchungen zur HF-Resonanzsonde", talk, Karlsruhe 1964; abstr. in *Phys. Verh. DPG* 4, 246 (1964).
- 59 W. Nässl, "Zeitaufgelöste Beobachtung von Linienprofilen mit Hilfe eines Bildwandlers", talk, Düsseldorf 1964; abstr. in *Phys. Verh. DPG* 4, 289 (1964).
- 60 B. Oswald, "Zur Erzeugung hoher stationärer Magnetfelder mit Hilfe wassergekühlter Spulen", *ETZ-A* 85, 481 (1964).
- 61 B. Oswald, "Hohe Magnetfelder und ihre Anwendung in der Plasmaphysik", *ETZ-A*, in press.
- 62 G. Peter, G. Müller, H. H. Rabben, "Untersuchungen mit der HF-Plasma-Resonanzsonde an einem Cs-Kontaktionsplasma". EURATOM-Mitteilung Nr. 1817.d (1964) under the terms of the joint research programme 003-61-1 FUAD.

- 63 F. Rau, G. H. Wolf, "Eine Methode zur automatischen Kompensierung von Totzeitverlusten", Nuclear Instruments and Methods 27, 321 (1964).
- 64 E. Rebhan, "Stationäre eindimensionale Plasmaströmung in gekreuzten elektrischen und magnetischen Feldern", talk, Karlsruhe 1964; abstr. in Phys. Verh. DPG 4, 242 (1964).
- 65 H. Ringler, "Experiments on Electric Arcs in Magnetic Fields", talk, Varenna 1964; Varenna Report under preparation.
- 66 H. Ringler, G. Zankl, "Messung der Wärmeleitfähigkeit eines Wasserstoffplasmas im Magnetfeld", talk, Karlsruhe 1964; abstr. in Phys. Verh. DPG 4, 236 (1964).
- 66 a A. Salat, A. Schlüter, "Plasma Diagnostics by Non-linear Resonant-Angle Scattering", Phys. Lett. 14, 106 (1965).
- 66 b A. Salat, A. Schlüter, "Plasmadiagnostik durch nichtlineare Resonanzwinkelstreuung", Z. Naturforsch. in press.
- 66 c A. Salat, "Lichtmischung in endlichen Plasmavolumen", Z. Naturforsch. in press.
- 66 d A. Salat, "On non-linear Resonant Light Mixing in Plasmas", Phys. Lett. 15, 139 (1965)
- 67 B. M. U. Scherzer, "Ionisationsmanometer in Öldampfatosphären - eine Deutung des Blears-Effekts", abstr. in Phys. Verh. DPG 4, 277 (1964).
- 68 P. P. J. M. Schram, "Kinetic Equations for Plasmas", EUR 1805.e
- 69 P. P. J. M. Schram, W. H. Kegel, "Radial Distribution Functions in a Two Component Plasma", eingereicht bei "The Physics of Fluids".
- 70 C.-R. Vidal, "Die relative Oszillatorenstärke von einigen Linien der scharfen und diffusen Nebenserien des Heliums", Z. Naturforsch. 19 a, 1018 (1964).
- 71 C.-R. Vidal, "Die Druckverbreiterung der Balmer-Linien und der diffusen Linien des Heliums", Z. Naturforsch. 19a, 947 (1964).
talk, Karlsruhe 1964; abstr. in Phys. Verh. DPG 4, 235 (1964).
- 72 H. Völk, "Electrostatic Stability of Plasmas", Phys. Lett. 12, 208 (1964).
- 73 G. Weiser, "A Rigid low-loss Polarizing Device for giant Pulse Lasers", Proc. IEEE 52, 966 (1964).
- 74 R. Wienecke, "Reaktionswärmeleitfähigkeit von Wasserstoff und einfach ionisiertem Helium in einer zylindersymmetrischen Entladung mit überlagertem axialen Magnetfeld", Z. Naturforsch. 19a, 676 (1964).
- 75 H. K. Wimmel, "Theory of the Plasma Resonance Probe", Z. Naturforsch. 19a, 1099 (1964).
talk, Karlsruhe 1964; abstr. in Phys. Verh. DPG 4, 246 (1964).
- 76 H. K. Wimmel, "Statistical Line Broadening in Plasmas: Erratum", J. Quant. Spectrosc. Radiat. Transfer 4, 497 (1964).